MOLECULAR MECHANISM OF INNATE IMMUNE RESPONSE DURING JAPANESE ENCEPHALITIS VIRUS INFECTION

M.Sc. Thesis
2015

Submitted to
Central Department of Biotechnology
Tribhuvan University
Kirtipur, Kathmandu, Nepal

Submitted by
Santosh Dahal

Supervisor
Dr. Tilak R. Shrestha

ACKNOWLEDGEMENT

I am deeply indebted to my supervisor Dr. Tilak R. Shrestha, Central Department of Biotechnology, Tribhuvan University for his supervision, continuous advice, support, encouragement, trust and recommending me to complete my thesis at such a prestigious institution, without which this research work would not have been possible. I am thankful to Dr. Rajani Malla, HOD, Central Department of Biotechnology, Tribhuvan University for providing every kind of facilities to undertake present study.

I would like to express my sincere gratitude to Dr. Shailendra K. Saxena, Senior Scientist & Project Leader, Infectious Diseases Laboratory, CCMB, for his supervision, his support, patience and encouragement throughout my thesis work. It is not often that one finds an advisor who is always down to earth and always finds the time for listening to even minute problem and roadblocks that I faced during my research and always provided advice to crop up the problems. I could not have imagined having a better advisor than him. His scintillating advice and lectures always motivated my zeal of working in the field of Infectious disease. As my supervisor, he has shown me, being an example himself, what a great scientist should be. I would also like to thank the Director, CCMB, Dr. Ch. Mohan Rao, for providing opportunity for students to have an exposure to a research environment through the thesis program.

I am highly in debt to Mr. M.L. Arvinda Swamy, Shirisha Cherukumu and Chitti Prasad who helped me throughout the course of my work. I whole-heartedly thank them for teaching me a lot of techniques in animal tissue culture, molecular biology and bio-informatics and giving me a strong foundation in this field.

I am also thankful to my friends Mitesh Shrestha, Rajindra Napit, Hari Haran Iyer, Gaurav Gupta, Gomati Pant and Aarati Poudel for accompanying me at CCMB during my dissertation. I feel pleasure to have friends like Nirmal Panthi, Mukesh Thapa, Rosan Nepal, Bimala Dhakal and Sandipty Kayastha, who always motivated me to move forward.

Last but not least, I express my heartiest gratitude to my parents for being a source of inexhaustible encouragement support and inspiration.

ABBREVIATION

PBS: Phosphate Buffer Saline

BSA: Bovine Serum Albumin

bp: Base Pair

DDW: Double Distilled Water

EDTA: Ethylene Diamine Tetra Acetic acid

Tris: Tris(hydroxymethyl) aminomethane

dNTP: Deoxynucleotide triphosphate

DNA: Deoxyribonucleic acid

RNA: Ribonucleic acid

Kb: Kilo Base

pM: Pico moles

µg: Micro gram

Taq: *Thermus aquaticus*

Pfu: Plaque forming units

DAPI: 4', 6'-diamidino-2-phenylindole

miR: micro RNA

p.i.: Post Infection

r.p.m.: Revolution per minute

TABLE OF CONTENTS

Chapters	Page No.
Title Page	**I**
Recommendation	**II**
Certificate	**III**
Certificate of Evaluation	**IV**
Acknowledgement	**V**
List of Abbreviation	**VI**
Table of Content	**VII**
List of Figures	**XII**
List of Tables	**XIV**
Abstract	**1**
Chapter 1: Introduction	**2-7**
1.1 Background	2-5
1.2 Hypothesis	6
1.3 Objectives	7
1.3.1 General Objective	7
1.3.2 Specific Objective	7
1.4 Rationale	7
Chapter 2: Literature Review	**8-20**
2.1 Epidemiology	8-11
2.1.1 Global outlook	8-9
2.1.2 Epidemiology in Nepal	9-11
2.2 Viral replication cycle	11-12

2.3 Vector and Transmission 12-13
2.4 Clinical presentation 13-14
2.5 Diagnosis 14-15
2.6 Pathology and Pathogenesis 15-17
2.7 Host immune response 17-19
2.8 Interleukin-10 19
2.9 NS3 Protein 20
2.10 Micro RNAs 20-21
Chapter 3: Materials and Methods 22-38
3.1 Cell culture and maintenance of cells for the study 22
3.1.1 Cell type used during the study 22
3.2 Determination of viral titre by plaque assay 22-24
3.2.1 Preparation of a monolayer of cells 22
3.2.2 Preparation of viral dilutions 23
3.2.3 Inoculation of virus 23
3.2.4 Preparation of agarose overlay 23
3.2.5 Fixation and staining of cells 23
3.2.6 Enumeration of plaques and determination of viral titre 23-24
3.3 Immunostaining 24-25
3.3.1 Cell culture 24
3.3.2 Cell Fixation 24
3.3.3 Cell permeabilization 24
3.3.4 Blocking 24
3.3.5 Incubate cells in primary antibody/antibodies 24
3.3.6 Incubate the cells in secondary antibody/antibodies 25

3.3.7 Mounting and visualization 25

3.4 Molecular characterization of NS3 protein 25-29

3.4.1 Viral RNA isolation by Trizol method 25

3.4.2 Determination of yield and quality of RNA 25

3.4.3 Preparation of cDNA by reverse transcriptase polymerase chain reaction (RT-PCR) 26

3.4.4 Primer designing and amplification of cDNA with PCR 26-27

3.4.5 Agarose gel electrophoresis of amplified viral cDNA 28

3.4.6 Sequencing PCR and Sequence plate processing 28-29

3.4.7 Sequence analysis 29

3.5 Interleukin-10 and miR Expression 30-36

3.5.1 Cell culture 30

3.5.2 Inoculation of virus 30

3.5.3 Time points collection 30

3.5.4 RNA isolation 30

3.5.5 Preparation OF cDNA BY reverse transcriptase polymerase chain reaction (RT-PCR) 31

3.5.6 MiR selection 31-34

3.5.7 Real Time polymerase chain reaction 34-36

3.6 Protein expression analysis of Interleukin-10 36-37

3.6.1 SDS-Polyacrylamide gel separation 36

3.6.2 Western Blotting 37

3.6.3 Detection by Western blotting 37

3.7 NS3 standard curve and Viral load analysis 37-38

Chapter 4: Results **39-56**

4.1 Characterization of serine protease domain of JEV NS3 protein 39-46

4.1.1 PCR amplification of NS3 gene 39

4.1.2 Sequence analysis of the NS3 protein 39-42

4.1.3 Phylogenetic tree (BLAST tree view) 43-45

4.2 Determination of viral titre by plaque assay 46-47

4.3 Immunostaining 47-48

4.4 Time Point Study for the expression of IL-10 and miRs 49-56

4.4.1 Cell culture and viral infection 49

4.4.2 Real time PCR for absolute quantification of viral RNA copies 50

4.4.3 Real time PCR for relative quantification of IL-10 51

4.4.4 Real time PCR for relative quantification of miR-98 52

4.4.5 Real time PCR for relative quantification of miR-27a 53

4.4.6 Real time PCR for relative quantification of miR-106b 54

4.4.7 Compared Relative expression 54-55

4.5 Protein expression analysis of Interleukin-10 56

Chapter 5: Discussion **57-60**

5.1 Study of sequence diversity in NS3 gene in the novel strain GP05 of Japanese encephalitis virus 57

5.1.1 Sequencing NS3 gene of JEV and performing phylogenetic analysis 57

5.1.2 Performing Homology Modeling of the NS3 protein from the obtained sequence and predict ligand binding sites on the protein 57-58

5.2 Study of the regulatory mechanism of Interleukin-10 production during Japanese encephalitis infection via micro RNAs 58-60

5.2.1 Determination of viral infection in cell culture 59

5.2.2 Relative expression of Interleuki-10 and selected microRNAs 59-60

Chapter 6: Summary and Conclusion **61-62**

Recommendation **63**

References **64-73**

Appendix **74-77**

LIST OF FIGURES

Figure 1: Japanese encephalitis virus structure and genome showing structural and non-structural proteins

Figure 2: Geographical distribution of Japanese Encephalitis Virus

Figure 3: Seasonal trend of Japanese Encephalitis in Nepal

Figure 4: JE infected districts of Nepal

Figure 5: Laboratory confirmed cases of Acute Encephalitis like Syndrome (AES) and Japanese encephalitis (JE) in the samples collected from the various districts of Nepal.

Figure 6: JEV replication Cycle

Figure 7: Transmission Cycle of JEV

Figure 8: Mechanism of neuroinvasion by JEV

Figure 9: Host innate immune response during JEV infection

Figure 10: Morphology of P388D1 and BHK-21 cells

Figure 11: Mouse miRs having the capability of binding with Interleukin-10 mRNA as predicted by Target scan software

Figure 12: Binding sites of the selected miRs in the 3'UTR of IL-10 mRNA as predicted by Target scan software

Figure 13: Binding sites of the selected miRs in the 3'UTR of IL-10 mRNA as predicted by miRanda software

Figure 14: Binding free energy between the selected miRs and IL-10 3'UTR as predicted by RNA hybrid software

Figure 15: The amplified PCR product of NS3 gene as examined on 1.2% agarose gel with 100 bp marker

Figure 16: Electropherogram results obtained from amplified DNA sequencing of NS3 gene

Figure 17: MultAlin analysis of nucleotide sequences of NS3 with reference GP78 JEV strain

Figure 18: Cladogram tree displaying the relative positions of the NS3 gene sequence in comparison with other JEV strains.

Figure 19: Predicted secondary structure of the NS3 protein exhibiting the regions where helix and beta sheets are present in the modelled protein.

Figure 20: 3D modelling structure of serine protease domain of GP05 NS3 protein

Figure 21: Immunostaining of JEV infected BHK-21 cells with monoclonal antibody against the envelope protein of the virus. Control cells were mock infected with plain medium

Figure 22: P388D1 cells as observed under microscope at different time points after JEV infection. Control cells are mock infected cells with plain medium.

Figure 23: Absolute Quantification of the viral copy number.

Figure 24: Real-time RT-PCR analysis of Interleukin-10 mRNA expression in the control and JEV infected P388D1 cells.

Figure 25: Real-time RT-PCR analysis of micro RNA 98 expression in the control and JEV infected P388D1 cells.

Figure 26: Real-time RT-PCR analysis of micro RNA 27a expression in the control and JEV infected P388D1 cells.

Figure 27: Real-time RT-PCR analysis of micro RNA 106b expression in the control and JEV infected P388D1 cells.

Figure 28: The relative expression of IL-10, miR-98, miR-27a and miR-106b was plotted on a single graph.

Figure 29: Protein expression analysis of Interleukin-10 in the JEV infected P388D1 cells by Western blotting.

LIST OF TABLES

Table 1: Reaction mixture for RT-PCR

Table 2: Primer sequence for the amplification of NS3 gene

Table 3: Reaction mixture for gradient PCR

Table 4: PCR conditions for the NS3 region amplification

Table 5: Reaction mixture for sequencing PCR

Table 6: Conditions for sequencing PCR with forward primers

Table 7: Conditions for sequencing PCR with reverse primers

Table 8: Reaction mixture for RT-PCR

Table 9: PCR condition for cDNA synthesis

Table 10: Predicted miR binding sites on Interleukin-10 mRNA

Table 11: Comparative view of predicted miR sites on 3' UTR region by miRWalk & other prediction programs

Table 12: Primers sequence for the target genes (GAPDH, IL-10, miR-98, miR-27a, miR-106b)

Table 13: Reaction mixture for Real Time PCR

Table 14: PCR reaction condition for GAPDH and IL-10

Table 15: PCR reaction condition for miRs

Table 16: Primers sequence for the absolute quantification of Viral RNA targeting NS3 gene

Table 17: Nucleotide variation in JEV gp05 compared to JEV gp78

Table 17: Viral titre (in pfu/mL) corresponding to control and viral dilutions 10^{-1} to 10^{-9}

ABSTRACT

Japanese encephalitis (JE) is an arboviral disease which accounts for significant pediatric mortality annually in Asia and Australia, including Nepal. Encephalitis is merely the result of viral invasion in CNS and pathological consequences. Neuronal loss is the outcome of both JEV infection of neurons and bystander damage caused by activated microglia. Recent studies have shown that micro RNAs (miRs) holds a major platform during JEV infection and modulate cellular pathways to determine the pathological condition. Therefore, the present study was planned to characterize the NS3 gene of gp05 and investigate the role of miRs in controlling the IL-10 expression (Th2 response) during JEV infection in macrophages. Sequencing analysis of the NS3 gene, taking the sequence of JEV gp78 as reference,showed high frequency of mutation in the gene. Although the NS3 is most conserved gene in JEV genome, result claimed that there is high frequency of mutation in the gene, which might be the cause for the emergence of more pathogenic strains of JEV. In this study, using a combination of bioinformatics and molecular approaches, we report that miR-98, miR-27a and miR-106b might have a possible role in posttranscriptional regulation of IL-10 gene expression during JEV infection. Our *in silico* analysis predicted the novel miRs having potential to bind with the 3'UTR region of IL-10 mRNA. From the predicted miRs, miR-98 and miR-27a were selected on the basis of published article showing their role in regulation of IL-10 expression. Novel micro RNA miR-106b was selected on the basis of free energy and prediction from the software. Normal PCR, real time PCR (RT-PCR) and western blotting was performed to validate the *in silico* data. Our results exhibited the correlation between the expression of IL-10 and three miRNAs mainly miR-98, miR-27a miR-106b during JEV infection. In summary, our result suggested that miR-98, miR-27a and miR-106 might have a role in regulation of IL-10 production during JEV infection, which, if unregulated, might be the probable reason for the adverse inflammatory condition present in the disease pathology.

Keywords: JEV gp05, Encephalitis, MicroRNA, Microglial cells, Th2 response, Interleukin-10, Non-structural protein 3

ABSTRACT

Japanese encephalitis (JE) is an arboviral disease which accounts for significant pediatric mortality annually in Asia and Australia, including Nepal. Encephalitis is merely the result of viral invasion in CNS and pathological consequences. Neuronal loss is the outcome of both JEV infection of neurons and bystander damage caused by activated microglia. Recent studies have shown that micro RNAs (miRs) holds a major platform during JEV infection and modulate cellular pathways to determine the pathological condition. Therefore, the present study was planned to characterize the NS3 gene of gp05 and investigate the role of miRs in controlling the IL-10 expression (Th2 response) during JEV infection in macrophages. Sequencing analysis of the NS3 gene, taking the sequence of JEV gp78 as reference,showed high frequency of mutation in the gene. Although the NS3 is most conserved gene in JEV genome, result claimed that there is high frequency of mutation in the gene, which might be the cause for the emergence of more pathogenic strains of JEV. In this study, using a combination of bioinformatics and molecular approaches, we report that miR-98, miR-27a and miR-106b might have a possible role in posttranscriptional regulation of IL-10 gene expression during JEV infection. Our *in silico* analysis predicted the novel miRs having potential to bind with the 3'UTR region of IL-10 mRNA. From the predicted miRs, miR-98 and miR-27a were selected on the basis of published article showing their role in regulation of IL-10 expression. Novel micro RNA miR-106b was selected on the basis of free energy and prediction from the software. Normal PCR, real time PCR (RT-PCR) and western blotting was performed to validate the *in silico* data. Our results exhibited the correlation between the expression of IL-10 and three miRNAs mainly miR-98, miR-27a miR-106b during JEV infection. In summary, our result suggested that miR-98, miR-27a and miR-106 might have a role in regulation of IL-10 production during JEV infection, which, if unregulated, might be the probable reason for the adverse inflammatory condition present in the disease pathology.

Keywords: MicroRNA, Microglial cells, Interleukin-10, Non-structural protein 3, Th2 response, JEV gp05

CHAPTER 1

INTRODUCTION

1.1 Background

Japanese Encephalitis Virus belongs to the family flaviviridae and genus Flavivirus. Flaviviridae family consists of three genera, namely Flavivirus, Pestivirus and Hepacivirus, of which the Flavivirus genus is the largest, with 53 species subdivided into 12 groups (Schweitzer and Chapman, 2009). Flaviviruses are a group of small, enveloped, positive-strand RNA viruses with yellow fever virus as the prototype member and the dengue viruses as the most clinically relevant members in terms of worldwide incidence of human disease (Guzman *et al*, 2010; Lindenbach and Rice, 2001). Within the genus, the viruses can be further subdivided into antigenic complexes according to serological criteria, or into clusters, clades and species on the basis of molecular phylogenetics (Lobigs and Diamond, 2012). However, the most common causes of diseases are associated with the Japanese encephalitis group viruses within the *Flavivirus* genus. The four most common disease causing species includes Japanese encephalitis virus (JEV), Murray Valley encephalitis virus (MVEV), St. Louis encephalitis virus (SLEV), and West Nile virus (WNV). The flaviviruses WNV, DENV, and JEV share some common features, such as transmission via mosquitoes, and cross-react with each other in serological tests. These cross-reactive responses could confound the interpretation during serological testing, including neutralization tests and enzyme-linked immunosorbent assay (Kuno, 2003).

Japanese encephalitis is mainly a disease of children, causing acute infection and inflammation of the brain. JE holds the position of the leading cause for the vaccine preventable arboviral encephalitis in eastern and southern Asia (van den Hurk *et al*, 2009). The virus undergoes enzootic transmission cycle involving waterbirds, domestic pigs and rice paddy-breeding mosquitoes, principally *Culex tritaeniorhynchus* (van den Hurk *et al*, 2009). Although humans and horses can develop fatal encephalitis, they are considered to be dead-end hosts of the virus, developing only low-level viremia (Endy and Nisalak, 2002). Though JEV infections were first described in 1871, it was only in 1934 that successful isolation was done from the brain of a fatal human encephalitis case, in Tokyo. Since its first outbreak, JE has taken a million lives and left survivors with severe neurological disabilities. Although most of the cases of JE are asymptomatic, 30,000 to 50,000 cases are reported annually, including 10,000 to 15,000 deaths (Tiwari *et al*, 2012). JE is a disease of the public health importance due to its epidemic potential and high fatality rate (25-30%). However the persons escaping from death will not fully recover to normal health, as the 50% of person who recovered from the disease will suffer from various forms of the neurological damage such as learning difficulties, behavioral problems, etc.

JEV circulates mainly in South-East Asia and is observed as two different epidemiological patterns according to the climatic conditions. In the temperate zones, periodic outbreaks are observed while in the tropical and sub-tropical regions sporadic outbreaks are seen throughout the year. With the spread of JEV to the region as far as northern Australia, JE is feared to become a global threat (Hanna *et al,* 1995). In Southeast Asia, the most important flaviviruses are JEV and dengue viruses (Mackenzie *et al*, 2004). In northern Australia, Kunjin virus is found to co-circulate with JEV (Hall *et al*, 2001), whereas in India evidence of WNV infection along with Japanese encephalitis in nonendemic areas and endemic areas were reported (Thakare *et al,* 2002).

Japanese Encephalitis Virus (JEV) is an enveloped virus belonging to the family Flaviviridae and genus Flavivirus. JEV is structurally spherical, having cubical symmetry and with the diameter ranging 40-50 nm. The viral genome consists of a single stranded, positive sense RNA approximately 11 Kb in length. The RNA consists of 5' cap, but lacks 3' poly A tail. The whole genome consists of a single open reading frame which translates into a polyprotein of ~3400 amino acids. These polyprotein is cleaved by the host and viral proteases to produce three structural (envelope (E), pre-membrane (prM) and core (C) proteins) and seven non-structural proteins (NS1, NS2a, NS2b, NS3, NS4a, NS4b and NS5). Host signal peptidase is responsible for cleavages between C/prM, prM/E, E/NS1, and 2K-NS4B. A virus-encoded serine protease, is responsible for cleavages between NS2A/NS2B, NS2B/NS3, NS3/NS4A, NS4A/2K, and NS4B/NS5 junctions (Lindenbach *et al*, 2007)

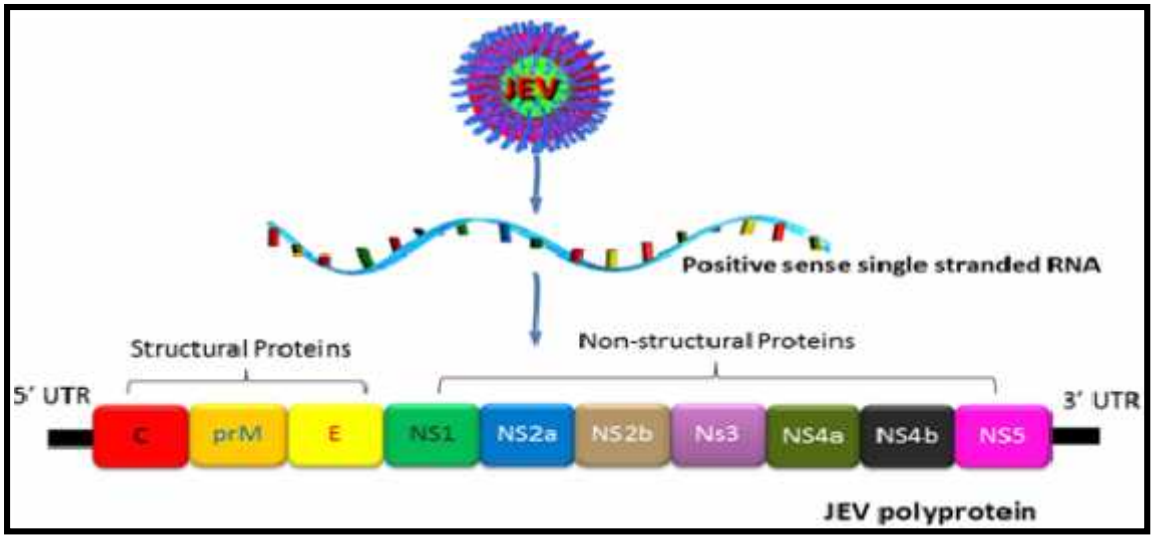

Figure 1: Japanese encephalitis virus structure and genome showing structural and non-structural proteins. C, prM and E refer to Core, Pre membrane and Envelope Proteins respectively and NS1 to NS5 refer to nonstructural proteins 1 to 5 respectively.

The virus consists of the genomic RNA complexed with the C protein, forming a nucleocapsid. The nucelocapsid is surrounded by the lipid bilayer, which embeds E protein and prM/M proteins (derived from the host cell). The prM proteins present in

the immature particles is cleaved into M proteins to form mature viral particles (Saxena *et al,* 2013).

NS3 protein serves as the major immunogen for T cell responses against JEV whereas E protein of virus defines itself as the major target of antibody response. NS3 is a multifunctional protein consisting of 619 amino acid residues. NS3 can be divided into N-terminal and C-terminal regions where the former is a serine protease and is responsible for the cleavage of viral poly protein at various junctions (NS2A-NS2B, NS2B- NS3, NS3-NS4A and NS4B-NS5) in association with NS2B (Murthy *et al*, 1999; Yamashita *et al*, 2008). DEXH helix motif and RNA helicase activity were demonstrated in the C - terminal region in JEV (Utama *et al*, 2000). The structural proteins, mainly regard to the antigenicity of the virus. On the other hand, the non-structural proteins are mainly involved with viral replication and processing (Tiwari et al, 2012). E protein is responsible for attachment of the virus to host membrane, pathogenicity and the protein also possesses a hydrophobic loop that accounts for fusion of viral and host membranes (Luca et al., 2012; Saxena, 2008). The error-prone nature of the polymerase largely contributes to the high mutation rates and the variability in strains observed in JEV (Saxena, 2008). Non-structural proteins are mainly responsible for the viral replication. NS1 protein has the molecular mass of approximately 46 kDa, which is expressed on the surface of and secreted extracellularly from infected cells (Lin *et al,* 1998). The NS2 is a membrane-spanning protein which consists of a C-terminal cysteine protease domain, and is responsible to cleave the NS2/3 junction. NS4A is the smallest NS protein, with 54 amino acid residues and having a molecular weight of 8kDA. NS4A serves as a cofactor of the serine protease by completing the fold of the protease domain and also facilitates recognition of RNA substrates by the full– length NS3 protease/helicase (Lindenbach *et al*, 2007). NS4B, having molecular weight of approximately 27 kDa, is an integral membrane protein and plays a critical role in organizing the membrane-bound replication complex. NS5 is a phosphoprotein with an important yet unclear role in RNA replication.

Interleukin-10 (IL-10) is an anti-inflammatory cytokine with a crucial role in preventing inflammatory and autoimmune pathologies. Although the absence of IL-10 confers better clearance of some pathogens, the absence of IL-10 can be accompanied by an immunopathology that is detrimental to the host but does not necessarily affect the pathogen load (Saraiva and Anne, 2010). IL-10 was originally recognizes as Th2 cytokine with an ability of indirectly repressing Th1 response. It is now evident that IL-10 is produced by various cell types, which include Dendritic Cells (DCs), B cells, macrophages, CD4 T cells, CD8 T cells, NK cells as well as innate and adaptive regulatory T cells (Wilson and Brooks, 2011). The dominant IL-10 producing cell type varies with different virus infections likely reflecting inherent differences in the pathogen-specific response as well as tissue-specific immune regulation (Wilson and Brooks, 2011).

MicroRNAs (miRNAs) are noncoding small RNAs that bind to the 3' untranslated region (UTR) of target mRNA and post-transcriptionally regulate gene expression via degradation of specific mRNAs and/or repression of their translation. They are single stranded molecules with approximately 20-22 nucleotides in length. They regulate the gene in a sequence specific manner. The miRNAs act as guide molecules, by base-pairing with the target mRNAs leading to translational repression and/or mRNA cleavage. Trancription of miRNA is done by RNA polymerase II to generate large precursor molecules called the primary precursor miRNA (pri-miRNA) (Lee *et al,* 2004). The primiRNA is processed in the nucleus by the ribonuclease Drosha/DGCR8 to produce the microRNA precursor (pre-miRNA) (Lee *et al,* 2003). Pre-miRNA is transported to the cytoplasm via Exportin 5 (Yi *et al,* 2003; Lund *et al*, 2004) and then processed by Dicer to generate an active, mature miRNA. There is a considerable difference between miRNA and traditional RNAs (e.g. mRNA, rRNA or snoRNA), since the mature miRNA is approximately 21 nts in length and the miRNA precursor exists as a stable hairpin (Schmittgen *et al,* 2008). It has been shown that miR-29b regulates JEV-induced expression of inducible nitric oxide synthase (iNOS) and COX-2 in BV-2 cells (Thounaojam *et al*, 2014). Cell culture based study on mouse cell line demonstrated that miR-29b and miR-98 holds a crucial position on regulation of Interleukin-10 production (Liu *et al*, 2011; Xie *et al*, 2014). In context of miR-106b, there is no specific data regarding the regulatory role of it on the regulation of IL-10 expression. However, miR-106a (which differs from miR-106b by single nucleotide base) has been shown to regulate the IL-10 expression in human cell (Sharma *et al*, 2009).

1.2 HYPOTHESIS

Since the first discovery of micro RNAs from the *Caenorhabditis elegans,* several miRs have been found in other organism which regulates the expression of various genes. Viruses rely on host cell functions for many aspects of their life cycle. As the miR pathway is an important part of the host's regulatory system, there is much potential for interplay between miRNA and viruses. This can modulate the pathological outcome during infection. In such manner host cell also have a regulatory mechanism to overcome adverse effects of the immune activation and inflammatory reactions. Interleukin-10 is one of the cytokine which plays a significant role in the immuno modulatory activity by inhibiting the synthesis of the inflammatory cytokines. Japanese encephalitis is the flaviviral disease cause by JEV and is characterized by the neuroinflammation resulting in death. Interleukin-10 has been shown to reduce during JEV infection when studied in mouse models. However, there is no data regarding the exact mechanism of regulation of IL-10 production during JEV infection. Thus we can hypothesize that there might be a potential role of three different micro RNAs (miR-27a, miR-98 and miR-106b) in the post-transcriptional regulation of IL-10 production during JEV infection.

1.3 OBJECTIVES

1.3.1 General Objectives

1. To study sequence diversity of NS3 gene in the novel strain gp05 of Japanese encephalitis virus
2. To study the regulatory mechanism of Interleukin-10 production during Japanese encephalitis infection via micro RNAs.

1.3.2 Specific Objectives

1. To sequence NS3 gene of JEV and perform phylogenetic analysis.
2. To perform homology modeling of the NS3 protein from the obtained sequence and predict ligand binding sites on the protein.
3. To infect P388D1 mouse cell line with Japanese Encephalitis Virus and isolate RNA from the infected cells at different time points.
4. To perform *insilico* analysis of the miRNAs having potential to bind with IL-10 mRNA.
5. To synthesize cDNA from the isolated RNA and perform Real Time PCR of Interleukin-10 and selected miRs (miR27a, miR98 and miR106b).
6. To analyze the regulatory role of miRs (miR27a, miR98 and miR106b) in regulation of IL-10 expression from the RT-PCR results.

1.4 RATIONALE

Japanese encephalitis has been typically described as the inflammation of the brain due to JEV infection. The pathological outcome thus is the combined effect of the JEV infection of the neurons and the damage by the activated microglial cells. In such behavior of the infection viral NS3 protein and host IL-10 protein has been found to play a major role in determining of the pathological outcome. Viral NS3 is considered as the major immunogen and serving multiple roles during the viral replication in the host cell. On the other hand host IL-10 protein regulates the host innate immune response. In such scenario understanding the regulatory mechanism of the IL-10 during infection provides a fruitful insight about the host defense mechanism and might also be helpful for discovery of the novel therapeutic approaches to treat the infection. Nonetheless, characterization of the NS3 protein can also be helpful for the finding the molecules which interact with the protein. This can give us the idea regarding science behind the importance of the NS3 protein for the pathological outcome during JEV infection. Characterization of the NS3 protein can also open new avenue for the modulation of the host immune response and effective clearance of the virus from the host system.

CHAPTER 2

LITERATURE REVIEW

2.1 Epidemiology

2.1.1 Global Outlook

JEV is epidemic to tropical and temperate regions of eastern and southern Asia. Its geographic range extends from eastern Asia (China, Japan, Korea, maritime Siberia, Taiwan, the Philippines, and Vietnam), to Southeast Asia and northern Australia (Cambodia, Indonesia, Laos, Malaysia, Papua New Guinea, Thailand, and the Torres Strait islands of northern Australia), and to southern Asia (Bangladesh, Bhutan, India, Myanmar, Nepal, and Sri Lanka) (Figure 2). Large epidemics of JE occur during summer months in the northern areas, roughly during May to October and in case of southern hemisphere encephalitis tend to occur throughout the year with a peak during rainy season.

The climatic conditions in addition to a variety of factors such as entomological factors, human activity as well as viral and cellular factors play a major role in the epidemiology of JE (Solomon, 2004). With the spread of the virus to the Torres Strait Islands of Australia and in Papua New Guinea, JE has increased its geographical distribution (Mackenzie *et al*, 2004). JE is usually a disease of rural areas, especially correlated with rice agriculture areas. Occupations like farming and animal husbandry are predominant in developing countries in Asia making JE infections more prone in these regions. Breeding mosquitoes in stagnant paddy fields are perfect vectors for the spread of virus. Moreover, man's associations with domestic animals such as pigs that maintain such high viral titres contribute to the epidemiology of JE. Migratory birds probably play an important role in the dissemination of the virus across countries.

The first reported cases of JE were from Japan in 1871. Clinical isolation of original prototype is given to Nakayama strain which was obtained from brain of a patient suffering from encephalitis in 1935 from Japan (Tiwari *et al*, 2012; Ghosh and Basu, 2009). Phylogenetic analysis on the basis of envelope (E) proteins has divided JEV strains on five genotypes (I-V) (Li *et al*, 2011; Solomon *et al*, 2003). Genotypes I and III are specific for Asia, including Japan, China, Korea, India, Philippines and Vietnam. Genotype II encompasses JEV isolates from southern Thailand, Indonesia, Malaysia, and northern Australia. Retreatment of genotype IV has been done only from Indonesia (Solomon *et al*, 2003). Isolation of Muar strain in Malaya in 1952 is regarded as genotype V [Li *et al*, 2011; Solomon *et al*, 2003; Mohammed *et al*, 2011). Newly isolated genotype V of JEV differ from Muar strain by 5 amino acid, which might be one possible reason for re-emergence and spread of genotype V JEV strain after nearly 57 years. And also the genotype differs significantly from other genotypes (I-IV) (Li *et al*, 2014). Although there

is evolution of new virus genotypes there are still cases of epidemics caused by the previous strains (Cao *et al*, 2011; Xu *et al*, 2013).

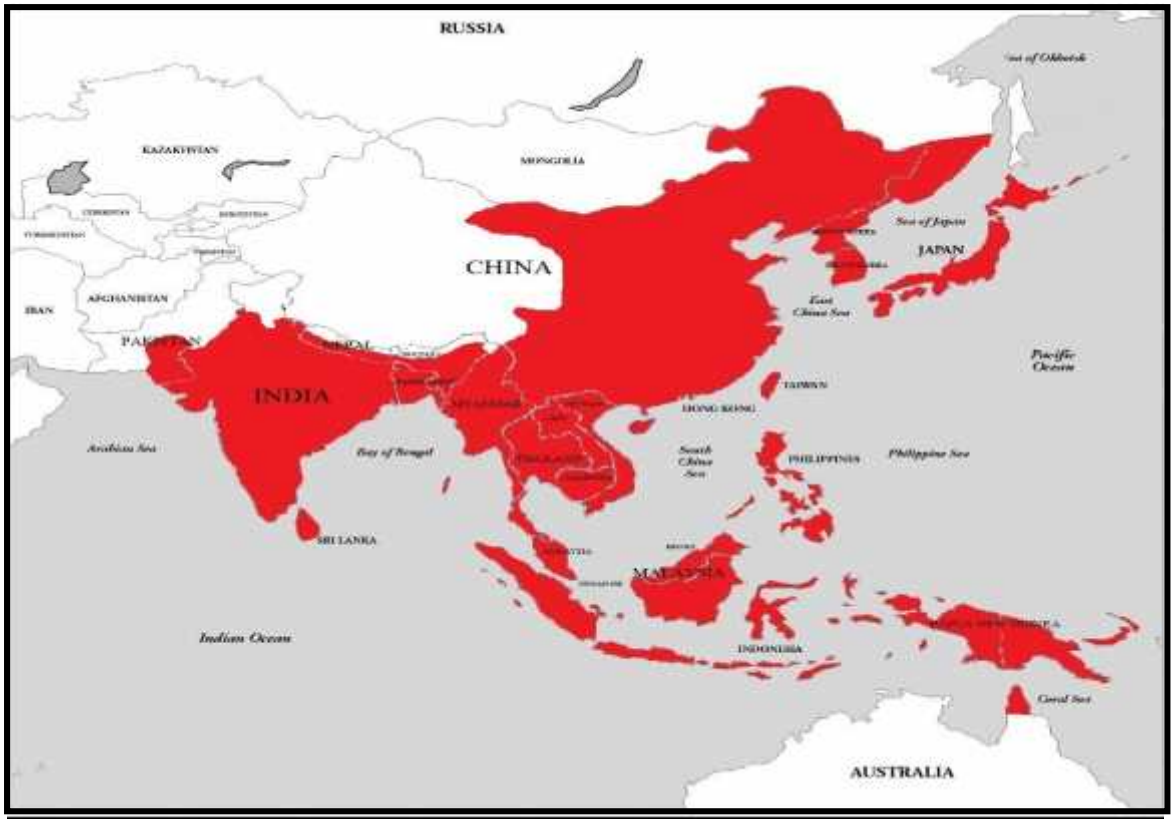

Figure 2: Geographical distribution of Japanese encephalitis virus

2.1.2 Epidemiology in Nepal

Japanese Encephalitis was first confirmed in western part of Nepal in 1978 however, endemic in Morang of the Eastern Region and Rupandehi district of the Western Development Region (Bista MB and Shrestha JM, 2005; Joshi *et al*, 2004). Since then, JE infection has been reported in animal reservoirs and in humans throughout the Terai region. JE is seasonally endemic in the Terai region of Nepal. JE outbreak outside Terai region has also been recorded, including Kathmandu valley, and a 2006 study reported JE endemicity in Kathmandu Valley (Zimmerman *et al*, 1997; Partridge *et al* 2007).

Geographically, Nepal is divided into three ecological regions termed as Mountainous, Hilly and Terai. Terai region is renowned for heavy rainfall ranging between 180- 225 cm, and also the humidity of Terai ranges between 80 to 90 percent during monsoon. Climatic condition is favorable for the breeding of the *Culex* mosquitoes, the proven vectors for JE.

Japanese Encephalitis is not a year around disease in Nepal like in other countries of South Asia. The transmission season in Nepal starts from June to October with a peak in August (Pant SD, 2009). The outbreaks occur after monsoon and coincide with Acute Encephalitis Syndrome outbreaks. Laboratory cases of AES and JE shows gradual decline

in the AES cases since 2010/11, however the number of JE patients remains same (Figure 5). Limited number of Japanese Encephalitis cases is then reported from November to March. This seasonal phenomenon is demonstrated in Figure 3.

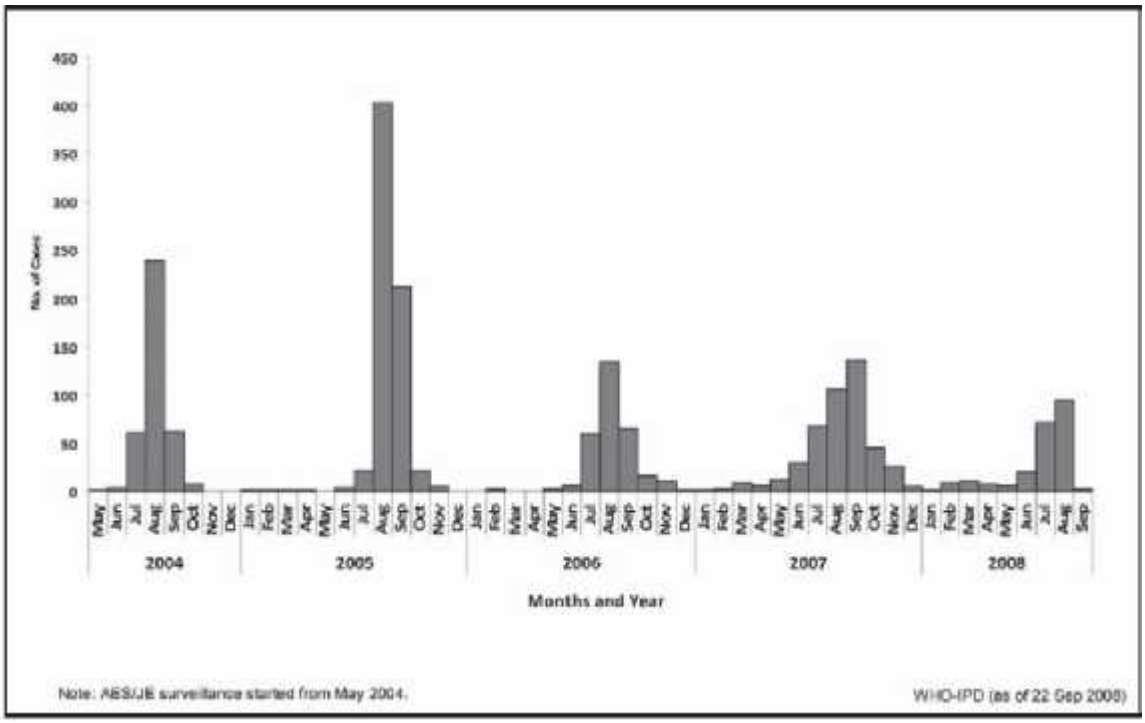

Figure 3: Seasonal trend of Japanese Encephalitis in Nepal **(Pant .S, JE Report, 2009)**

Additionally, since 1997 there have been reports of JEV transmission expanding from the Terai region to the hill region (altitude of 1,300 m) of Nepal with a significant number of cases appearing in the Kathmandu Valley (Bhattachan *et al*, 2009; Partridge *et al*, 2007). Since then, Japanese Encephalitis have been confirmed in 54 districts of Nepal (Figure 4).

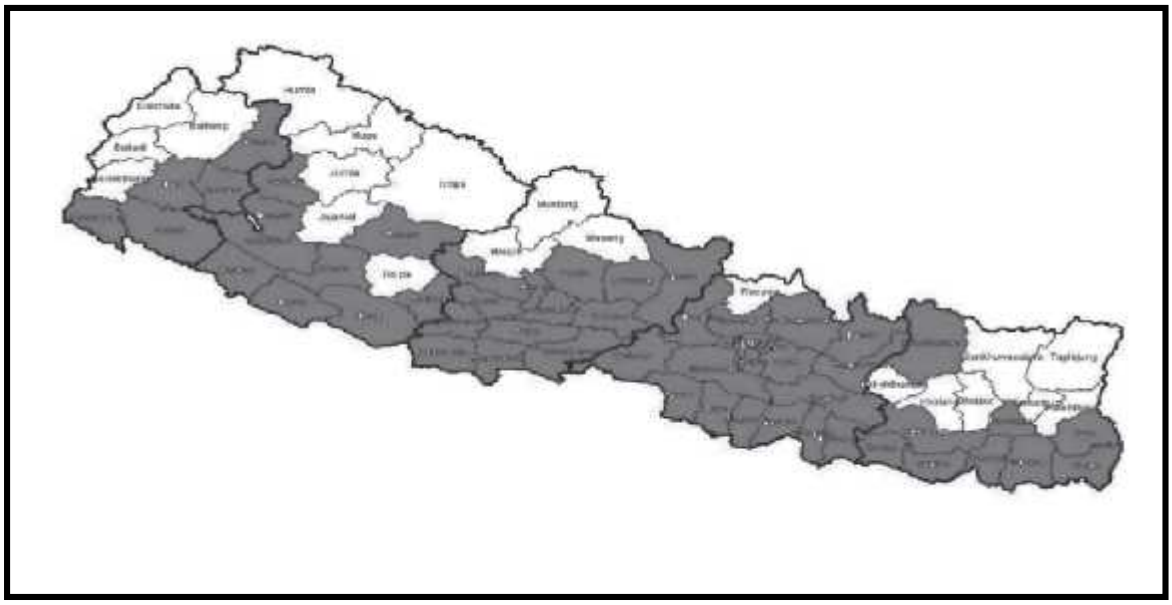

Figure 4: JE infected districts of Nepal **(Pant .S, JE Report, 2009)**

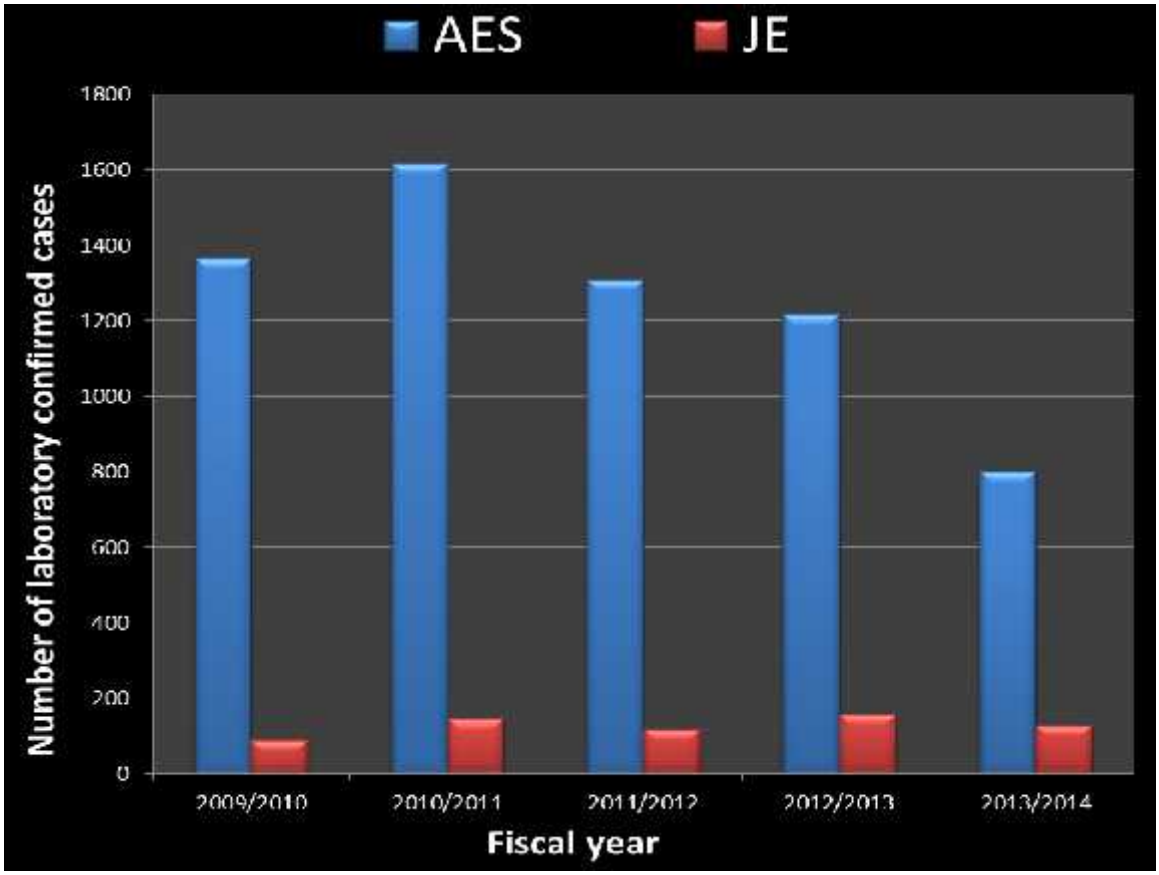

Figure 5: Laboratory confirmed cases of Acute Encephalitis like Syndrome (AES) and Japanese encephalitis (JE) in the samples collected from the various districts of Nepal. **(Source: Annual Report, Department of Health Science)**

2.2 Viral replication cycle

The exact mechanism of JEV entry is unknown. Various studies have shown that the entry mechanism of JEV differs according to the cell types. JEV is found to utilize caveola mediated endocytosis in case of rat neuroblastoma cells, clathrin and cholesterol dependent endocytosis in case of kidney epithelial PK15 cell, whereas, in neuronal cells JEV utilizes clathrin-independent mechanism (Zhu *et al*, 2012; Yang *et al*, 2013; Kalia *et al*, 2012). The decrease in pH of the endosome is a required for irreversible trimerization of the flaviviral E protein that leads to the fusion of the cellular and viral membranes (Allison *et al*, 1995). Once the fusion has occurred, the nucleocapsid is released into the cytoplasm. The capsid protein then dissociates from the RNA genome and replication of the RNA genome is initiated (Lindenbach and Rice, 2003; Brinton, 2002). JE virus undergoes trans-type maturation in that viral RNA replication and protein synthesis occur on smooth and rough endoplasmic reticulum respectively, with resultant release of the products into the cisternae (Hase *et al*, 1990). The immature viral particles that are initially formed in the lumen of the endoplasmic reticulum (ER) are non-infectious. The presence of the Pre-membrane (prM) protein bound to the Envelope (E) protein

masks the fusion loop of the E protein and prevents the virus from cell attachment and fusion rendering them non-infectious (Li *et al*, 2008; Rodenhuis-Zybert *et al*, 2011). When the virus reaches the trans-Golgi network, the prM is cleaved from the prM-E heterodimer which leads to the formation of mature, infectious particles. Finally, the mature viral particles are released from the host cells by exocytosis. The viral replication cycle is summarized in figure 6.

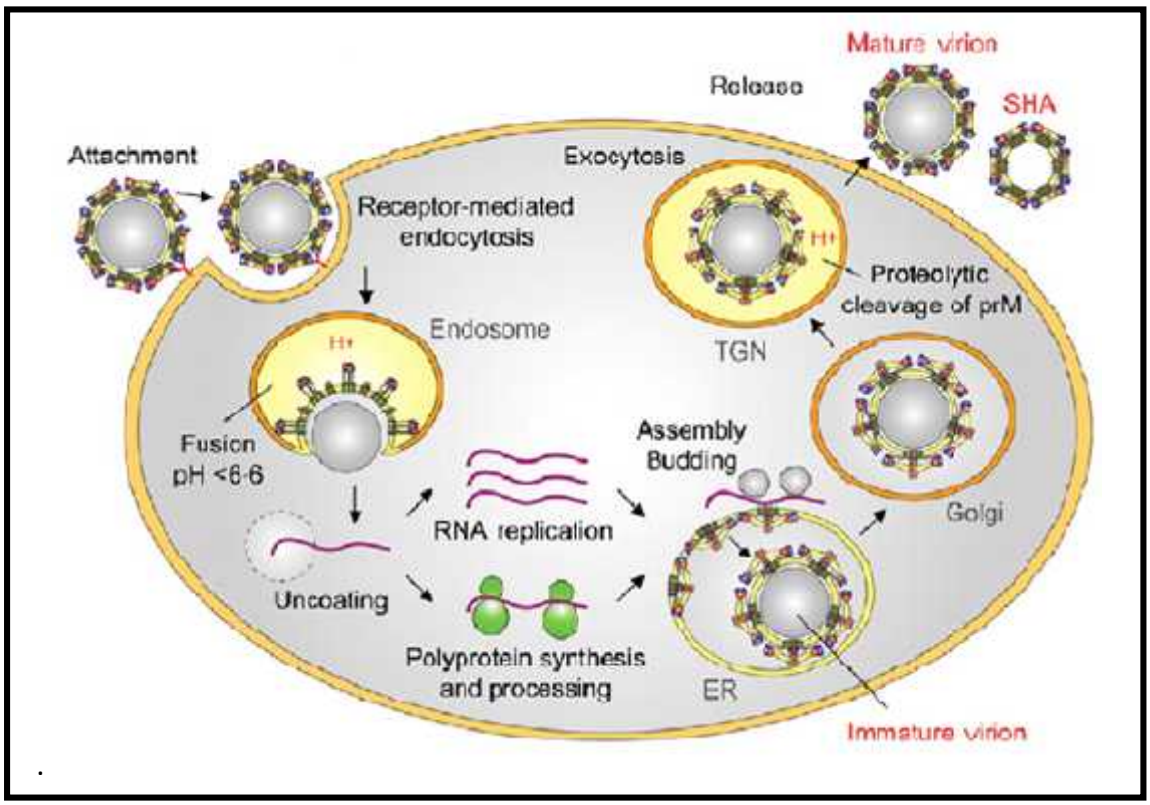

Figure 6: Replication Cycle of JEV. ER-Endoplasmic Reticulum, TGN-Trans Golgi Network, SHA-sedimentation hemagglutinin particles, prM- Pre-membrane.

2.3 Vector and transmission

JE virus maintains zoonotic cycles encompassing mosquitoes, birds, pigs and several vertebrates including human. Mosquitoes, typically *Culex tritaeniorhyncus* and *Culex gelidus* serve as a vector for the transmission of the disease from the pigs and birds to the human. Humans hold a position of the accidental, dead end hosts owing to the low transient viremia and clearance of virus once the illness begins (Ghosh and Basu, 2009). Pigs and birds (pond heron, cattle egret and so on) on the other hand serve as an amplifying hosts increasing number of virus (Khan *et al*, 2014; Duong *et al*, 2011). Rice fields, water pools filled with stagnant water and standing puddles, irrigation canals, open sewers, fish ponds etc. are breeding places for these vectors. Birds help to perpetuate and maintain the virus in the environment and also increase the geographic distribution of the same. Pigs, the vital link of the cycle, develop viremia approximately four days after an infectious mosquito bite (Weaver and Barrett, 2004). Transmission of JE virus varies accordance to environmental conditions like human density, elevation

and temperatures (Wang *et al*, 2014), and also as mosquitos are cold blooded organisms they are active only during summer and autumn.

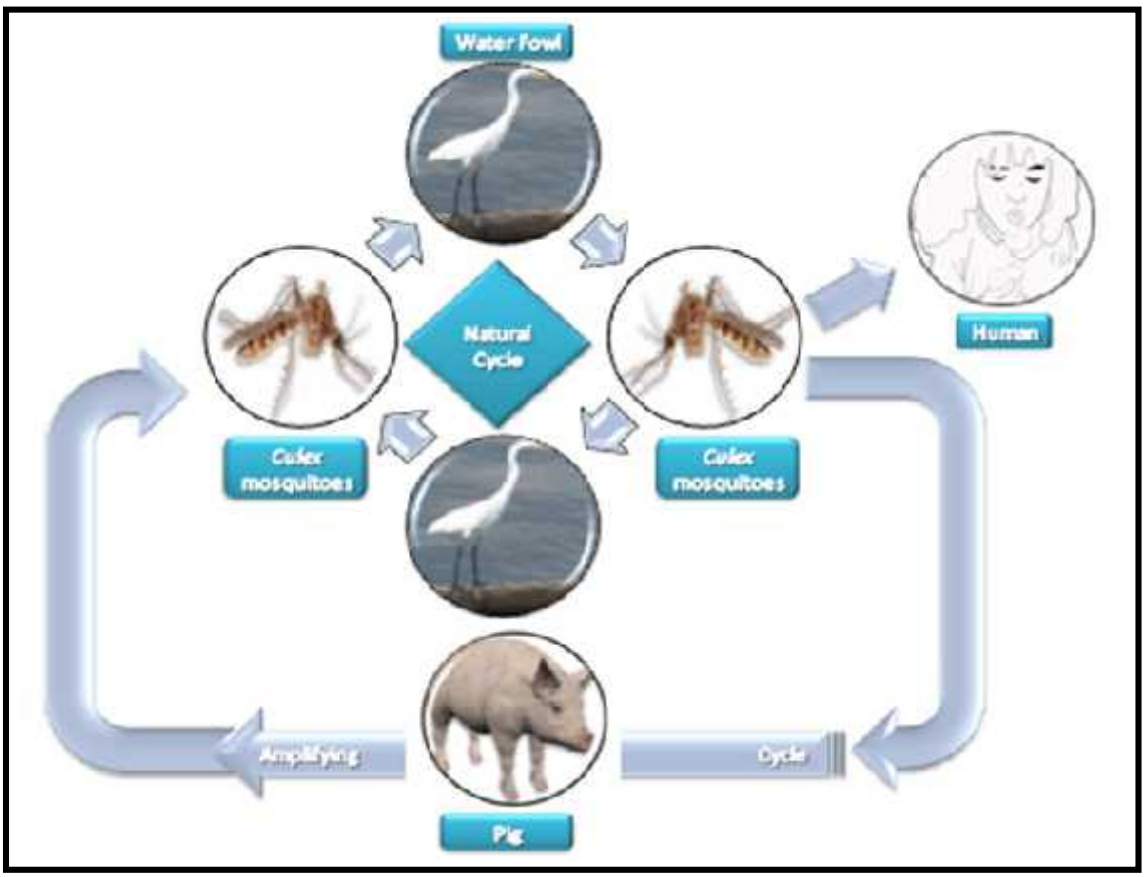

Figure 7: Transmission cycle of JEV

JEV infection transmits from mother to fetus through vertical mode of transmission. This may be due to persistent maternal infection or due to pregnancy induced reactivation of virus. An animal model of congenital infection with JEV has been described and trans-placental transmission of the virus during consecutive pregnancies in mice has been shown experimentally (Mathur *et al.,* 1981).

2.4 Clinical presentation

A typical incubation period of 6-16 days is observed in humans before the first symptom of JE is observed. Most JE patients die within 24 to 48 hours of admission (Saxena, 2008). General clinical manifestation of JE includes fever, headache, vomiting, diarrhoea, seizures, signs of meningeal irritation, and altered consciousness (Kakoti *et al*, 2013). Fever is the most common symptom in both adults and children whereas, higher percentage of pediatric patients has been found to have neck rigidity, convulsions, abnormal behavior, seizures and elevated aspartate transaminase (Borah *et al*, 2011). The course of the disease can be divided into three stages: a prodromal stage, an encephalitic stage, and a late stage characterized by recovery or persistence of signs of CNS injury. The prodromal stage lasts for 2-3 days accompanied by non-specific fever and gastrointestinal-like symptoms. This is followed by the acute encephalitic stage of 3-

4 days involving reduced consciousness levels followed by convulsions. The last stage lasts for 4-7 weeks and is called late convalescent or sequelae stage wherein acute inflammation takes place together with subsidence of fever and recovery with neurological impairment. In severe cases, fever reoccurs and leads to severe cerebral complications which are often fatal (Saxena, 2008). Other features include multiple persistent seizures, motor seizures, symptoms of Parkinson syndrome and polio-like acute flaccid paralysis. These are accompanied by neurological features such as periodic lateralized epileptiform discharge and inflammation in basal ganglia can be diagnosed by encephalography and neuroimaging techniques like CT scan and MRI (Solomon, 2004).

2.5 Diagnosis

Most laboratory diagnostic tests for JE are serological based and detect the presence of antibodies or viral proteins in serum or cerebro-spinal fluid (CSF) samples. However, due to low transient viremia, isolation and detection of virus and anti-viral antibodies are achieved with greater success in CSF samples than from serum (Solomon *et al*, 2000). Detectable levels of IgM antibody can be found in CSF and serum within fourth day of infection, whereas while IgA and IgG antibody levels are not detected until the sixth day (Han *et al*, 1988). Laboratory diagnosis of JE is done by JEV specific IgM capture ELISA on CSF or serum. Diagnosis by detection of IgM in CSF through IgM capture ELISA is a reliable technique throughout the disease period while in case of serum definitive results are obtained only on day 9 or later (Chanama *et al*, 2005). Anti-JEV antibodies, targeting mainly pre-membrane (prM) and envelope (E) proteins of virus, can be detected with the use of classical techniques such as haemagglutination inhibition (HAI) assays, reverse passive haemagglutination assay (RPHA), complement fixation tests (CFT) and so on. These techniques, however, lacked the ability to detect JEV at early stages. Detection of IgM antibodies by indirect immunofluorescence could be used over HI for early diagnosis (Mathur *et al*, 1990) but is not widely used due its practical limitations. Plaque reduction neutralization tests (PRNT), used as a gold standard technique to identify JE infections, is very efficient and can differentiate between closely related flaviviruses but is technically challenging and requires the use of live viruses. Recent research, however, demonstrated that even NS1 protein can also be used for diagnosis with its potential to be used in the surveillance program to distinguish natural infection from vaccination and to monitor vaccine effectiveness (Chao *et al*, 2015; Kumar *et al*, 2011). The use of bead based agglutination assays using antibody coated hydroxy-appatite or latex beads has been recently introduced for JE diagnosis and can be developed into rapid expedient on-field kits to detect JE. The novel use of gold coated magnetic beads in an electrochemical immunoassay appears to be a potential tool for clinical diagnosis in the near future (Li *et al*, 2011).

Introduction of molecular diagnosis such as use of nucleic acid sequence-based amplification (NASBA) and quantitative reverse transcription polymerase chain reaction (qRT-PCR) ensued detection of JEV with remarkable sensitivity and specificity. RT-PCR

can be used as a supplement for diagnosis from CSF at early stage of infection (Swami *et al*, 2008), as the technique has high specificity, but holds a drawback of having a low sensitivity since virus is cleared from peripheral blood/CSF eventually. Leap in the diagnosis of JEV infection was development of reverse transcription loop-mediated isothermal amplification (RT-LAMP). The method proved to be efficient and rapid in nature as compared with previously used techniques (Deng *et al*, 2014). Recently, RT-LAMP coupled with Lateral Flow Dipstick (LFD) showed higher efficiency than individual techniques. The technique demanded less amount of RNA, as less as 50pg, and providing no false positive result. Considering these facts RT-LAMP coupled with LFD recognizes itself as a next generation method for more sensitive, rapid and reliable technique for the diagnosis of JEV.

2.6 Pathology and pathogenesis

Pathological condition during JEV infection is combined outcome of both JEV infection of neurons and bystander damage caused by the activated microglial cells (Chen *et al*, 2012; Chen *et al*, 2010). The incubation period of JEV ranges between 6-16 days. After the bite of the infected mosquito the virus replicates in dendritic cells of skin, which is then transported to lymph nodes via lymphatic system. Virus then enters in the circulatory system from the lymphoid tissues via lymphatic and thoracic system. Virus then infects and amplifies in extra neural tissues like connective tissue, skeletal muscle, myocardium, smooth muscle, lymph reticular tissues, and endocrine and exocrine glands. If infection is limited to the extraneural tissues then the signs will be mild or apparent, whereas entry of virus into CNS results in fatal encephalitis case. Thus entry of virus in CNS is the major concern during JEV infection. Invasion of the virus into CNS is supposed to be via Blood Brain Barrier (BBB), which is structurally and functionally compromised during infection (Chen *et al*, 2014; Sharma *et al*, 2014) or by 'Trojan horse' mechanism along with infiltrating infected macrophages (Thongtan *et al*, 2012). On the other hand replication in the endothelial cells might also help the virus to dessiminate into CNS (Mishra *et al*, 2009).

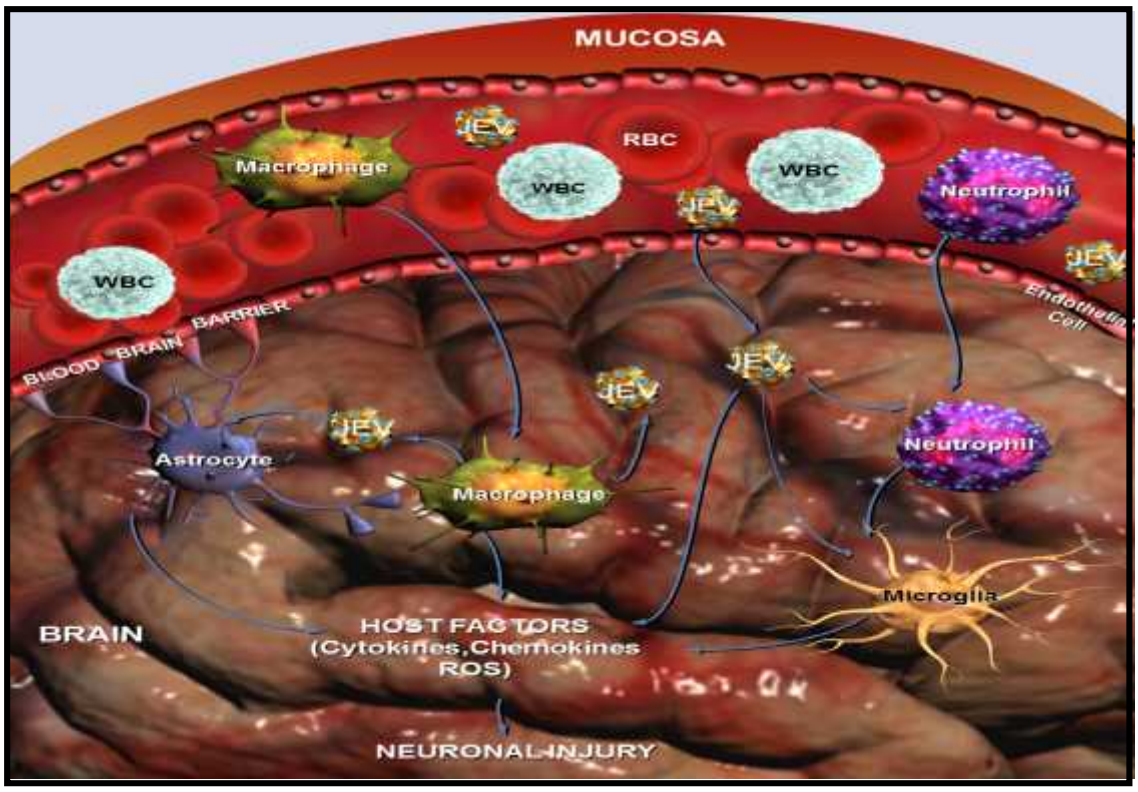

Figure 8: Mechanism of neuroinvasion by JEV

Immune evasion strategies of virus hold a major position to define the pathogenic ability. JEV is found to modulate dendritic cells (DCs) and Macrophages (Mϕ) via various mechanisms, including of myd88 molecule dependent and independent pathway (Aleyas *et al*, 2009), increasing expression of programmed cell death 1 ligand 1 (PD1-L1) on dendritic cells (Gupta *et al*, 2014), blocking of Interferon-Induced Jak-Stat Signaling by viral NS5 protein (Lin *et al*, 2006). Modulation of Mϕ and DCs results in the alteration in other antiviral mechanisms such as ross-presentation of soluble and cell-associated antigens (Aleyas *et al*, 2012), alteration of cytokine production along with proliferation and polarization of T helper cells towards Th1 phenotype (Aleyas *et al*, 2009; Gupta *et al*, 2014), alteration in autophagy machinery (Sharma *et al*, 2014; Jin *et al*, 2013). Activated microglia has been shown to release glutamate ensuing abnormal accumulation of extracellular glutamate (Chen *et al*, 2012), which is highly toxic to neurons due to dysregulated calcium influx through NMDA-type glutamate receptor. Infection results in neuronal cell death with morphological features corresponding to apoptosis with activation of astrocytes, microglial and endothelial cells (Myint *et al*, 2014). Endothelial cells were also found to express MHCII antigen and TNF-α showing its role as inflammatory mediator and potential contributor in immune response, glial activation and blood brain barrier breakdown.

JE predominately affects the thalamus, anterior horn cells of the spinal cord, cerebral cortex, and cerebellum. During the acute stage of illness, congestion, edema, and herniation are found in the brain. Microscopic lesions include meningeal inflammation, perivascular lymphocytic cuffing, neuronal degeneration and neuronophagia, and

microglial proliferation forming glial nodules. These changes usually occur in gray matter and predominantly affect diencephalic, mesencephalic, and brainstem structures. The brain parenchyma is congested with focal petechiae or hemorrhage in the grey matter. Blotchy necrolytic zones are seen when survival is prolonged beyond seven days. The white matter usually appears normal. In some patients, the grey matter of the spinal cord is confluent discolored, resembling that of poliomyelitis.

2.7 Host immune response

Host immune response during JEV infection is modulated by both innate and adaptive immune system. Innate immune system relies in the capabilities of recognition of conserved structures termed as Pathogen Associated Molecular Patterns (PAMPs) by Pattern Recognition Receptors (PRR) (Ye *et al*, 2013; Mogensen, 2009). Viral invasion is rapidly detected through the triggering of pattern recognition receptors like toll like receptors (TLRs) and the retinoic acid-inducible gene 1-like helicases (RIG-I). Recognition of PAMPs by PRR stimulates the production of antiviral molecules such as Type I interferon (i.e. IFN α and β). Type I interferons checks early viral replication by directly inducing apoptosis or hindering proliferation of virally infected cells, as well as stimulating cytotoxic natural killer (NK) cells (Wilson and Brooks, 2011). They are secreted by different cell types, and their secretion induces adjoining cells to express genes with potent antiviral affects, so called interferon stimulated gene (ISGs) via JAK/STAT pathway (Mogensen, 2009). IFN-α also has other important immunoregulatory functions during host innate immune response such as activation of monocytes, enhancement of chemokine expression and Major Histocompatibility Complex class I and II induction. Activation of transcription factors IRF-3, IRF-7 and NFκB, either through TLR pathway or RIG-I pathway also results in production of IFN-α/β (Ye *et al*, 2013; Mogensen, 2009). It has been shown that neurons also express adaptor molecule called as Stimulator of Interferon Gene (STING) on surface of endoplasmic reticulum, and involves in neuronal innate immune response (Nazmi *et al*, 2012). Induction of inducible Nitric Oxide Synthase (iNOS) might be one of the antiviral mechainsm of host defense as correlated with enhanced enzyme activity observed during JEV infection (Saxena *et al*, 2001).

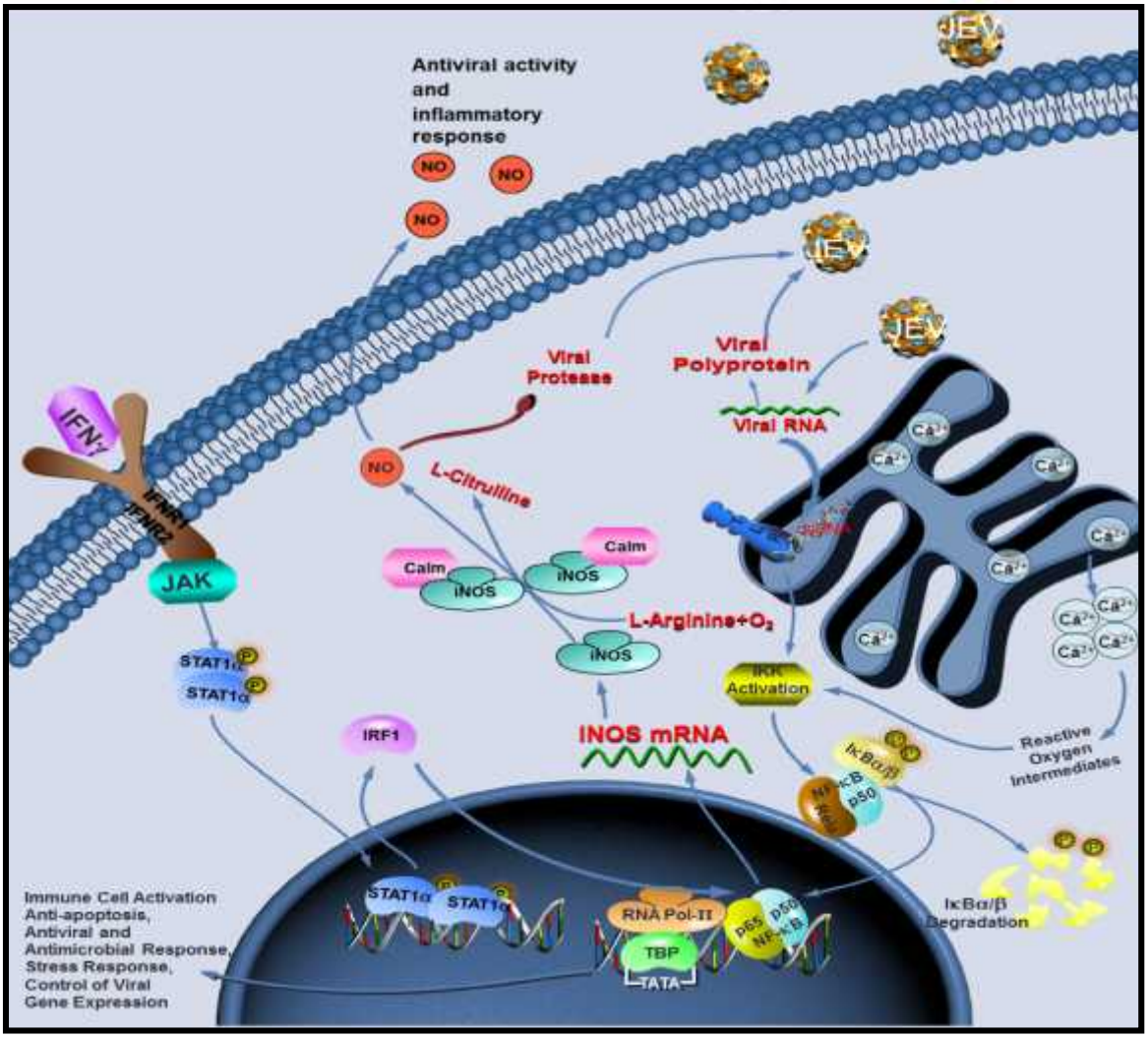

Figure 9: Host innate immune response during JEV infection

Along with innate immune response, adaptive immune response also coordinates for viral clearance. Adaptive immune response is the combined activity of T cell and JEV specific antibodies produced by activated B cell. It has been shown that mice deficient in JEV specific cytotoxic T cell (CD8+ T cell) resulted in increased viral load in CNS and reduced disease severity than wild type mice (Larena *et al*, 2013). Number of activated CD8+ T cell and trafficking of virus-immune CD8+ T cells into CNS are generally accounted during infection (Larena *et al*, 2011). Study on knock-out mice and passive cell transfer showed pivotal role of T cells in protection and recovery from JEV infection (Larena *et al*, 2011; Biswas *et al*, 2009). Adoptive transfer of JEV specific CD8+ T cells in CNS of infected mice resulted in viral clearance but only in presence of CD4+ T cells. Major role of CD4+ T cell in protection against JEV can be demonstrated by the outcome where mice receiving CD4+ T cell depleted immune splenocytes showed lower survival rate than mice receiving CD8+ T cell depleted immune splenocytes. In spite of the protective role of T cells in protection against JEV, recent study showed that excessive infiltration of Treg cells in brain results in bias towards Th1 cytokine profile and also inhibits intra-cerebral cell-mediated immunity (Shirai *et al*, 2015). Infection of B cell

deficient mice with JEV resulted in uniformly high mortality than wild type mice sketching the role of humoral response against JEV infection. Presence of IgM antibody specific for the viral proteins is observed within 5-7 days in patients infected with JEV. However level of IgM antibody will be increased in serum but not in CSF in case of asymptomatic patients. Level of IgM antibody reaches maximum on 9 days after onset of clinical features. On patient bypassing the fatal outcome of encephalitis class switching occurs producing IgG antibody after 30 days. Kinetics of antibody production in sera of mice acutely infected with JEV infection revealed an increase in JEV specific IgM production from day 4 p.i. Passive immunization with anti-JEV antibodies has shown to confer protection in mice (Kimura-Kuroda and Yasui, 1988), defining the necessity of humoral immune response against the virus.

2.8 Interleukin-10

Interleukin-10 (IL-10), also termed as cytokine synthesis inhibitory factor (CSIF), is a potent anti-inflammatory and immunosuppressive cytokine. IL-10 possesses the feature to suppress the production of IFN-γ, IL-2, and other proinflammatory cytokines. It works in parallel during host defense against various pathogens, and checks over exuberant immune responses and prevents reactivity to self to limit host damage (Brooks *et al*, 2006). IL-10 also inhibit ongoing T cell activity to viral infections, decrease stimulatory molecule expression on Antigen presenting cells, alter cytokine production and prevent maturation of T cells (Wilson and Brooks, 2011). In contrast to its negative role, IL-10 can positively stimulate NK cells, in some instances CD8 T cells and induce B cell proliferation and antibody production (Wilson and Brooks, 2011).

Focusing on viral infection IL-10 has been shown to have important role in determining the pathogenic outcome. Expression of IL-10 is critical during the course of major viral diseases in the CNS and promotes survival of neurons and microglial cells in the brain by blocking the effects of proinflammatory cytokines and by promoting expression of cell survival signals. IL-10 was found to be decreased during JEV infection. A study on mouse model of JEV, reported that IL-10 level progressively declines during JEV infection, providing one possible reason for the neuropathological condition (Swarup *et al*, 2007). Same study conducted on N2a cells concerning the role of IL-10 during infection demonstrated that IL-10 inhibits IL-1β and TNF-α mediated microglial Cox-2 and ROS production. Other features included inhibition of the bystander neuronal death following microglial activation and inhibition of direct neuronal death following viral infection (Swarup *et al*, 2007). In contrast, other study described increased secretion of IL-10 by DC cells during infection, whereas secretion of IL-10 by macrophages remains unchanged (Aleyas *et al*, 2009; Cao *et al*, 2011). In case of other flavivirus such as dengue virus and West Nile Virus, IL-10 level has been found to increase, thus guiding enhance pathology (Bai *et al*, 2009).

2.9 NS3 protein

Structural proteins play a major role in the viral attachment and eliciting host immune response, but the role of non-structural proteins and its molecular mechanism of action, infection, replication and pathogenesis during JEV infection are not completely elucidated. NS3 protein being in the center of non-structural region has triphosphatase activity (unwinding the double stranded RNA intermediate during replication), role in intracellular trafficking of various viral components, viral packaging (Liu *et al*, 2002). NS3 protein is also associated with tumor susceptibility gene protein 101 (TSG101) and microtubules (Chiou *et al*, 2003). A study in pigs as an *in vivo* model of JEV showed that the virus possesses the ability to infect pyramidal neurons, small cells, granule cells and Purkinje cells of the cerebellum as early as 12 hours after infection (Deng *et al*, 2011).

In the context of the host immune response NS3 protein has been shown to be the most frequently targeted antigen, and has the capability of eliciting highest level of proliferation of T cell and IFN-γ secretion as compared with E protein, NS1 protein and NS5 protein (kumar *et al*, 2004). The flavivirus NS3 protein has also been shown as a dominant source of antigenic peptides (Lobigs *et al*., 1994). Immunogenic capability of the NS3 protein can also be outlined by the report demonstrating the ability of more than two independent HLA alleles to bind to and present epitopes from NS3 (kumar *et al*, 2004).

2.10 Micro RNAs

Recent studies have shown that micro RNAs (miRs) holds a major platform during JEV infection and modulate cellular pathways to determine the pathological condition. *In vitro* study of mouse microglial cell lines has shown significant up regulation of miRs such as miR-29b and miR155 during JEV infection, addressing its role in microglia activation, modulation of inflammatory response and host innate immune response (Thounaojam *et al*, 2014; Pareek *et al*, 2014). MiR-29b governs microglial activation by targeting tumor necrosis factor alpha induced protein 3 (TNFAIP3) thereby regulating expression of nuclear factor-kappa B (NF-κB). Whereas miR155 has been shown to target Src homology 2-containing inositol phosphatase 1 (SHIP1) and enhance CD45 expression, reduce pro-inflammatory cytokines and Complement Factor H (CFH) expression by targeting several key genes, and suppress JEV replication in microglial cells.

Considering the ability of miRs to regulate diverse gene expression, IL-10 also serves as one of the targets of miRs post transcriptional regulation. As described before there is a dynamic difference in the expression of IL-10 during various flavivirus infection and surplus to it, expression also differs according to the cell types. Several miRs have already been shown to have regulatory activity in IL-10 expression during various pathological conditions. However the role of miRs in the regulation of IL-10 during

flaviviral infection particularly JEV remains uncovered. Study in human cell cultures showed that hsa-miR-106a regulates the expression of IL-10, thus modulating the immune function (Sharma *et al*, 2009). Whereas in context of has-miR-106b, which differs by only one nucleotide base has minimal effect on the IL-10 expression (Sharma *et al*, 2009). This reflects the sequence specific functionality of miRs. Similar studies on mouse cell cultures demonstrated that IL-10 is regulated by mmu-miR-27a and mmu-miR-98, thus playing a crucial role in immune modulatory activities (Liu *et al*, 2011; Xie *et al*, 2014).

CHAPTER 3

MATERIALS AND METHODS

3.1 Cell culture and maintenance of cells for the study

Cell culture studies were performed to validate the stated hypothesis. P388D1 and BHK-21 cell type were used to perform the study. Cells were cultured and infected with JEV gp05, isolated from JEV infected patients during 2005 epidemic, and further molecular analysis was performed. Detail of the study is described in the following sections.

3.1.1 Cell type used during the study: P388D1 and BHK-21

P388D1, a mouse macrophage like cells were cultured in Rosewell Park Memorial Institute media (RPMI-1640, Gibco, Life technologies, Cat. No. 22400-089) supplemented with 10% serum. Cells were maintained by changing media three times a week and sub culturing repeatedly when they were 90-95% confluent. BHK-21 cells were cultured in Dulbeccos Modified Eagles Medium (DMEM, Gibco, Life technologies, Cat. No. 12430) with 10% serum and maintained by sub culturing similarly as P388D1 cells.

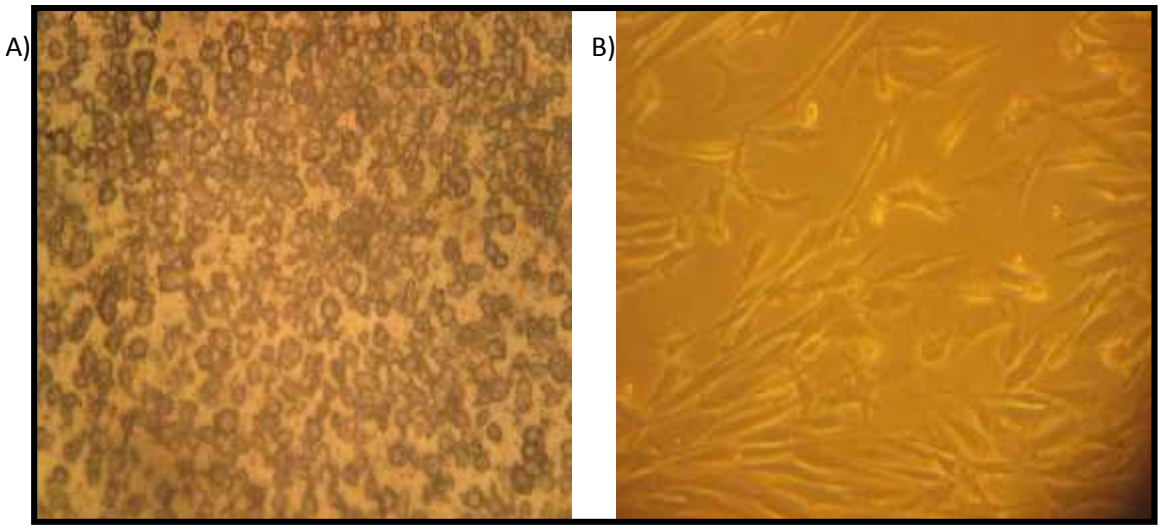

Figure 10: Morphology of cultured cells as observed under bright field microscope under 40X objective. A) Cultured P388D1 cells, B) Cultured BHK-21 cells

3.2 Determination of viral titre by plaque assay

3.2.1 Preparation of a monolayer of cells

BHK-21 cells cryopreserved on liquid nitrogen were revived and seeded into T-25 flasks and cultured on DMEM medium with 10% serum and 1% Anti-Anti Antibiotic. After the cells were 90-95% confluence, they were sub cultured into T-75 flasks. Sub culturing was done by enzymatic method using 1mg/ml trypsin and number of viable cells was counted with the help of hemocytometer using trypan blue stain. Cells were then seeded in 6 well plate (Nunc) each containing around $0.3X10^6$ viable cells per well.

3.2.2 Preparation of viral dilutions

A series of 10-fold dilutions (10^{-1} to 10^{-10}) of virus were prepared from viral stock in chilled incomplete DMEM medium. These dilutions were stored at -30°C until further use.

3.2.3 Inoculation of virus

When the cells were 40-50% confluent, culture medium was removed and the cells were washed twice with 1X PBS. Well 1 was selected as control while wells 2, 3, 4, 5 and 6 were selected as tests and inoculated with 50µL of viral dilutions: 10^{-1}, 10^{-3}, 10^{-5}, 10^{-7}, 10^{-9} respectively. In control well 100 µl of the plain medium was added. This was then incubated in the CO_2 incubator at 37°C for 2 hours with intermittent rocking every 15 minutes for uniform viral adsorption. After 2 hours, the viral adsorption is stopped by removing the culture media and washing twice with 1X PBS.

3.2.4 Preparation of agarose overlay

After infection 2% low melting point agarose (UltraPure LMP Agarose, Invitrogen, Cat. No. 16520-050) was prepared by dissolving 600mg of agarose in 30ml of incomplete DMEM. Agarose solution was boiled for approximately 2 minutes until the agarose dissolved completely. Low melting agarose solution was allowed to cool in the biosafety cabin and serum at 5% concentration was added (1 µl) when the temperature reached 60-65°C. When the temperature of agar reached 37-40°C, it was added evenly in all the wells and left 10-15 minutes for solidification. Once solidified, the plate was incubated in the CO_2 incubator (5% CO_2) at 37°C.

3.2.5 Fixation and staining of cells

Plaques were observed on fourth day of viral inoculation. 2ml of 4% formaldehyde solution prepared in 1X PBS was added on the top of agarose overlay and incubated at 37°C for overnight. After the cells are fixed, residual agarose was removed by gentle pipetting up and down. Cells were then washed twice with 1X PBS. Fixed cells were stained with 0.2% crystal violet stain for 1 minute and excess of stain were removed by washing with 1X PBS. Then the clear zones were identified as plaques under the microscope.

3.2.6 Enumeration of plaques and determination of viral titre

Plaques were visualized under the microscope and the numbers of plaques were counted. Viral titre was determined as plaque forming units (pfu) per mL at each dilution with the help of the following formula:

$$\text{Viral titer (pfu/mL)} = \frac{N \times 10^{d}}{\text{Volume of inoculum}}$$

Where,
N = number of plaques
d = dilution factor

3.3 Immunostaining

Immunostaining was performed for the confirmation of infection and active viral replication in BHK-21 cells. Mouse monoclonal antibody specific for envelope protein of JEV was used as primary antibody and anti-mouse IgG (H+L) antibody with 3 conjugates (FITC, Cy3 and Cy5) was used as secondary antibody. Immunostaining protocol was then followed as below.

3.3.1 Cell culture

Coverslips were sterilized by autoclaving and placed in 6 well plates in sterile environment. 1-2 ml of cell suspension in DMEM supplied with 10% serum was added on the wells and the cells were grown at 37°C in a humidified CO2 incubator until they are 50-70% confluent. Cells were then infected with JEV for 2 hours with intermittent rocking every 15 minutes for uniform viral adsorption. One well was taken as a control with no infection. Infected cells were incubated for different time points (12 hour- 60 hour) and preceded to fixation.

3.3.2 Cell Fixation

After the specific time point culture medium was aspirated and gently washed twice with 1X PBS at room temperature. Then cells were fixed by incubating them in 4% (v/v) formaldehyde in PBS for 20 minutes at room temperature. After fixation cells were washed thrice with 1X PBS. Fixed cells were stored in 0.02% (w/v) sodium azide in PBS at 4°C until further use.

3.3.3 Cell Permeabilization

Cells were incubated in 0.1% Triton X-100 in PBS for 15 minutes at room temperature and washed 3 times with 1X PBS.

3.3.4 Blocking

Cells were incubated in 3% BSA in 1X PBS for an hour at room temperature. After blocking cells were washed thrice 1X PBS, each for 10 minutes.

3.3.5 Incubation of cells in primary antibody/antibodies

1% BSA was prepared in 1X PBS. Primary antibody specific for envelope protein of JEV (MAB8734, Chemicon International, Lot no. 051101599-1) was diluted in 1% BSA in a ratio 1:1000. Cells were then incubated overnight at 4°C with diluted primary antibody. After incubation cells were washed thrice with 1X PBS, each for 5 minutes.

3.3.6 Incubation of the cells in secondary antibody/antibodies

Fluorophore conjugated secondary antibody (Goat-anti mouse IgG (H+L), CY 3 conjugate, Invitrogen, Lot No. 1385359) was diluted with 3% BSA prepared in 1X PBS in a ratio 1:2000. Anti-mouse IgG antibody was used having 3 conjugates i.e Cy3, Cy5 and FITC. Cells were incubated with diluted secondary antibody for 2 hours at room temperature, away from light and washed 3 times with 1X PBS. Cells were then incubated in diluted DAPI (300ng/ml) in 1%BSA for 10 minutes.

3.3.7 Mounting and visualization

Cells were incubated in 1µl (300ng/ml) of DAPI for 1 minute. After incubation, cells were washed with 1X PBS. A drop of glycerol was added to the coverslips and each coverslips were then carefully placed on the glass slides with the cell side facing down. Then the cells were visualized under fluorescent microscope.

3.4 Molecular characterization of NS3 protein

Viral cDNA was synthesized using Promega kit (Cat. No. A3500) from the RNA isolated from culture supernatant of infected P388D1 cells. The protocol was followed as below:

3.4.1 Viral RNA isolation by Trizol method

200µL sample (culture supernatant of infected P388D1 cells) was taken into a microfuge tube and 800µL of Trizol reagent (Ambion, Life Technologies, Cat. No. 15596018) was added and incubated at room temperature for 10 minutes. This was then centrifuged at 12,000 RPM for 10 minutes and the supernatant was aspirated into another tube to which chloroform was added (For every 1ml of Trizol used 0.2 ml of chloroform was added). The sample was then vigorously mixed using vortex shaker and incubated at room temperature for 15 minutes, after which the samples were centrifuged again at 12,000 RPM for 15 minutes at 4°C. The aqueous phase (containing RNA) was carefully collected into a fresh microfuge tube without disturbing the pellet (containing DNA and proteins). To this, 0.5 ml of isopropanol alcohol was added for 1ml of Trizol used. Samples are then incubated for 10 minutes at room temperature and centrifuged at 12,000 RPM for 10 minutes at 4°C. The pellet was washed with 75% ethanol and centrifuged at 12,000 RPM for 5 minutes at 4°C. Air dried the pellet and dissolved in RNase free water with incubation at 55-60°C for 10-15 minutes.

3.4.2 Determination of yield and quality of RNA

RNA concentration and purity was checked by Nanodrop instrument. Mili-Q water was taken as blank to determine the concentration and purity of the isolated RNA. The ratio of absorbance at 260/280 and 260/230 was taken into consideration. After checking the concentration and purity, RNA samples were stored at -30°C until further use.

3.4.3 Preparation of cDNA by reverse transcriptase polymerase chain reaction (RT-PCR)

Reverse transcription PCR was performed using Promega kit (Cat. No. A3500) to synthesize cDNA from the isolated RNA. RNA preserved at -30°C was kept at 70°C for 10 minutes. Then the cDNA synthesis protocol was followed, using 1 µg of RNA, as instructed. 20µl reaction mixture was prepared using random primers (Table 1).

Table 1: Reaction mixture for RT-PCR

Sample	Volume (in µL)
25Mm $Mgcl_2$	4.0
Reverse Transcription 10X Buffer	2.0
dNTP Mixture, 10mM	2.0
Recombinant RNasin® Ribonuclease Inhibitor (25 U)	0.5
AMV Reverse Transcriptase (High Conc.) (15 U)	0.6
Random Primers (0.5 µg/ml)	1.5
RNA sample (about 1 µg)	1
Nuclease-Free Water	8.4
Total	20

Samples were kept at room temperature for 10 minutes and after pop spin kept in PCR condition. The reaction setup consists of 1 hour at 47°C, 5 minutes at 95°C and 7 minutes at 0°C. Thus synthesized cDNA was stored at -30°C until further use.

3.4.4 Primer designing and amplification of cDNA with Polymerase chain reaction

Forward and reverse primers were designed using primer 3 software. Primers were designed taking sequence of JEV strain gp78 (Accession no. AF075723) as reference and were designed in such a way that PCR products overlap in 100 bp for the convenience in aligning after sequencing (Table 2). NS2 and NS3 gene sequence obtained from the published JEV strain gp78 (Accession no. AF075723) was utilized to obtain the full N terminal sequence. PCR reaction mix is prepared and cDNA is added to each and placed in the PCR machine for amplification (Table 3 and Table 4).

Table 2: Primer sequence for the amplification of NS3 gene

Primers	Sequence	Melting Temperature (Tm)	GC content
1)	NS3F1: 5'GCGCATGTCTTATATTGG3' NS3R1: 5'TCTGCGGCAGAATTTTCC3'	48°C 48°C	50% 50%
2)	NS3F2: 5'GCAATGGAGTTGAGCTTG3' NS3R2: 5'CCGCATATTCTGTGATCC3'	48°C 48°C	50% 50%

Reaction mix:

Table 3: Reaction mixture for gradient PCR

SAMPLE	Volume in µL
10x PCR Buffer	2.0
25Mm $Mgcl_2$	1.5
5mM dNTPs	1.0
10pM Forward primer	O.3
10pM Reverse primer	O.3
3 units/µl Taq polymerase	0.4
Milli-Q	12.5
cDNA	2.0
Total	20

PCR conditions:

Table 4: PCR conditions for the NS3 region amplification

Stage		Temperature	Time
Primary denaturation		94°C	6 min
35 cycles	Denaturation	94°C	40 sec
	Annealing	48°C	40 sec
	Extension	72°C	50 sec
Final extension		72°C	8 min
Hold		4°C	∞

3.4.5 Agarose gel electrophoresis of amplified viral cDNA

Agarose gel electrophoresis is a widely used method for separation of nucleic acids according to their size. Ethidium bromide is used to visualize the DNA bands, due to its intercalating nature with DNA, and fluorescence under UV light.

1.2% agarose gel was prepared by dissolving 0.42 gm agarose in 35 ml 1X TAE buffer in a 100ml conical flask. The solution is boiled to ensure the agarose dissolves completely. 1.75µl ethidium bromide was added from stock solution to make a final concentration of 0.5µg/ml. The gel was cooled down to 60°C, poured into a gel casting tray containing a well-forming comb and was allowed to set. 2 µl of 6X gel loading dye (New England Biolab) was mixed with the 8µl DNA sample which was loaded in wells along with a 100 bp molecular ladder. Electrophoresis was then carried out at a constant voltage of 110V. After 30-35 minutes of run, the gel was observed under UV trans-illuminator by using Gel doc software.

3.4.6 Sequencing PCR and Sequence plate processing

A master mix was prepared in a 1.5 ml Eppendorf tube and then 4µl of it is dispensed equally into 96 well plate followed by 1 µl of the amplified RNA sample. The PCR of the Micro Amp plates containing the PCR product, gene specific primers and sequencing mixture was carried out in the Thermocycler at following conditions (Table 5, Table 6 and Table 7).

Table 5: Reaction mixture for sequencing PCR

Requirements	Forward primer
Big dye	0.25 µl
Sequencing buffer	1.75 µl
Primer (10pm)	0.25 µl
MilliQ water	1.75 µl
Sample	1 µl

Table 6: Conditions for sequencing PCR with forward primers

Stage		Temperature	Time
Primary denaturation		94°C	5 sec
30 cycles	Extension	55°C	10 sec
Final extension		60°C	4 min
Hold		4°C	∞

Table 7: Conditions for sequencing PCR with reverse primers

Stage		Temperature	Time
Primary denaturation		94°C	5 sec
30 cycles	Extension	57.5°C	10 sec
Final extension		60°C	4 min
Hold		4°C	∞

Three millilitres of absolute ethanol was added to 130µl of 3 M sodium acetate (pH 7.5) in a tube and mixed thoroughly and 25µl of the above mixture was added to each well of the plate. The plate containing sequencing PCR product and above reaction mixture was centrifuged at 4000 rpm for 15 min in eppendorf centrifuge at 16°C. The plate was then inverted (rocked) to remove the supernatant. Hundred microlitres of fresh 80% ethanol was added to each well and again centrifuged at 4000 rpm for 12 min at 20°C. The plate was once again inverted to discard the supernatant and cover the plate with filter paper and give it a short spin for few seconds at 750 rpm to remove remaining alcohol. The plate was kept at room temperature, avoiding direct light, to air dry for 15 minutes. The plate was covered properly with fresh foil. At the time of sequencing, 10 µl of 50% formamide was added to all the wells. The sample plates were kept and run in the ABI DNA Analyzer (for sequencing).

3.4.7 Sequence analysis

The Nucleotide sequences obtained from sequencing was analysed through Chromas lite free online software and the sequences was edited appropriately using the editing tools from the software. The nucleotide sequence was tested for the sequence homology using NCBI BLAST analysis tool with the available JEV sequences in the database and phylogenetic tree was obtained using the same NCBI software.

Nucleotide sequences were then translated into amino acid sequences by using the online software (Nucleotide translator tool from EMBLK Expasy softwares). Thus obtained amino acid sequence was then utilized for the homology protein modeling using the online software Phyre2. Phyre2 software predicts the protein structures based on the Crystal structures and NMR structures available in the PDB (Protein Data Bank) with high confidence rates. The predicted structure will be selected based on high sequence identity, coverage and confidence.

Predicted 3D structure of NS3 protein was tested for the ligand/drug binding properties available in the database using the online software 3D ligand binding site. This software is useful to find out the possible amino acid positions crucial for binding of the drugs or ligands to the specific amino acids and it will be helpful in targeting those amino acids for active testing of the drugs.

3.5 Interleukin-10 and Micro RNAs Expression

3.5.1 Cell culture

P388D1 cells cryopreserved in liquid nitrogen were revived and seeded into T-25 flasks and cultured on RPMI1640 medium with 10% serum and 1% anti-anti antibody. After the cells were 90-95% confluence, they were sub cultured into T-75 flasks. Sub culturing was done by enzymatic method using 1mg/ml trypsin and number of viable cells were counted with the help of hemocytometer using trypan blue stain. Cells were then seeded in 6 well plate (Nunc) each containing around 0.3 X 10^6 viable cells per well.

3.5.2 Inoculation of virus

When the cells were 40-50% confluent, culture medium was removed and the cells were washed twice with plain medium. Viral inoculation was performed with 10^{-1} dilution as described earlier. Cells were then incubated in the CO_2 incubator at 37°C at 5% CO_2. Control was kept for each test well without infection.

3.5.3 Time points collection

At every 12 hour time point, supernatant was collected and cells were lysed with trizol reagent for 5 minutes and stored at -30°C for further processing.

3.5.4 RNA isolation

Cell extracts in trizol reagent were thawed and incubated at room temperature for 10 minutes. After incubation it was centrifuged at 12,000 g for 10 min at 4°C and supernatant was collected. Two hundred microliters of chloroform was added to the supernatant, shook vigorously and incubated at room temperature for 15 min. Then it was centrifuged at 12,000 g for 15 min at 4°C. Aqueous phase containing RNA was carefully collected considering there is no contamination with the interphase. 500µl of chilled isopropanol was added to the aqueous phase and incubated at -20°C for 2.5 hours and centrifuged at 12,000 g for 10 min at 4°C. Supernatant was discarded and pellet was washed with chilled 75% ethanol, mixed by vortexing and centrifuged at 7500 g for 5 minutes at 4°C. Washing step was performed 2-3 times. Pellet was air dried for 5-15 minutes. After drying RNA pellet was resuspended on 20µl of nuclease free water. The RNA solution was incubated in a water bath at 55-60°C for 10-15 minutes. RNA concentration and purity was measured by Thermo Scientific NanoDrop™ 1000 Spectrophotometer and was proceed for cDNA synthesis.

3.5.5 Preparation of cDNA by reverse transcriptase polymerase chain reaction (RT-PCR) using promega kit:

RNA was kept at 70°C for 10 minutes. Then the PCR was prepared and RT-PCR was carried out in thermocycler (Table 8).

Table 8: Reaction mixture for RT-PCR

Sample	Volume (in µL)
25Mm $Mgcl_2$	4.0
10X RT buffer	2.0
10Mm d NTP'S	2.0
RNase inhibitor (25 units)	0.5
Reverse Transcriptase(15 units)	0.6
Random Primers (0.5 µg/ml)	1.5
Milli Q	7.4
RNA (1µg)	02
Total	22

Samples were kept at room temperature for 10 minutes and after pop spin, tubes were kept in PCR condition as in table 9.

Table 9: PCR condition for cDNA synthesis

Temperature (°C)	Time
47	60 minutes
95	5 minutes
4	6 minutes
4	hold

After cDNA synthesis, the samples were stored at -20°C until further use.

3.5.6 miR selection

All micro RNAs having potential of binding with the Interleukin-10 mRNA was checked using the miRwalk software. MiR 27a and miR-98 were selected for the study in accordance with the previously published paper which has been shown to regulate the expression of mouse interleukin-10 (Liu *et al*, 2011; Xie *et al*, 2014). Novel microRNA was selected using miRWALK software based on having potential of binding with the 3'UTR region of IL-10 mRNA. MicroRNAs having binding energy more than -20kcal were omitted out. To outweigh the overprediction, further selection was done using three widely used softwares (Target Scan, miRanda and RNA hybrid) to predict the miRNAs targeting IL-10. Only those miRNAs showing the potential binding with the IL-10 mRNAs were selected for the further analysis (Table 10 and Table 11).

Table 10: Predicted miR binding sites on Interleukin-10 mRNA

Gene Name	RefSeqID	MicroRNA	Seed Length	Start	Sequence	End	Region of IL-10 gene	P-value
IL-10	NM_010548	mmu-miR-106b	7	886	UAAAGUG	880	3 UTR	0.0419
IL-10	NM_010548	mmu-miR-98	7	762	UGAGGUA	756	3 UTR	0.0419
IL-10	NM_010548	mmu-miR-27a	7	799	UUCACAG	793	3 UTR	0.0419

Table 11: Comparative view of predicted miR sites on 3' UTR region by miRWalk & other prediction programs

Gene Name	MicroRNA	miRanda	miRDB	miRWalk	RNAhybrid	RNA22	Targetscan
IL-10	mmu-miR-27a	1	0	1	1	0	1
IL-10	mmu-miR-98	1	0	1	0	0	1
IL-10	mmu-miR-106b	1	0	1	0	0	1

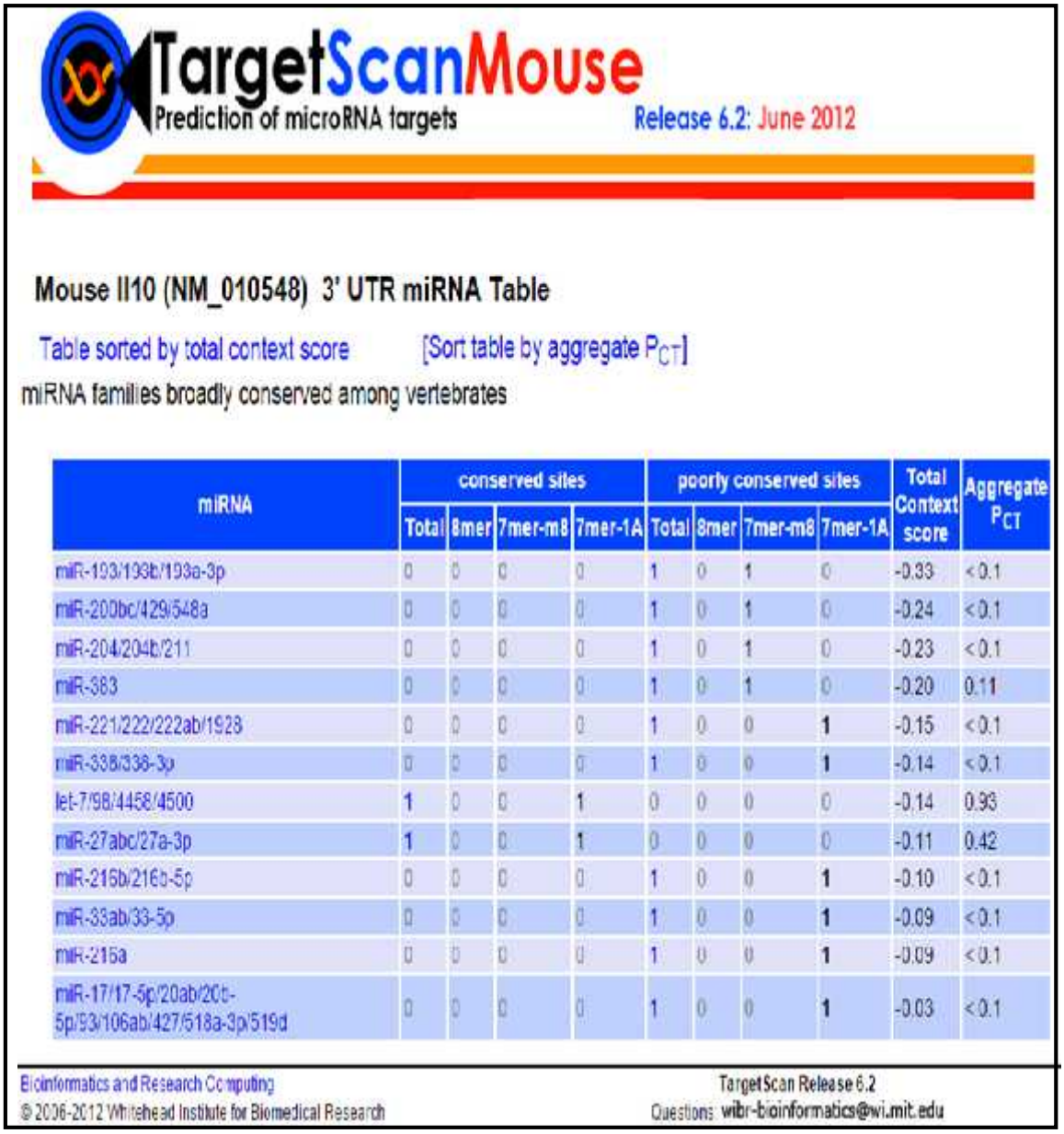

TargetScanMouse
Prediction of microRNA targets
Release 6.2: June 2012

Mouse Il10 (NM_010548) 3' UTR miRNA Table

Table sorted by total context score [Sort table by aggregate P_{CT}]

miRNA families broadly conserved among vertebrates

miRNA	conserved sites				poorly conserved sites				Total Context score	Aggregate P_{CT}
	Total	8mer	7mer-m8	7mer-1A	Total	8mer	7mer-m8	7mer-1A		
miR-193/193b/193a-3p	0	0	0	0	1	0	1	0	-0.33	<0.1
miR-200bc/429/548a	0	0	0	0	1	0	1	0	-0.24	<0.1
miR-204/204b/211	0	0	0	0	1	0	1	0	-0.23	<0.1
miR-383	0	0	0	0	1	0	1	0	-0.20	0.11
miR-221/222/222ab/1928	0	0	0	0	1	0	0	1	-0.15	<0.1
miR-338/338-3p	0	0	0	0	1	0	0	1	-0.14	<0.1
let-7/98/4458/4500	1	0	0	1	0	0	0	0	-0.14	0.93
miR-27abc/27a-3p	1	0	0	1	0	0	0	0	-0.11	0.42
miR-216b/216b-5p	0	0	0	0	1	0	0	1	-0.10	<0.1
miR-33ab/33-5p	0	0	0	0	1	0	0	1	-0.09	<0.1
miR-216a	0	0	0	0	1	0	0	1	-0.09	<0.1
miR-17/17-5p/20ab/20b-5p/93/106ab/427/518a-3p/519d	0	0	0	0	1	0	0	1	-0.03	<0.1

Bioinformatics and Research Computing
© 2006-2012 Whitehead Institute for Biomedical Research

TargetScan Release 6.2
Questions: wibr-bioinformatics@wi.mit.edu

Figure 11: Mouse miRs having the capability of binding with Interleukin-10 mRNA as predicted by Target scan tool

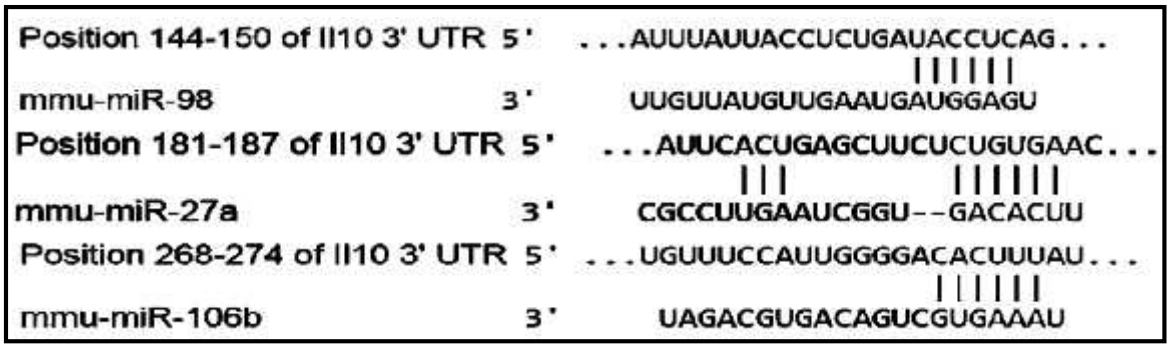

Figure 12: Binding sites of the selected miRs in the 3'UTR of IL-10 mRNA as predicted by Target scan software

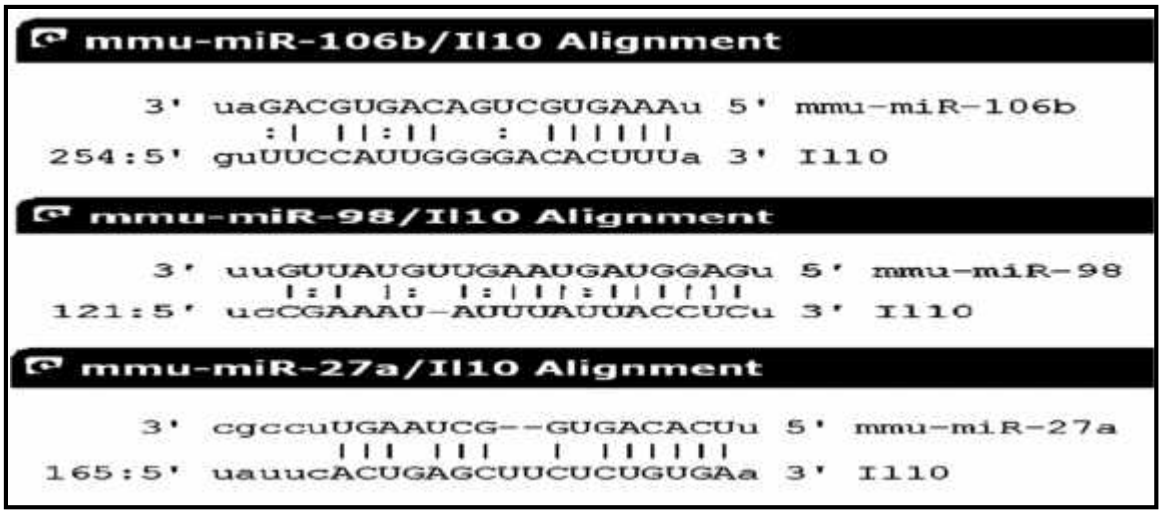

Figure 13: Binding sites of the selected miRs in the 3'UTR of IL-10 mRNA as predicted by miRanda software

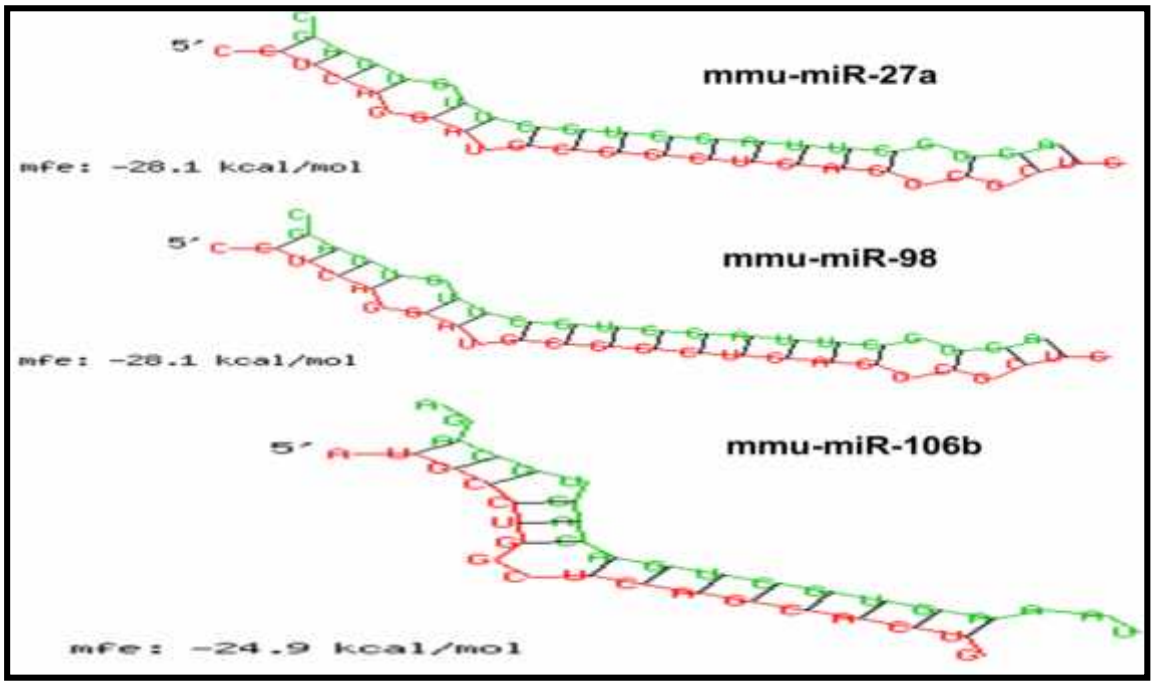

Figure 14: Binding free energy between the selected miRs and IL-10 3'UTR as predicted by RNA hybrid software

3.5.7 Real Time polymerase chain reaction:

Real Time Polymerase Chain Reaction (RT-PCR) or quantitative Polymerase Chain Reaction (qPCR) commonly used in molecular biology for amplification of specific sequences delimited by primers and detection of amplification in Real time. Forward and reverse primers were designed using primer 3 software specified for qPCR (Table 12). PCR mix was prepared in white 96 well RT-PCR plates (ROCHE) using the USB veriquest SYBR Green qPCR Master Mix (2X) in a final volume of 20 µl. Dilution at 1:10 of

synthesized cDNA was used for the reaction (Table 13). PCR reaction was carried out in Roche Light cycler 480.

Table 12: Primers sequence for the target genes (GAPDH, IL-10, miR-98, miR-27a, miR-106b)

Target Gene	Primers	Melting temperature (T_m)	GC content
GAPDH	GF: 5'AGTATGACTCCACTCACGGCA-3' GR: 5'ATGGTGGTGAAGACACCAGT-3'	54°C 52°C	52.38% 50.00%
IL-10	IF: 5'CCCTGGGTGAGAAGCTGAAG 3' IR: 5'CACTGCCTTGCTCTTATTTTCACA 3'	60.04°C 60.02°C	60.00% 41.67%
miR-98	M98F: 5'ACATGCTGGGGTGAGGTAGT3' M98R: 5'GCCACACACCAAGGAAAGTAG3'	59.5°C 60.0°C	55% 47.4%
miR-27a	M27F: 5'GAGCAGGGCTTAGCTGCTTG 3' M27R: 5'CCAGGGGGCGGAACTTAG 3'	62.6°C 62.8°C	60.0% 66.7%
miR-106b	M106F: 5'TGCTGGGACTAAAGTGCTGA 3' M106R: 5' GGAGCAGCAAGTACCCACA 3'	59.6°C 60.2°C	50% 57.9%

Table 13: Reaction mixture for Real Time PCR

Sample	Concentration	Volume
PCR buffer (veriquest)	2X	10 µl
Forward Primer	10 pm/µl	0.5 µl
Reverse Primer	10 pm/µl	0.5 µl
Diluted cDNA	1:10 dilution	2 µl
Nuclease Free Water	-	7 µl
Total		20 µl

Real time PCR was conducted for the all the gene of interest using specific primers on 96 well plates (Table 14 and Table 15). PCR was run on Roche light cycler 480 instruments.

Table 14: PCR reaction condition for GAPDH and IL-10

Steps		Temperature (°C)	Time	Cycles
Initial Denaturation and Taq activation		95	5 min	1
Amplification	Denaturation	98	10 sec	45
	Annealing	52	20 sec	
	Extension	72	30 sec	
Melting Curve		98	1 min	1
		52	1 min	
		98	continuous	
Cooling		40	5 min	-

Table 15: PCR reaction condition for miRs

Steps		Temperature (°C)	Time	Cycles
Initial Denaturation and Taq activation		95	5 min	1
Amplification	Denaturation	98	10 sec	45
	Annealing	56	20 sec	
	Extension	72	30 sec	
Melting Curve		98	1 min	1
		52	1 min	
		98	continuous	
Cooling		40	5 min	-

After amplification, data were analysed using light cycler 480 software and relative expression was analysed taking GAPDH as calibrator. Relative expression in the test samples was determined with reference to the control cells without infection.

3.6 Protein expression analysis of Interleukin-10

3.6.1 SDS-Polyacrylamide gel separation

Cell culture supernatants acquired at different time points were mixed with 5x protein loading dye in a ratio of 1:4 which were then placed in boiling water bath for 15 minutes. For the positive control serum samples from the Balb/c mice, which were induced for the Interleukin-10 production, were used. The serum samples were kind gift from the animal house facility at CCMB. For the negative control normal Fetal Bovine serum was used.

Discontinuous gel electrophoresis was performed with the help of resolving gel and stacking gel. Stacking gel helps concentrates the sample into a tight band with the help of glycinate ions and chloride ions present in the stacking gel. Gel assembly was prepared by aligning two glass plates with spacers in between them. Freshly prepared separating gel was poured between the two plates. The gel was layered with 1 ml of water and allowed to set for around 30 minutes at room temperature. Later water was removed and stacking gel solution was poured and the comb was fitted in between the plates. The gel was left undisturbed till the stacking gel was set. Then, 30µl of samples prepared were loaded in the wells. The gel was run at 100V in stacking and at 180V in resolving gel till the dye front reaches the end in 1X SDS PAGE running buffer.

3.6.2 Western Blotting

A stacking portion of the gel was cut and removed. The separation portion of the gel was transferred to pre-chilled transfer buffer in glass tray for 10-15 minutes for equilibration. PVDF membrane being hydrophilic is dipped in methanol for 5 mins for enhancing the binding properties. PVDF membrane was then transferred to 1X transfer buffer. The blot paper and fiber sponge were also transferred to transfer buffer for equilibration. Transfer sandwich was assembled with blot at the cathode and gel at the anode considering no air bubble is trapped in the sandwich. The cassette was placed in the transfer tank maintained at 4°C and ice block was placed in the tank. The protein was transferred for an hour at 100V.

3.6.3 Detection by Western blotting

After the transfer, blots were incubated in 5% milk powder in 1X PBST for at least 1 hr, blots were then washed with 1X PBST and incubated with fresh primary antibody (Rat anti mouse IL-10 antibody, dilution 1:5000) for 2 hrs at room temperature. Then blots were washed thrice with 1X PBST 10 mins each. Blots were incubated with secondary antibody (anti Rat IgG conjugated with Horseradish Peroxidase), diluted in the ratio 1:10,000 in PBST, for 40mins. Blots were again washed thrice with 1X PBST 10mins each. ECL (Enhanced Chemi Luminescence) substrate which binds to secondary antibody and imparts chemiluminiscence was evenly added, blots were then viewed under Chemi- doc instrument (Vilber lourmat chemiluminiscence documentation) and image was captured.

3.7 NS3 standard curve and Viral load analysis

Viral titer obtained from the plaque assay was utilized for the generation of standard curve for the viral RNA molecules. Primers were designed for the NS3 protein using primer 3 plus software (Table 16).

Table 16: Primers sequence for the absolute quantification of Viral RNA targeting NS3 gene

Target Gene	Primers	Melting Temperature (°C)	GC content (%)
NS3	NS3F3: 5'ATACCAGACAGGGCATGGAG3' NS3R3: 5'GACTTGCGGTTGAGTTGGAT3'	60 60.1	55.0 50.0

200µl of the serial diluted viral sample with known viral load was used for the isolation of viral RNA molecules. Trizol method was utilized for the RNA isolation. Thus obtained RNA was measured on Nanodrop and the number of RNA molecules present was calculated. One microgram of RNA was taken for the cDNA synthesis. cDNA thus synthesized was serially diluted to reach 10-5 dilution. Serially diluted cDNA sample was

amplified by Real time PCR using NS3 specific primers. A standard curve was generated for the amplified products using light cycler software release 1.5.0.

RTPCR was conducted for the cDNA samples obtained from the different time points of the infected P388D1 cells. Absolute quantification of the viral RNA in different time points was done using the prepared standard curve.

CHAPTER 4

RESULTS

4.1 Characterization of serine protease domain of JEV NS3 protein

4.1.1 PCR amplification of NS3 gene

The NS3 gene of the gp05 strain was amplified with the help of PCR using specific primers to target our gene of interest. Electrophoresis was carried out on an agarose gel with a 100 base pair ladder from New England Biolabs. The amplified product was seen on the gel which showed that the amplified product of around 614 bp (Figure 15). The DNA was further processed for sequencing analysis.

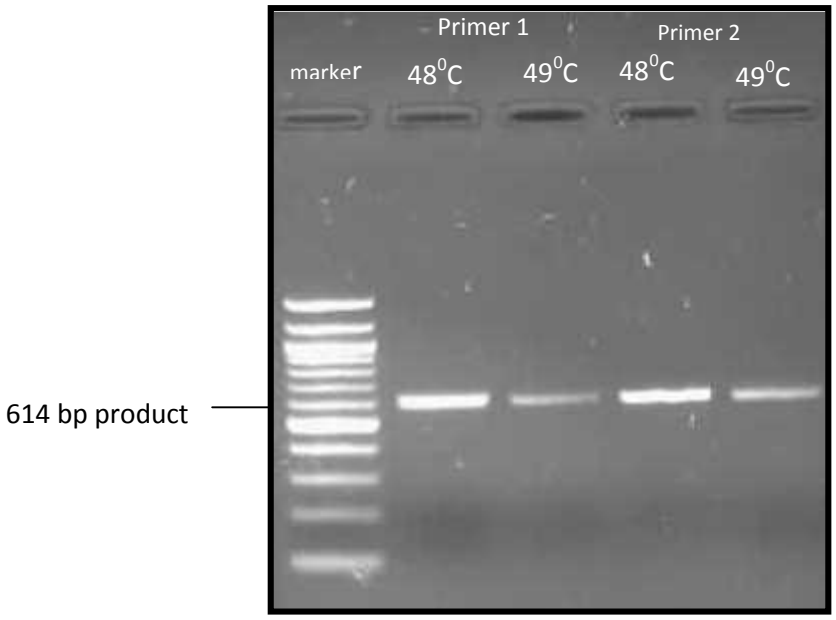

Figure 15: The amplified PCR product of the NS3 gene. NS3 gene was amplified from the cDNA using specific primer. The PCR product was examined on 1.2% agarose gel with 100 bp marker.

4.1.2 Sequence analysis of the NS3 protein

The amplified products of NS3 gene were subjected to sequencing PCR, the sequencing plates were processed well and were put in ABI 3730 sequence analyser. Then, with the help of chromas lite software the sample sequence was aligned with the reference sequence and was analysed (Figure 16).

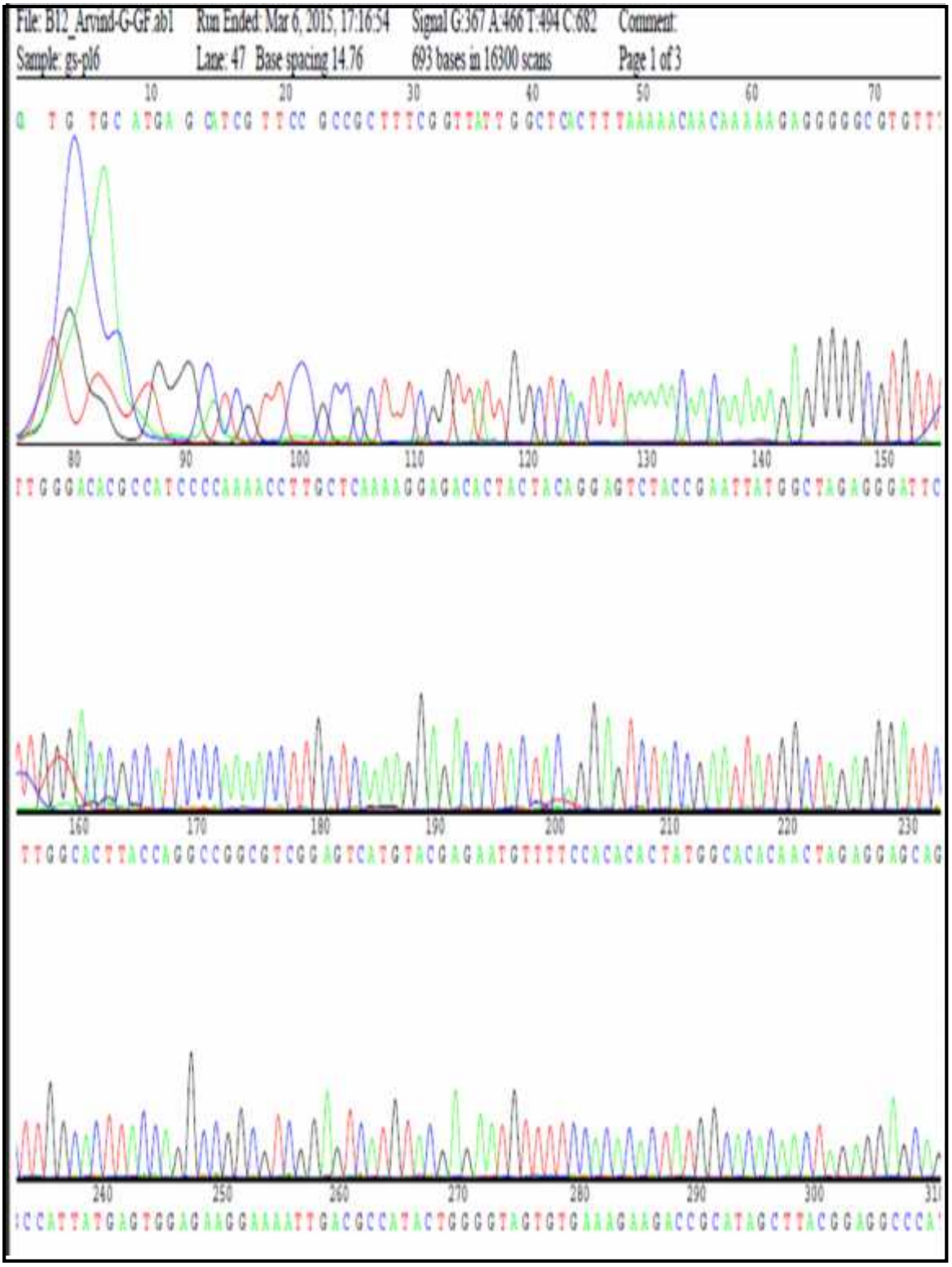

Figure 16: Electropherogram results obtained from amplified DNA sequencing of NS3 gene. The amplified PCR product was subjected to sequencing PCR using ABI sequence analyser and the sequence was obtained using chromas lite software. Each coloured peaks show the specific nucleotide base present in the sequence.

Retrieved sequence of the NS3 gene of JEV gp05 was compared with the reported JEV gp78 sequence in NCBI. This was done with the help of CLUSTALW software which performs multiple sequence alignment to the sequence variation between these two strains.

```
gp05_NS3        GGGGGCGTGTTTTGGGACACGCCATCCCCAAAACCTTGCTCAAAAGGAGACACTACTACA
gp78_NS3        GGGGGCGTGTTTTGGGACACGCCATCCCCAAAACCTTGCTCAAAAGGAGACACCACTACA
                ************************************************** ******

gp05_NS3        GGAGTCTACCGAATTATGGCTAGAGGGATTCTTGGCACTTACCAGGCCGGCGTCGGAGTC
gp78_NS3        GGAGTCTACCGAATTATGGCTAGAGGGATTTTTGGCACTCACCAGGCCGGTGTTGGAGTC
                ***************************** ******** ********** ** ******

gp05_NS3        ATGTACGAGAATGTTTTCCACACACTATGGCACACAACTAGAGGAGCAGCCATTATGAGT
gp78_NS3        ATGTATGAGAATGTTTTCCACACACTATGGCACACAACTAGAGGAGCAGCCATTATGAGT
                ***** ************************************************** 

gp05_NS3        GGAGAAGGAAAATTGACGCCATACTGGGGTAGTGTGAAAGAAGACCGCATAGCTTACGGA
gp78_NS3        GGAGAAGGAAAATTGACGCCGTACTGGGGTAGTGTGAAAGAAGACCGCATAGCTTACGGA
                ******************** ************************************

gp05_NS3        GGCCCATGGAGGTTTGACCGAAAATGGAATGGAACAGATGACGTGCAAGTGATCGTGGTA
gp78_NS3        GGCCCATGGAGGTTTGACCGAAAATGGAATGGAACAGATGACGTGCAAGTGATCGTGGTA
                ************************************************************

gp05_NS3        GAACCGGGGAAGGCTGCAGTAAACATCCAGACAAAACCAGGAGTGTTTCGGACTCCCTTC
gp78_NS3        GAACCGGGGAAGGCTGCAGCAAACATCCAGACAAAACCAGGAGTGTTTCGGACTCCCTTC
                ******************** ************************************

gp05_NS3        GGGGAGGTTGGGGCTGTTAGTCTGGATTACCCGCGAGGAACATCCGGCTCACCCATTCTG
gp78_NS3        GGGGAGGTTGGGGCTGTTAGTCTGGATTACCCGCGAGGAACATCCGGCTCACCCATTCTG
                ************************************************************

gp05_NS3        GATTCTAATGGAGACATCATAGGCCTATACG-CAATGGAGTTGAGCTTGGCGATGGCTCA
gp78_NS3        GATTCCAATGGAGACATCATAGGCCTATATGGCAATGGAGTTGAGCTTGGCGATGGCTCA
                ***** ********************** * ****************************

gp05_NS3        TACGTCAGCGCCATCGTGCAGGG-GACCGTCAGGAGGAACCAGTCCCAGAAGCTTACACC
gp78_NS3        TACGTCAGCGCCATCGTGCAGGGTGAACGTCAGGAGGAACCAGTCCCAGAAGCTTACACC
                ********************** ** ********************************

gp05_NS3        CCAAACATGTTGAGAAAGAGACAGATGACTGTGCTAGATTTGC-CCCTGGCTCAGGGAAG
gp78_NS3        CCAAATATGTTGAGAAAGAGACAGCTGACTGTGCTAGATTTGCACCCTGGTTTAGGAAAA
                ***** ****************** ****************** ****** * *** **

gp05_NS3        ACCAGGAAAATTCTGCCACAGATAATCAAGGACGCCATCCAGCAACGCCTAAAAACAGCT
gp78_NS3        ACCAGGAAAATTCTGCCGCAGATAATTAAGGACGCTATCCAGCAGCACCTAAGAACAGCT
                ***************** ******** ******** ******** * ***** *******

gp05_NS3        GTGCTGGCACCGACGCGGGTGGTAGCAGCAGAAATGGCAGAAGCTTTGAGAGGGCTCCCA
gp78_NS3        GTGTTGGCACCGACGCGGGTGGTGGCAGCAGAGATGGCAGAAGCTTTGAGAGGGCTCCCA
                *** ******************* ******** ***************************

gp05_NS3        GTGCGATTTCAAACTTCAGCAGTGCACAGAGAGCACCAAGGGAATGAAATAGTGGATGTG
gp78_NS3        GTACGATATCAAACTTCAGCAGTGCAGAGAGAGCACCAAGGGAATGAAATAGTGGATGTG
                ** **** ****************** ********************************

gp05_NS3        ATGTGCCACGCCACTCTGACCCATAGACTGATGTCACCGAACAGAGTGCCCAACTACAAC
gp78_NS3        ATGTGCCATGCCACTCTGACCCATAGACTGATGTCACCGAACAGAGTGCCCAACTACAAC
                ******** ************************************************

gp05_NS3        CTATTTGTCATGGATGAAGCTCATTTCACTGACCCAGCCTGCAGAGCCGCACGAGGATAC
gp78_NS3        CTATTCGTCATGGATGAAGCTCACTTCACCGACCCAGCCAGTATAGCCGCACGAGGATAC
                ***** ***************** ***** ********* * * ****************
```

```
gp05_NS3        ATTGCTACCAAGGTGGAATTAGGGGAGGCAGCAGCCATCTTCATGACAGCGACCCCGCCT
gp78_NS3        ATTGCTACCAAGGTGGAATTGGGGGAGGCAGCAGCCATTTTCATGACAGCGACTTCGCCT
                ********************* ***************** **************  *****

gp05_NS3        GGAACCACGGATCCTTTTCCTGACTCATATGCCCCAATCCATGATTTGCCAGATGAGATA
gp78_NS3        GGAACCACGGATCCTTTTCCTGACTCCAATGCTCCAATCCATGACTTGCAAGATGAGATA
                ************************  **** *********** **** **********

gp05_NS3        CCAGACAGGGCATGGAGCAGTGGATACGAAT
gp78_NS3        CCAGACAGGGCATGGAGCAGTGGATACGGAT
                ***************************** **
```

Figure 17: Multiple alignment analysis of nucleotide sequences of gp05 NS3 sequence with reference gp78 JEV strain. NS3 sequence obtained from the sequencing was aligned with GP78 sequence using CLUSTALW software. The vacant space below the sequence indicate variation in the nucleotides.

Multiple sequence alignment showed the presence of nucleotide variations in the NS3 gene of JEV GP05 strain. Nucleotide variation in transition from T to C was found more frequently than other mutation (Table 17).

Table 17: Nucleotide variation in JEV gp05 compared to JEV gp78

Nucleotide sequence variation in JEVgp05 compared to JEVgp78	Number of variation	Position
A to G	4	597,600,647,723
G to A	7	201,618,645,653,684,693,921
A to C	2	507,1010
C to A	2	565,987
A to T	3	728,988,880
T to A	0	
G to C	1	747
C to G	0	
G to T	0	
T to G	1	884
C to T	8	54,100,320,426,846,864,870,1005
T to C	17	91,114,111,126,450,546,591,593,627,636,664,789,955,954,993,882,939

4.1.3 Phylogenetic tree (BLAST tree view)

Further, the NS3 sequence was compared against the nucleotide database in NCBI using BLAST tool and phylogenetic tree was created with all the BLAST hits. The results showed that the NS3 sequence of GP05 is closely related to the Japanese strain JaoArS982 which was isolated from infected mosquitoes in 1982 (figure 18).

The nucleotide sequence was then translated into an amino acid sequence by using an Expasy software translation tool for further analysis on sequence divergence and homology modelling studies (Figure 18). Result showed that there is the presence of 14 α-helix and Thus obtained protein sequence was tested for the homology protein modeling using the free online software Phre2.

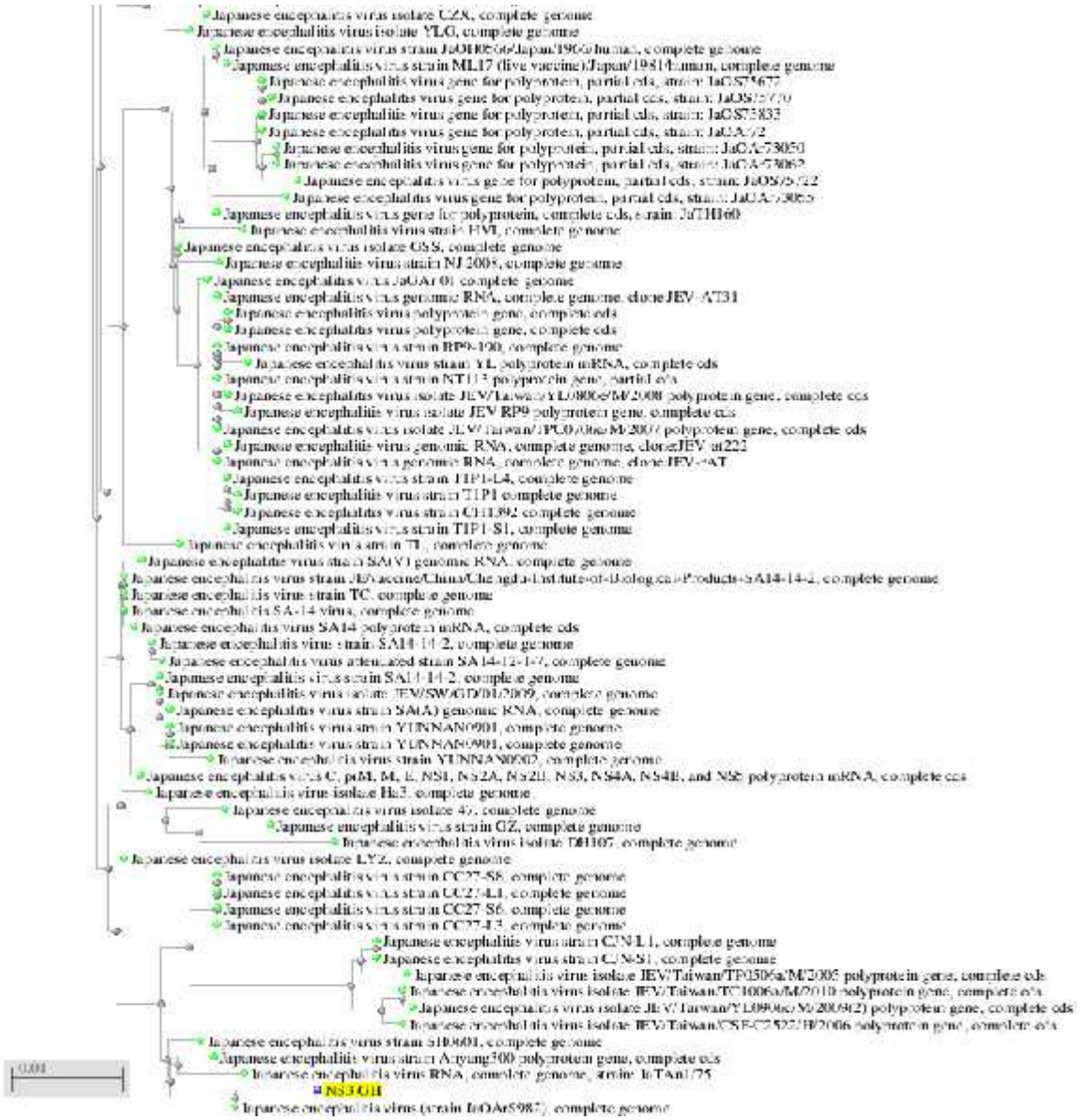

Figure 18: Cladogram tree displaying the relative positions of the NS3 gene sequence in comparison with other JEV strains. Phylogenetic analysis shows the close relationship of the obtained NS3 sequence with Japanese strain JaoArS982.

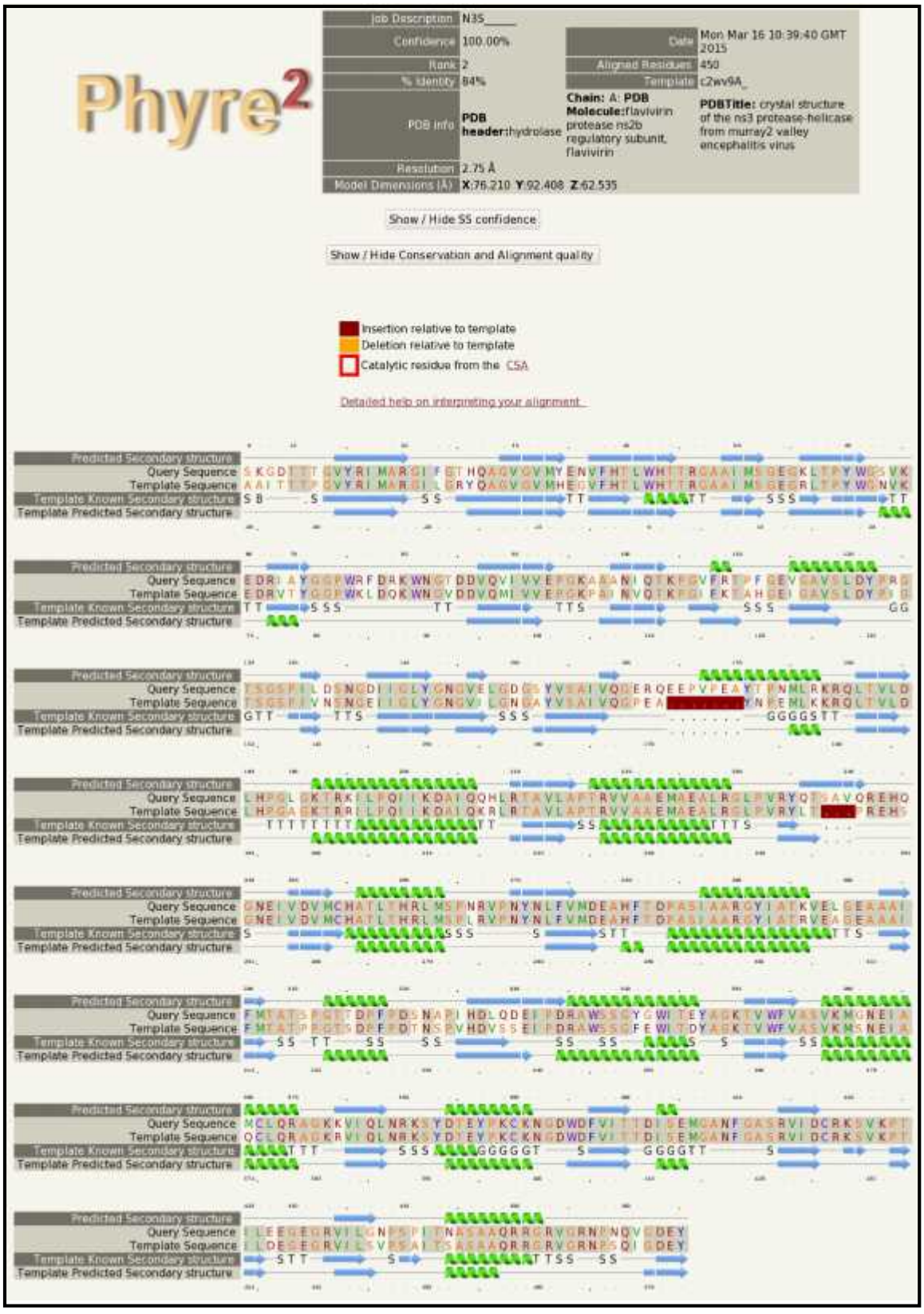

Figure 19: Predicted secondary structure of the NS3 protein. Obtained NS3 sequence was translated to the amino acid sequence using the Phyre 2 software and possible secondary structure was predicted using the same software. The figure shows the translated amino acid sequence and the regions where helix and beta sheets are present in the modelled protein.

Further 3D structure was predicted from the obtained sequence. The structure was predicted by 3D ligand binding site software. The same software was utilized to predict the ligand binding site on the serine protease domain of the NS3 gene. 3D-ligand binding analysis showed the amino acids Threonine, Tyrosine, Leucine, Histidine, Proline, Glycine, Leucine, Glycine, Lysine, Threonine, Arginine, Glutamine, Aspargine and Arginine at positions 58, 60, 186, 187, 188, 189, 190, 191, 192, 193, 194, 278, 409 and 456 respectively are important ligand binding sites as the molecule ADP and Magnesiunm (Mg) interacted with this position. The ligand biding analysis showed that the amino acid residues 186 to 194 serve as a hot spot for ligand binding.

A)

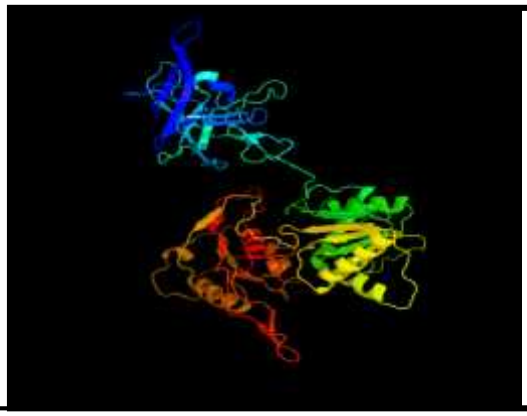

B)

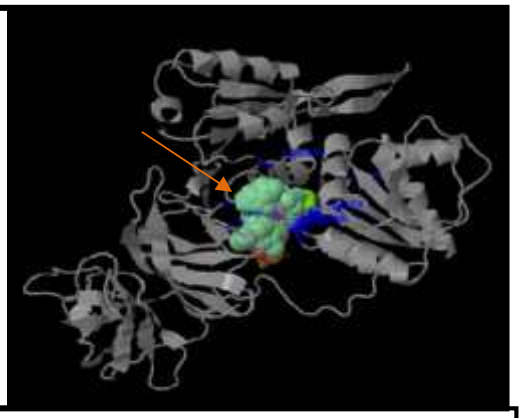

C)

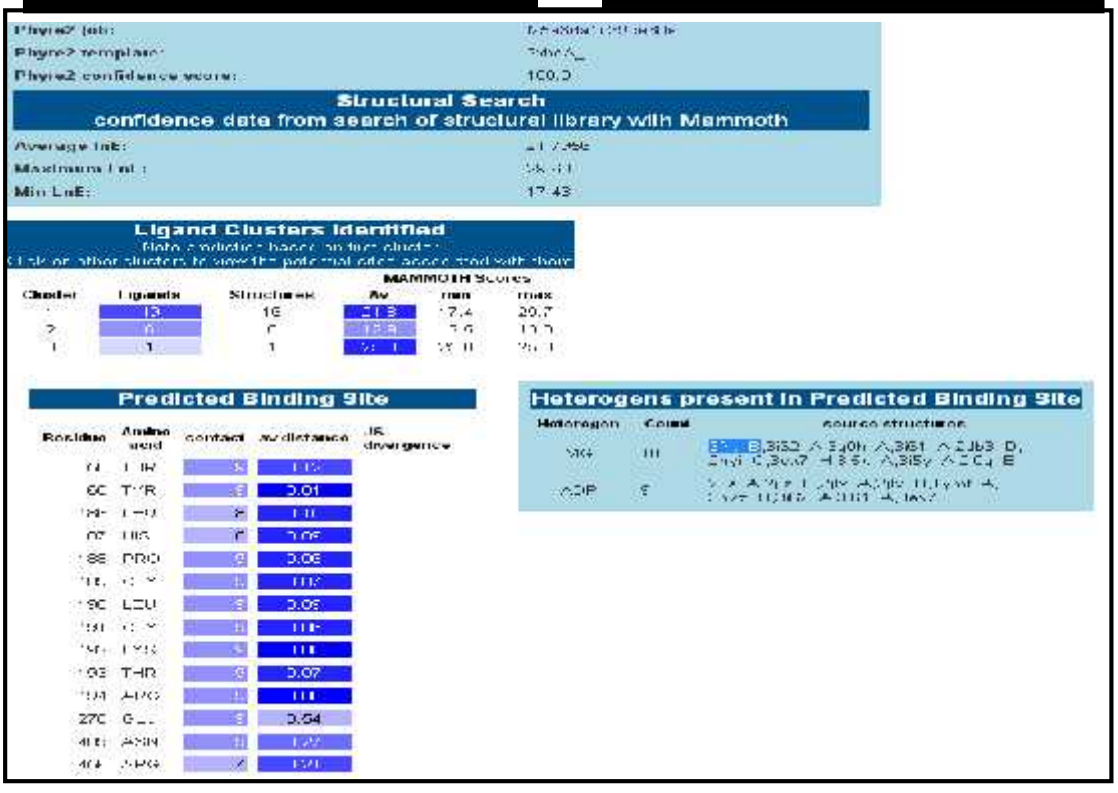

Figure 20: Predicted 3D structure and possible ligand binding sites for the modelled protein. A) 3D ligand binding software was utilized to predict the 3D modelling structure of serine protease domain of GP05 NS3 protein. B) 3D model of predicted NS3 serine protease domain showing binding of possible ligands. C) Amino acid positions critical for binding in NS3 proteins as predicted using the 3D ligand binding site.

4.2 DETERMINATION OF VIRAL TITRE BY PLAQUE ASSAY

Plaque assay was performed as discussed in the materials and methods in order to determine the viral titre. Plaques were calculated according to the dilutions used; 10^{-1}, 10^{-3}, 10^{-5}, $10^{-7}$and 10^{-9} and tabulated below (Table 18). The viral titre was calculated to be around 10^{11} pfu/ml. Due to the high viral load in the first three dilutions, it was difficult to distinguish clear plaques especially, since most plaques had fused together. The sizes of the plaques were microscopic in nature, thus visible only under microscope.

Table 18: Viral titre (in pfu/mL) of BHK-21 cell line corresponding to control and viral dilutions 10^{-1} to 10^{-9}

Viral dilution	Plaques	No. of plaques per well	Viral titre (pfu/ml)
Control	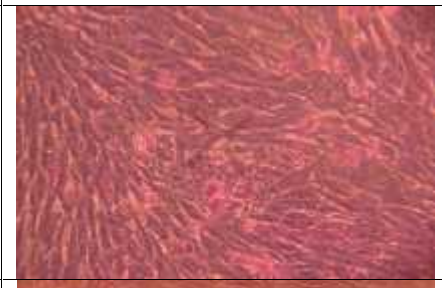	**0**	**0**
10^{-1}		**Not Determined (High viral infection)**	**-**
10^{-3}	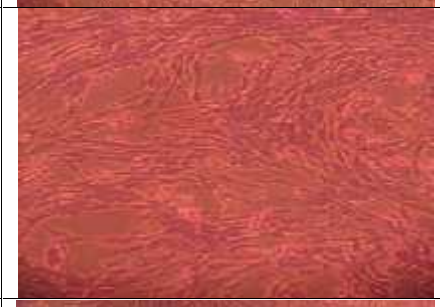	**Not Determined (High viral infection)**	**-**
10^{-5}		**Not Determined (High viral infection)**	**-**

10^{-7}	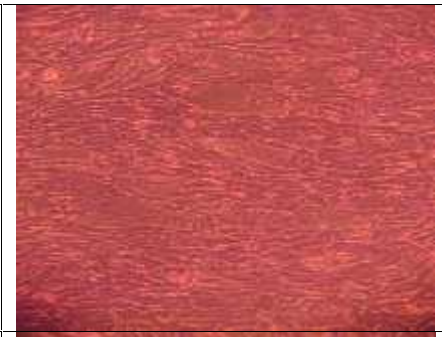	**87**	**$8.7X10^{10}$**
10-9	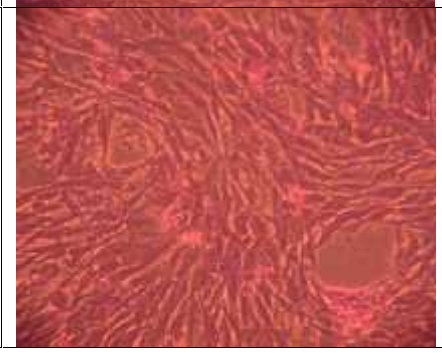	**5**	**$1X10^{11}$**

4.3 Immunostaining

Immunostaining performed using monoclonal antibody specific for envelope protein of JEV showed presence of infection and active viral replication. Blue fluorescence was showing the position of nucleus as stained with DAPI. Green and red fluorescence of FITC and CY3 respectively was observed when viewed under a fluorescence microscope, which shows the position of the envelope protein of JEV. Fluorescence due to FITC and CY3 conjugated secondary antibody was observed mostly in the cytoplasm signifying the presence of the target antigen in the cytoplasm. The number of cells declined progressively as observed in various time points. Fluorescence intensity was maximal at 36 and 48 hours signifying high viral replication at such time points (Figure 21).

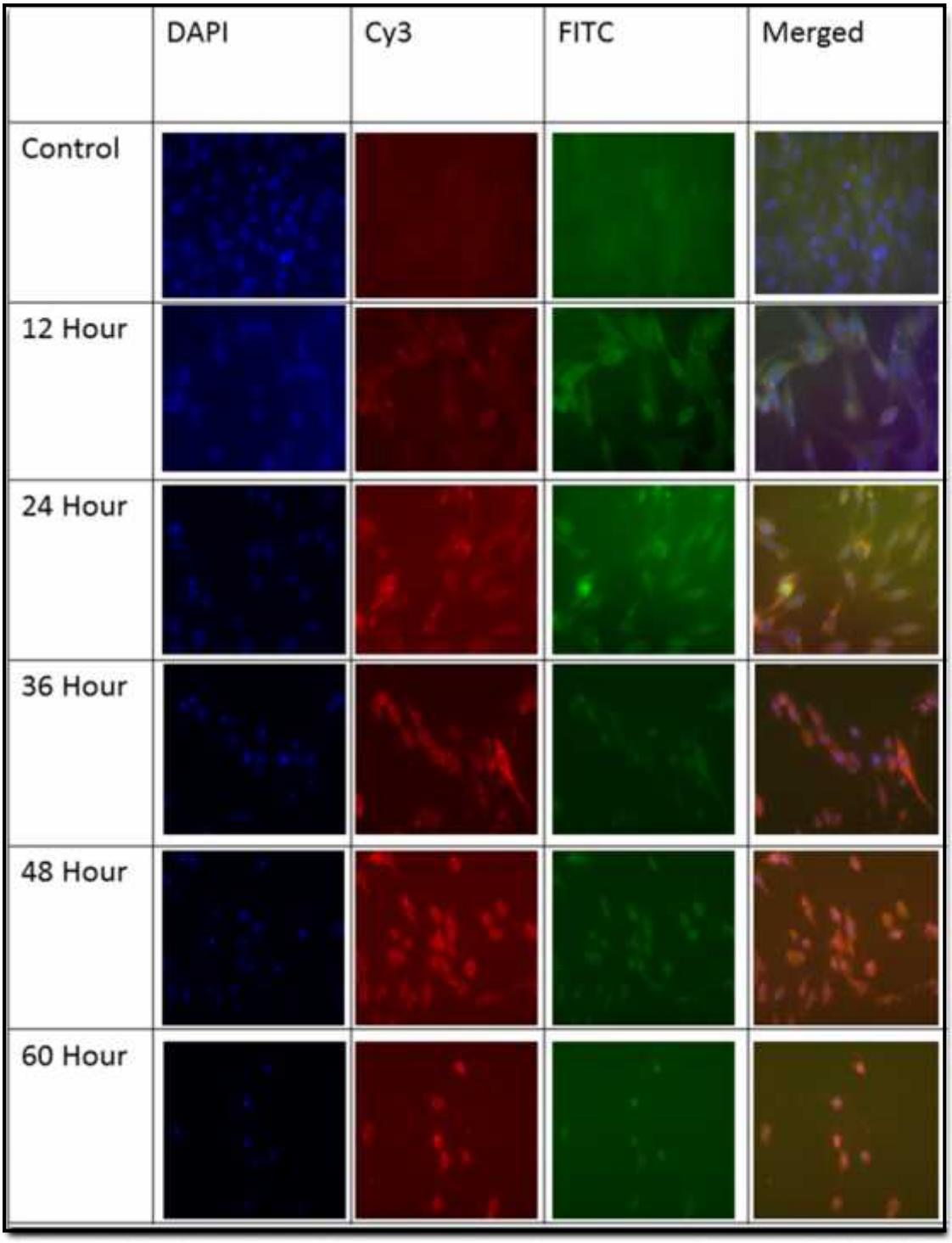

Figure 21: Immunostaining of JEV infected BHK-21 cells. Immunostaining was performed at each time point using monoclonal antibody specific for envelope protein of virus and secondary antibody labelled with FITC and CY3 fluorescent dyes. DAPI was used to label the nucleus and to determine the position of cells. Blue, red and green color indicates the fluorescence of DAPI, CY3 and FITC respectively. Immunostaining shows maximal fluorescence at 36 and 48 hours signifying high viral replication at such time points.

4.4 Time Point Study for the expression of IL-10 and miRs

4.4.1 Cell culture and viral infection

Cells were cultured in 6 well plates and infected with a virus for the time points study of interleukin-10 and selected miRs expression (materials and method). For each time point control was kept which were mock infected with plain culture medium. Cells were observed under microscope at each time point and microscopic image were obtained for both control and test samples. Microscopic image showed the cell number in the test samples decreased after 36 hours p.i., whereas, in control cells the cell density increased gradually till 72 hours (Figure 22).

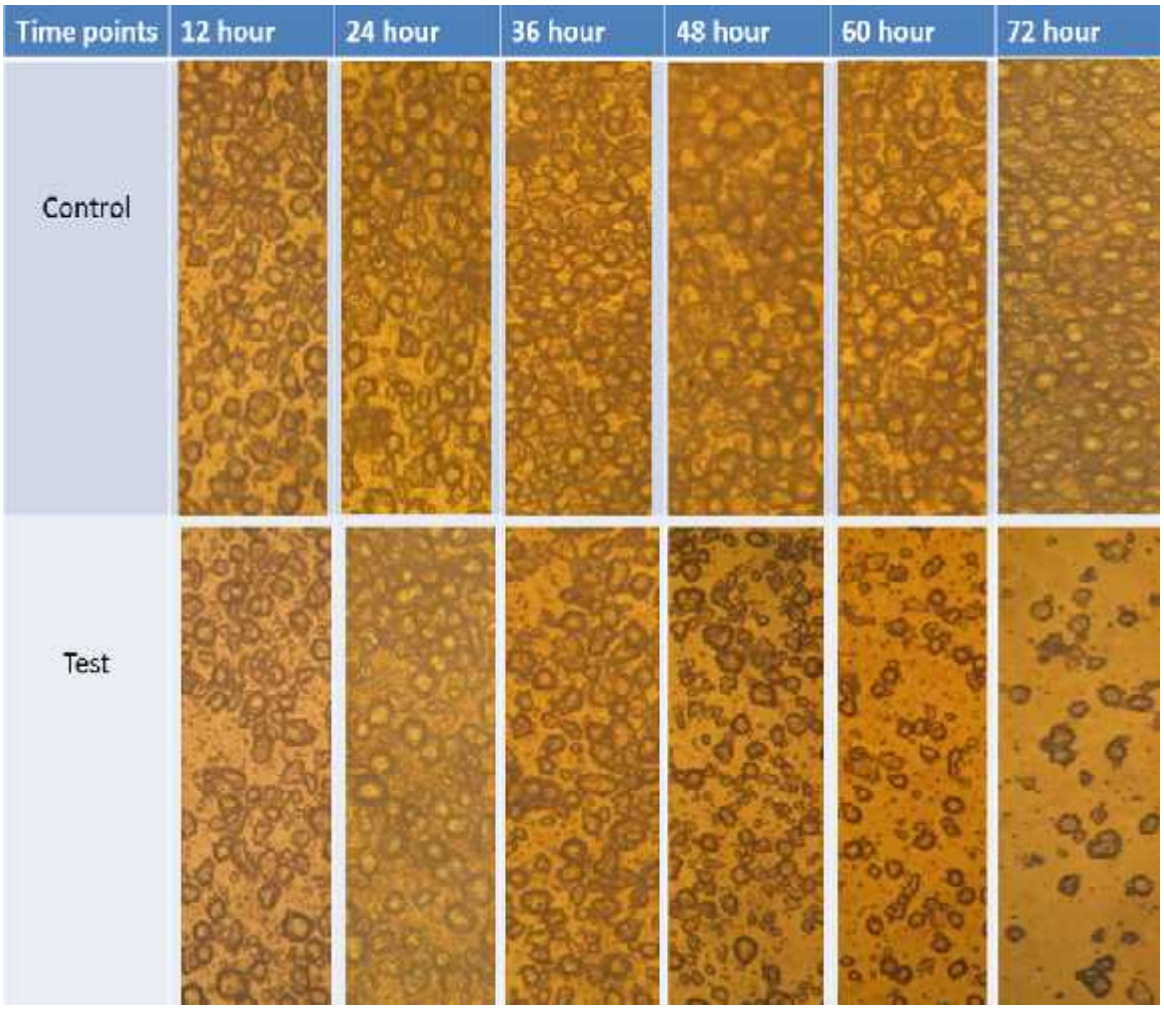

Figure 22: P388D1 cells as observed under microscope at different time points after JEV infection. P388D1 cells were cultured in 6 well culture plates and test cells were infected with JEV. Control cells were mock infected cells with plain medium. The figure shows decrease in cell number in the test sample after 36 hour post infection, whereas in control cells the cell number increased gradually till 72 hours.

4.4.2 Real time PCR for absolute quantification of viral RNA copies

Absolute quantification of the viral RNA copies was performed for the confirmation of infection and viral replication. Primer specific for the viral NS3 gene (NS3F3 and NS3R3) were used quantitatively relying on the information regarding NS3 gene as the most conserved gene in the viral genome. Primers were designed using primer3 software. Real time data showed increases in the viral RNA copies sequentially from 12 hrs p.i. and reached maximum viral RNA copies at 60 hrs p.i. (Figure 23). Increase in viral RNA copies gradually signifies active viral infection and replication in P388D1 cells.

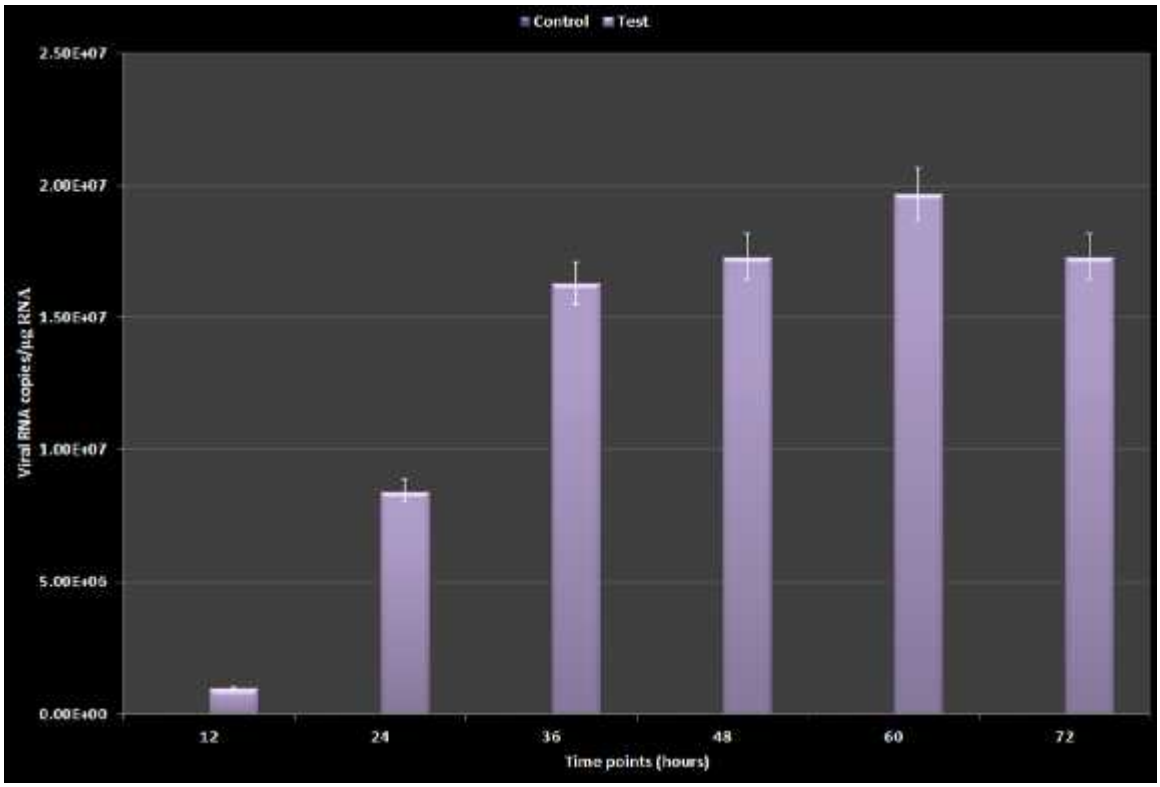

Figure 23: Absolute Quantification of the viral copy number. Total RNA was isolated from the JEV infected P388D1 cells at different time points. Isolated RNA was converted into cDNA using random primers and amplified using primer specific for viral NS3 gene using Real time PCR. Graph was plotted using the viral copy number at different time points as obtained from the real time PCR. As shown in the figure the viral RNA copies increased sequentially from 12 hrs p.i. and reached maximum viral RNA copies at 60 hrs p.i.

4.4.3 REAL TIME PCR for relative quantification of IL-10

Real time PCR was performed to check the expression of interleukin-10 mRNA during JEV infection in p388D1 cells. Total RNA was isolated from the JEV infected and mock infected cells. Isolated RNA was converted into cDNA using random primers. Synthesized cDNA was diluted into optimal concentration and real time PCR was performed using specific primer for mouse IL-10. After plotting a bar graph of the obtained real time PCR data it was observed that IL-10 gene expression increased significantly at 36 hrs p.i. And reached a peak at 48hrs. After 48 hours expression of IL-10 gene declined gradually (Figure 24).

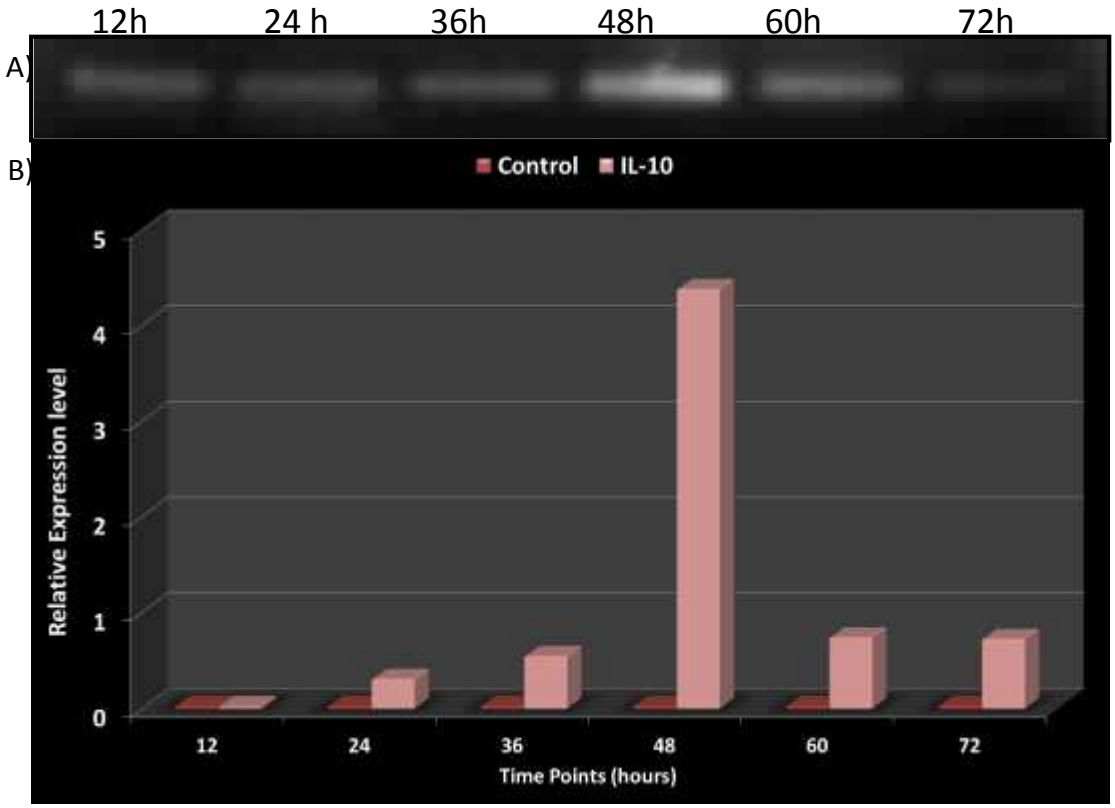

Figure 24: Real-time RT-PCR analysis of Interleukin-10 mRNA expression in the control and JEV infected P388D1 cells. At each time point total RNA was isolated from the P388D1 cells infected with JEV. RNA was then converted to cDNA using random hexamer primers and was then amplified by Real time PCR using primer specific for mouse IL-10 gene (IF and IR). (A) The amplified PCR product of IL-10 mRNA at different time points as examined on 1.2% agarose gel. (B) Bar graph representing the fold changes of mRNA levels quantified by normalizing to the GAPDH as an internal control.

4.4.4 REAL TIME PCR for relative quantification of miR-98

Expression of miR-98 was checked using Real Time PCR from the total RNA isolated from the infected and control P388D1 cells. Total RNA was isolated from the JEV infected cells and the mock infected control cells at each time point and converted into cDNA using random primers. Dilution was performed to get the optimum concentration of cDNA and Real time PCR was done to amplify precursor miR-98 using specific primers. Plotting bar graph from the obtained data shows miR-98 expression increased gradually and reached peak at 48 hrs p.i. and declined after 48 hrs p.i. (Figure 25).

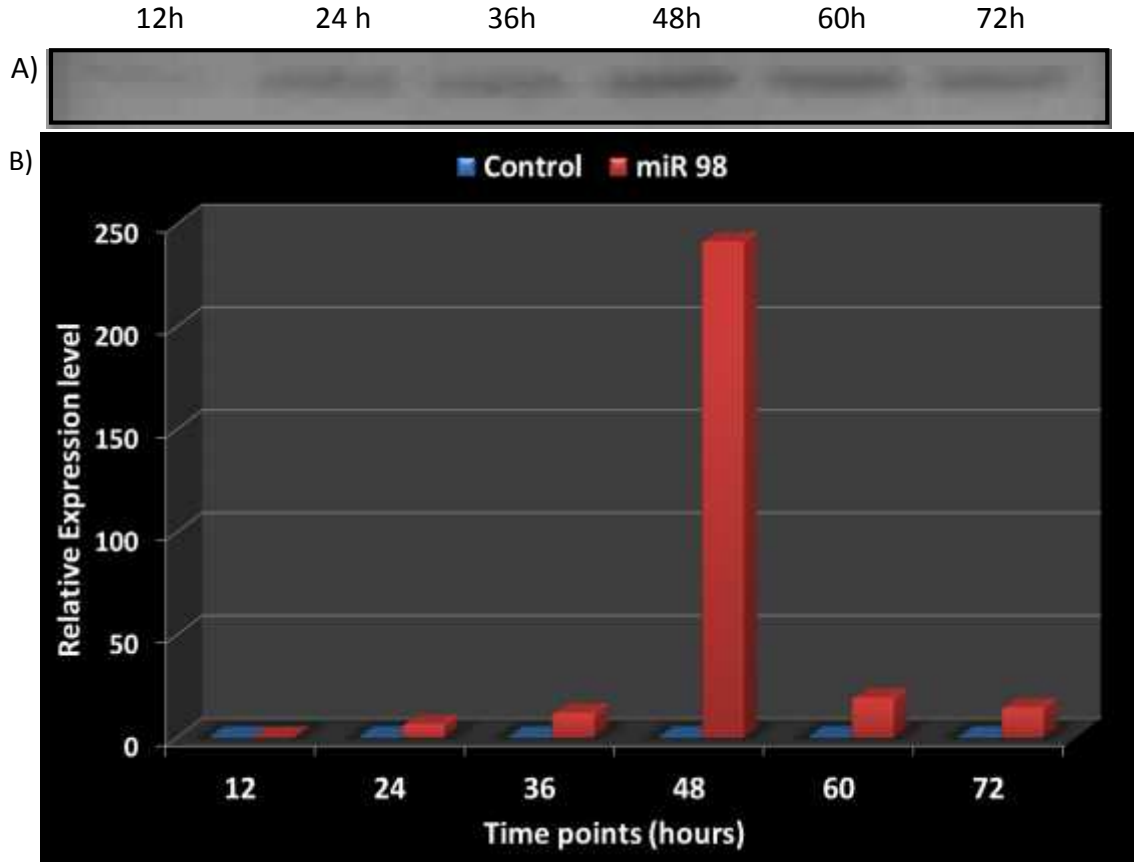

Figure 25: Real-time RT-PCR analysis of micro RNA 98 expression in the control and JEV infected P388D1 cells. Synthesized cDNA from the isolated RNA from the JEV infected and control P388D1 cells were amplified using primer specific for miR-98 (M98F and M98R). Real time PCR was performed to analyze the relative expression of miR-98. (A) The amplified PCR product miR-98 at different time points as examined on 1.2% agarose gel. (B) Bar graph representing the fold changes of more quantified by normalizing to the GAPDH as an internal control.

4.4.5 REAL TIME PCR for relative quantification of miR-27a

Real time PCR was also performed using primers specific for miR-27a in the JEV infected and mock infected P388D1 cells. RNA isolated from the control and test samples were converted into cDNA. Dilution of synthesized cDNA was performed to get the optimum concentration and Real time PCR was performed using primers designed for miR-27a. Bar graph was plotted from the Real time PCR data which shows that the expression of miR-27a remains at low level till 36 hrs p.i. and shows high level of expression at 48 hrs p.i. The expression level of miR-27a again decreased after 48 hrs p.i. as shown in figure 26.

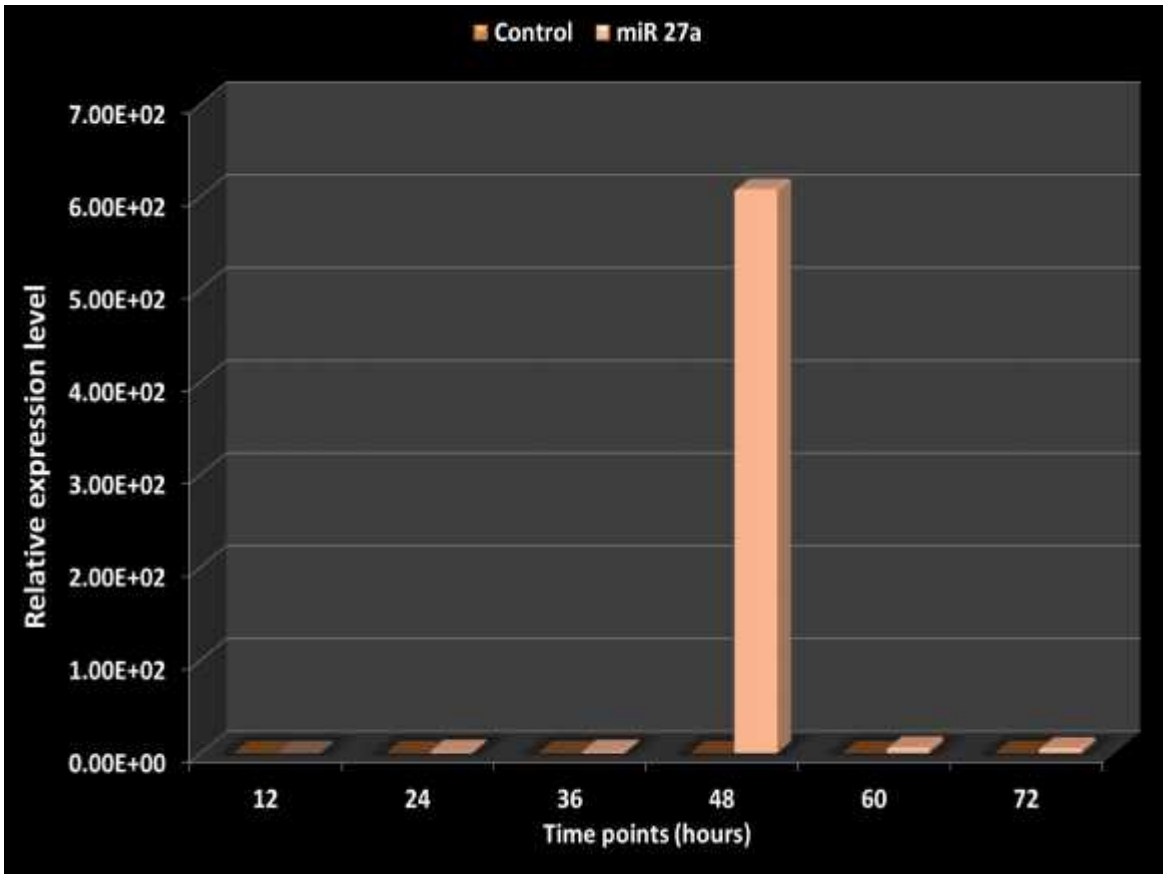

Figure 26: Real-time RT-PCR analysis of micro RNA 27a expression in the control and JEV infected P388D1 cells. Prepared cDNA from the total RNA isolated from the control and JEV infected P388D1 cells. Real time PCR was carried out from the cDNA using primer specific for miR-27a (M27F and M27R) with SYBR green reaction mixture. Bar graph representing the fold changes of miR-27a quantified by normalizing to the GAPDH as an internal control was plotted as shown in the figure.

4.4.6 REAL TIME PCR for relative quantification of miR-106b

Expression of miR-106 was checked using Real Time PCR from the total RNA isolated from the JEV infected and mock infected control P388D1 cells. RNA was isolated from the JEV infected cells and the mock infected control cells at each time point and cDNA was synthesized using random primers. Dilution of the synthesized cDNA was performed to get the optimum concentration of cDNA and Real time PCR was done to amplify precursor miR-106b using specific primers. Plotting bar graph from the obtained data shows miR-106b expression remains at low level till 36 hrs p.i. and shows high level of expression at 48 hrs p.i. The expression level of miR-106b again decreased after 48 hrs p.i. (Figure 27).

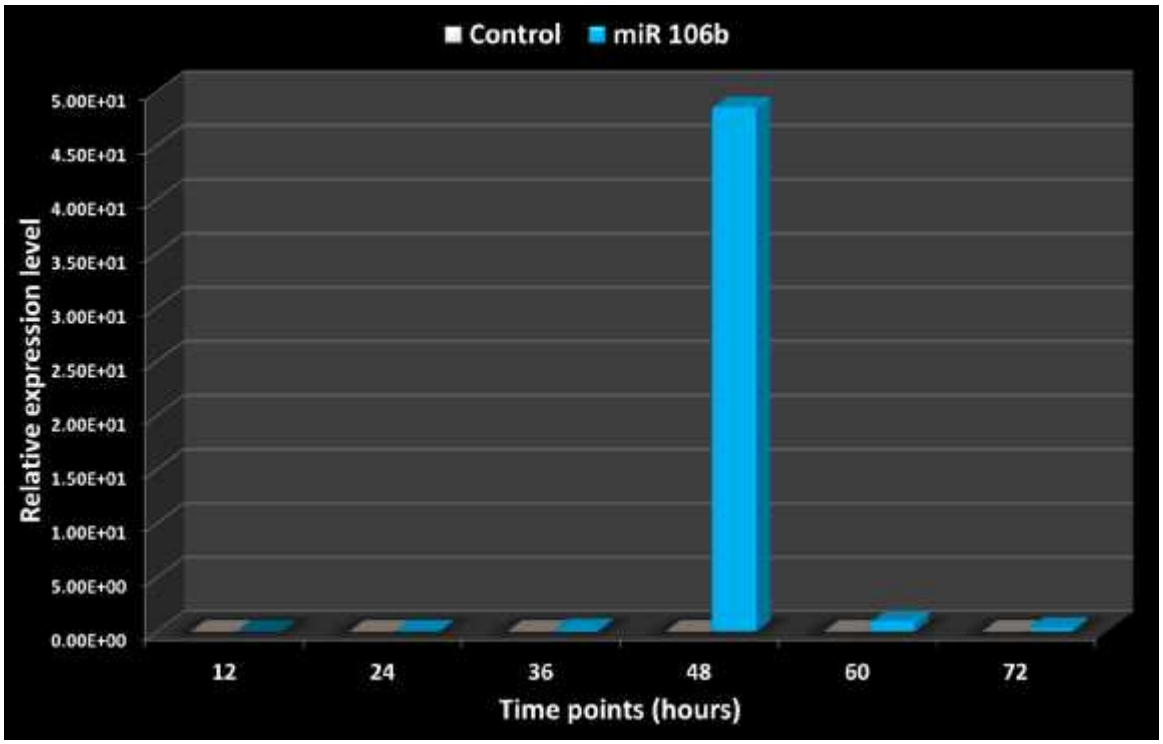

Figure 27: Real-time RT-PCR analysis of micro RNA 106b expression in the control and JEV infected P388D1 cells. Prepared cDNA from the total RNA isolated from the control and JEV infected P388D1 cells. Real time PCR was carried out from the cDNA using primer specific for miR-106b (M106F and M106R) with SYBR green reaction mixture. The relative expression value quantified by normalizing to the GAPDH as an internal control was plotted as Bar Graph as shown in the figure.

4.4.7 Compared Relative expression

Graph was plotted to compare the expression of miR-98, mi-27a and miR-106b in relation to the expression of IL-10 in the JEV infected P388D1 cells. In case of micro RNAs i.e miR-98, miR-27a and miR-106b concordant result was observed with the maximum expression at 48 hrs p.i. The expression level was relatively higher in miR-27a, followed by miR-98 and miR-106b respectively as shown in the figure 28.

A)

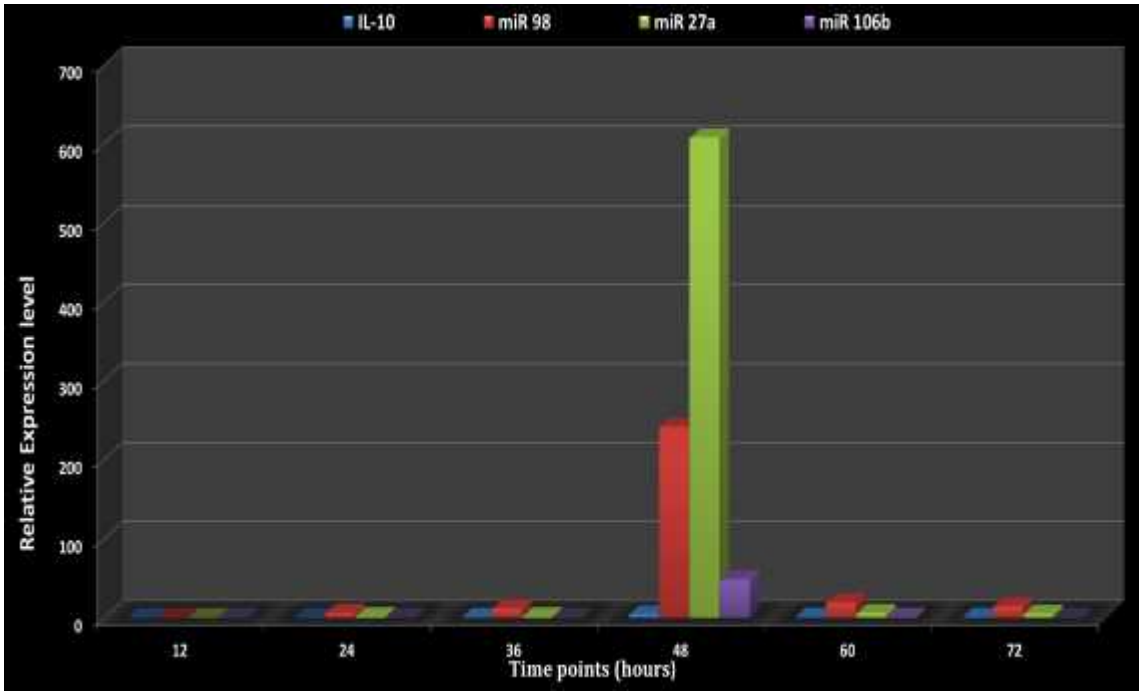

B)

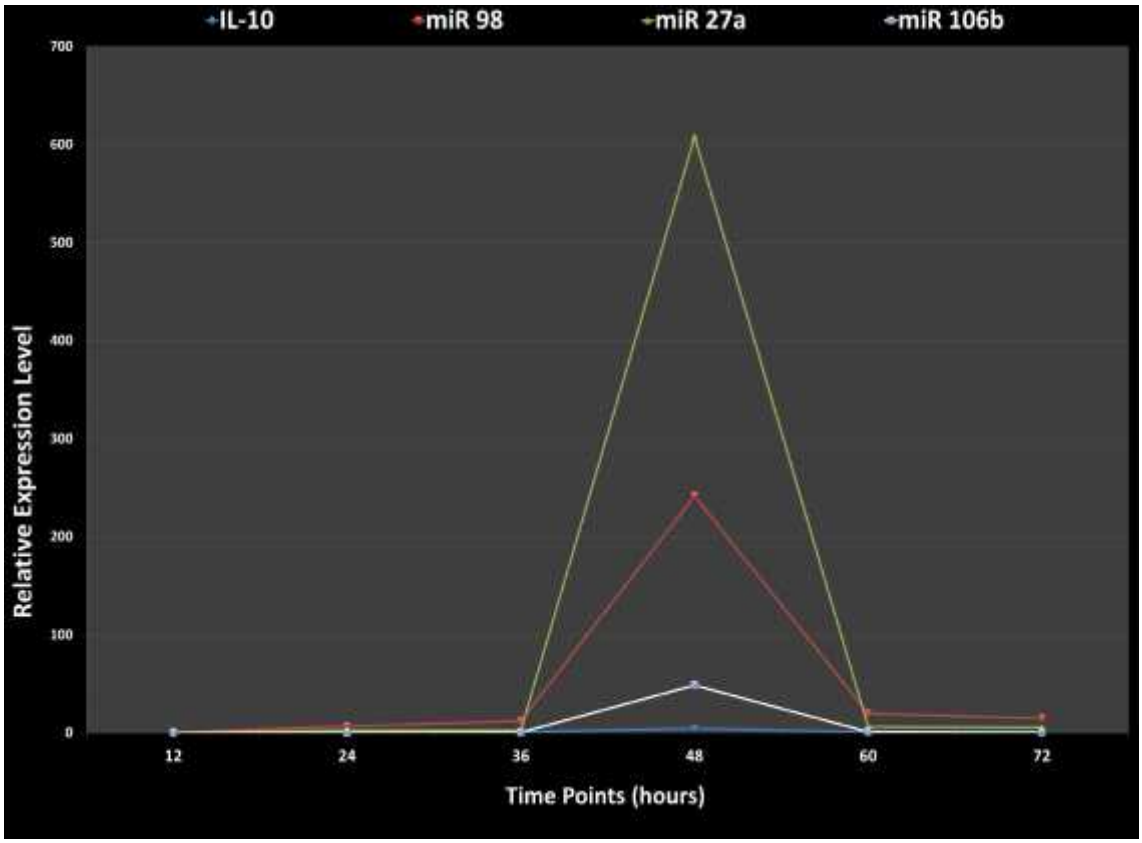

Figure 28: The relative expression of IL-10, miR-98, miR-27a and miR-106b was plotted on a single graph. (A) Comparative view of the relative expression of mouse Interleukin-10 mRNA and micro RNAs during JEV infection. (B) Graphical representation of the gradual change in the expression mouse interleukin-10 mRNA and micro RNAs after JEV infection.

4.5 Protein expression analysis of Interleukin-10

Expression of Interleukin-10 protein was studied on P388D1 cell lines by western blotting. Figure 29 show the expression of IL-10 in the JEV infected P388D1 cells. Serum from the LPS infected Bal b/c mice was used as the positive control and normal serum was used as a negative control to detect the expression level of IL-10. P388D1 cells were cultured overnight in RPMI media constituted with 10% FBS in 5% CO_2 incubator and were infected with JEV. At an interval of 12 hours, culture supernatant was collected and the expression of IL-10 protein was checked by western blotting. Expression of IL-10 in the test samples was below the detection level of western blotting in all the time points signifying very low expression of IL-10 protein.

Figure 29: Protein expression analysis of Interleukin-10 in the JEV infected P388D1 cells by Western blotting. Cells were infected with JEV and the expression of IL-10 was checked at different time points using monoclonal antibody specific for mouse IL-10. Serum samples from the infected Bal b/c mice was used as a positive control and for negative control normal fetal bovine serum was used.

CHAPTER 5

DISCUSSION

5.1 Study of sequence diversity in NS3 gene in the novel strain GP05 of Japanese encephalitis virus

In flavivirus, the NS3 protein plays an important role in immune response along with the viral replication and packing. Among all the non-structural proteins, NS3 is extensively studied due to its role in the replication and pathogenesis of the virus. In the context of the host immune response NS3 protein has been shown to be the most frequently targeted antigen, has the capability of eliciting highest level of proliferation of T cell and IFN-γ secretion as compared with E protein, NS1 protein and NS5 protein (kumar *et al*, 2004).

5.1.1 Sequencing the NS3 gene of JEV and performing phylogenetic analysis

Results from the CLUSTALW multiple alignment of obtained NS3 sequence showed the presence of nucleotide variation in multiple positions of the NS3 gene in JEV gp05 strain in comparison to the JEV gp78 strain reported in NCBI gene bank (Figure 17). Nucleotide Transitions from T to C were found to be more frequent than other mutations (Table 17).

Phylogenetic analysis of NS3 gene sequence of JEV gp05 showed homology with the Japanese Strain JaoArS982 rather than the reference sequence JEV gp78 (Figure 18). JaoArS982 was the first JEV strain to be completely sequenced and referred as the prototype JEV sequence (Vrati *et al*, 1999). This provides an insight about the frequency of mutation occurring in the JEV genome, which accounts for the antigenic shift among the variants, causing the emergence of the more pathogenic and resistance virus. However, incomplete sequence data were obtained so far due to the technical difficulties, the exact phylogenetic position and relationship are yet to be determined. Thus the complete DNA sequence of NS3 region of JEV gp05 is required to validate the data and claim a premise.

5.1.2 Performing Homology Modeling of the NS3 protein from the obtained sequence and predict ligand binding sites on the protein

3D-ligand binding analysis showed the amino acids Threonine, Tyrosine, Leucine, Histidine, Proline, Glycine, Leucine, Glycine, Lysine, Threonine, Arginine, Glutamine, Aspargine and Arginine at positions 58, 60, 186, 187, 188, 189, 190, 191, 192, 193, 194, 278, 409 and 456 respectively are important ligand binding sites as the molecule ADP

and Magnesium (Mg) interacted with this position (Figure 20). The ligand binding analysis showed that the amino acid residues 186 to 194 serve as a hot spot for ligand binding. As the NS3 protein is an enzyme, efficient binding of ADP and Mg is critical for its functioning. Any changes in these amino acid positions can alter the enzyme efficiency. The complete information obtained after the further study and validation of the present research work can be utilized for the drug development against the JEV infection.

5.2 Study of the regulatory mechanism of Interleukin-10 production during Japanese encephalitis infection via micro RNAs.

Host pathogen interaction plays a crucial role in determining pathological consequences during various viral infections. On one side, host defense mechanisms have required on-going adaptation to combat infection, whereas, under survival pressure from sophisticated defense mechanisms, viruses have evolved immune-evasion strategies. In such cases, optimal regulation is vital for significant immune response while limiting the errant immunopathological consequences. This feature is maintained by the immunomodulatory cytokines, which governs the immune response during infections and assure the optimal level of immune response.

Interleukin-10 (IL-10), also termed as cytokine synthesis inhibitory factor (CSIF), is a potent anti-inflammatory and immunosuppressive cytokine. IL-10 is produced by various cell types, which include DC, B cells, macrophages, CD4 T cells, CD8 T cells, NK cells as well as innate and adaptive regulatory T cells (Wilson and Brooks, 2011) and is a major factor of Th2 immune response. It works in parallel during host defense against various pathogens, and checks over exuberant immune responses and prevents reactivity to self to limit host damage (Brooks et al, 2006). IL-10 also promotes survival of neurons and all glial cells in the brain by blocking the effects of proinflammatory cytokines and by promoting expression of cell survival signals.

Pathological outcome during JEV infection is the combined effect of infection of neurons by JEV and damage caused by activated microglia. This activated microglia provokes the production of the inflammatory cytokines such as TNF-α and IFN-γ. Neuroinflammation results in the neuronal loss which can be fatal sometimes. Even though the fatality rate of JE is 25-30%, 50% of the persons escaping death will have various neurological sequels such as learning difficulties, behavioral problems, etc. IL-10 in such case balances this adverse inflammatory reaction thus protecting the host cell. Thus, regulation of IL-10 level during JEV infection plays a crucial role in determining the pathological outcome.

5.2.1 Determination of viral infection in cell culture

To check the presence of the live and actively replicating virus, plaque assay and Immuno staining was performed in BHK-21 cells. BHK-21 cells were selected for the study as they replicated fast and show active viral replication in them. Immuno staining technique was performed by using primary antibody specific for the envelope protein of JEV for the confirmation of the viral infection and viral replication. The immunostaining observation showed efficient viral infection and viral replication in BHK-21 cells. The cell number decreased gradually along with the time points and certain cytosolic changes such as shrinkage of cells were observed, fluorescence was observed in the cytosolic region of the cell indicating viral replication. Fluorescence was observed only in the cytosolic region of the cells, indicating that the viral replication and translation occur primarily in the cytosol. The nucleus of the cells was intact and round, which shows that virus do not cause any nuclear damage during the replication.

The plaque assay was carried out to check for the viral titre. Microscopic plaques were observed on 4^{th} day post infection. The plaque assay results showed that the viral stock solution contains 1 x 10^{11} PFU/ml viruses. Result from the plaque assay and immunostaining showed that viral inoculum consists of the live and actively replicating viruses. They are also capable of efficiently infecting the cells and causing cellular damage, as correlated with the formation of plaques and decrease of cell number. P388D1 cells were selected for the study as the virus shows active replication in these cells. During the study cells were cultured in RPMI 1640 medium and were infected with JEV. When observed in the microscope the cell number decreased gradually in the test samples, which were infected with JEV, showing viral infection in cells.

5.2.2 Relative expression of Interleuki-10 and selected microRNAs

With the discovery of microRNAs, various studies have been performed to understand their role in the post transcriptional regulation of gene expression. Concerning about the popularity of microRNAs, they have been shown to play a critical role in determining pathological outcome during viral infections, including JE. Expression of miR-155 has been shown to increase, in correlation with target genes, during JEV infection in time dependent manner (Thounaojam *et al*, 2014; Pareek *et al*, 2014). The miR-155 has been demonstrated to inhibit expression of Src homology 2-containing inositol phosphatase 1 (SHIP1) protein, enhance CD45 expression, reduce pro-inflammatory cytokines and Complement Factor H (CFH) expression by targeting several key genes, and suppress JEV replication in microglial cells (Thounaojam *et al*, 2014; Pareek *et al*, 2014). Furthermore, miR-29b has been shown to modulate the inflammatory response during JEV infection by targeting tumor necrosis factor alpha-induced protein 3 (Thounaojam *et al*, 2014).

Earlier studies have revealed a role of miR-98 and miR-27a in mouse cell culture when induced by lipopolysaccharide (Liu *et al*, 2011; Xie *et al*, 2014). These microRNAs have been shown to negatively regulate the expression of IL-10 in the LPS induced macrophages. Our *in silico* studies have given an insight for miR-106b as a possible regulator of the IL-10 expression (material and methods). The present study indicated the significant IL-10 mRNA expression that starts from 36 hrs p.i., with maximum expression at 48 hrs p.i., followed by a gradual decline (Figure 24). This shows that IL-10 expression occurs during JEV infection to balance the inflammatory reaction. A similar feature was observed in case of miR-98, miR-27a and miR-106b also (Figure 25, 26 and 27). However, expression of miR-27a was relatively higher as compared to miR-98 and miR-106b, signifying that miR-27a might be having a more potent role in regulation of IL-10 expression than miR-98 and miR-106b (Figure 28). In spite of the increase in the expression of IL-10 mRNA during JEV infection, the level of IL-10 protein was below detection levels by Western blotting in all the time points (Figure 29). This observation, in some ways, can be explained by the post transcriptional regulation of IL-10 gene by the microRNAs. With this it is concluded that miRs might be regulating the expression of IL-10 at the posttranscriptional level. Therefore, combining both *in silico* and *in vitro* data, it can be proposed that miR-98, miR-27a and miR-106b might have a potential role in posttranscriptional regulation of IL-10 expression during JEV gp05 infection.

Thus with the utilization of anti-miR, the level of IL-10 can be regulated and maintain an immunological homeostasis during JEV infection. This can be fruitful to prevent the neurological damage caused by the activated microglial cells. Along with this, the identification of the potent epitope in NS3 protein can be utilized to design the DNA vaccine against JEV in the future.

CHAPTER 6

SUMMARY AND CONCLUSION

6.1 SUMMARY

In the present research work novel JEV strain gp05 was used to study the host immune response focussing on IL-10 expression and its regulation via micro RNAs. DNA sequence analysis of NS3 gene of JEV gp05 was performed. Primer specific for NS3 gene were used to perform normal PCR, which was followed by DNA sequencing PCR. The sequence thus obtained was utilized to perform the phylogenetic analysis of JEV gp05 strain. The sequence was further translated *in silico* into corresponding amino acids and probable protein structure, as well as ligand binding sites were predicted using phyre2 and 3D ligand binding software. In context of the host immune response, cell culture based studies were done. Micro RNAs were selected on the basis of previously published papers (miR-98 and miR-27a) and *in silico* analysis (miR-106b). From the *in silico* analysis miR-106b was found to the potent microRNAs having ability to bind with the 3'UTR of IL-10 mRNA. P388D1 cells were cultured and infected with JEV gp05. At each time points from 12 hrs to 72 hrs p.i., infected cells were lysed and total RNA was isolated. The RNA thus obtained was utilized for cDNA synthesis. Expression analysis of IL-10 and selected microRNAs were done using Real Time PCR from the synthesized cDNA. To analyse the expression of IL-10 protein, western blotting was done using primary monoclonal antibody specific for mouse IL-10 protein.

Phylogenetic analysis showed that the novel strain JEV gp05 have a close relationship with the Japanese stain JaoArS982 on the basis of NS3 gene sequence. The 3D-ligand binding analysis showed the amino acids Threonine, Tyrosine, Leucine, Histidine, Proline, Glycine, Leucine, Glycine, Lysine, Threonine, Arginine, Glutamine, Aspargine and Arginine at positions 58, 60, 186, 187, 188, 189, 190, 191, 192, 193, 194, 278, 409 and 456 respectively are important ligand binding sites as the molecule ADP and Magnesium (Mg) interacted with these position. Results obtained from Real Time PCR showed significant IL-10 mRNA expression that starts from 36 hrs p.i., with maximum expression at 48 hrs p.i., followed by a gradual decline. Similar results were obtained in case of microRNAs (miR-98, miR-27a and miR-106b) expression also. In this experiment, although the increase in expression of IL-10 mRNA was observed during JEV infection, protein levels were below detection levels in all the time points indicating the fact that the translation of IL-10 mRNA was hindered by those selected microRNAs. From this observation we can propose that these micro RNAs (miR-98, miR-27a and miR-106b) might have a potential role in post transcriptional regulation of the expression of IL-10 during JEV infection.

6.2 CONCLUSION

Since the first reported cases of JEV from Japan in 1871, there have been various epidemics in various countries of Asia. Spread of JE as far as Australia and evolution of new genotypes, made the virus potential to be a global threat. In such scenario understanding of the viral genome, pathogenesis and host defence mechanism can provide a new avenue for the therapeutic approach against JE. In context of JE, as the disease is a result of immune pathogenesis due to viral infection, primary focus is targeted to viral NS3 protein and host Interleukin-10 protein. Thus the experiment was conducted to cover both the aspects of pathogenesis of JEV, including immunogenic protein of virus and major immune-regulatory protein of host defence.

NS3 is also the most conserved gene in the viral genome and is also found to be the most potent immunogen. Sequencing and proteomic analysis was done in order to explore the nucleotide variation in the NS3 gene of Novel JEV strain gp05. From the present experiment, the novel strain JEV gp05 has been shown to have various nucleotide variations as compared to JEV gp78. Transition from T to C was found to be more frequent than other nucleotide variation. Phylogenetic analysis showed that NS3 gene of JEV gp05 shows close relationship with the Japanese Strain JaoArS982. The proteomic analysis of serine protease domain of NS3 protein shows its ability to bind with the two co-factors ADP and Mg, which are required for the proper functioning of the protein.

The present also study illustrates that Interleukin-10 level mRNA expression increases at the 36 hrs p.i. to compensate the inflammatory response during JEV infection. However, this increase in the IL-10 mRNA level is in parallel with the increase in the expression of miR-98, miR-27a and miR-106b. Although there is increase in the expression of IL-10 mRNA during JEV infection, the level of IL-10 protein was below detection levels. Thus, from the experiment we may conclude that these micro RNAs might be having a potential role in posttranscriptional regulation of Interleukin-10 expression during Japanese encephalitis virus infection.

RECOMMENDATIONS

- To understand the molecular basis of immunity of JEV infection, complete sequence of the genome is required.

- Complete molecular characterization of JEV gp05 genome need to be done to obtain the reliable phylogenetic characterization of the strain.

- Confirmation of the antigenic efficacy of the NS3 protein should be done in order to use it as a candidate epitope to design genetic vaccine against JEV gp05.

- Further analysis of the post transcriptional regulation of IL-10 by micro RNAs is necessary, using robust micro RNA expression analysis techniques, cloning techniques and expression analysis of IL-10 protein.

- Study needs to be done using all the microRNAs which have the capability of binding with 3'UTR region of IL-10.

REFERENCES

Aleyas AG, George JA, Han YW, Rahman MM, Kim SJ, Han SB, Kim BS, Kim K, Eo SK (2009) Functional modulation of dendritic cells and macrophages by Japanese encephalitis virus through MyD88 adaptor molecule-dependent and -independent pathways. *J Immunol*. **183**(4): 2462-2474

Aleyas AG, Han YW, Patil AM, Kim SB, Kim K, Eo SK (2012) Impaired cross-presentation of CD8α+ CD11c+ dendritic cells by Japanese encephalitis virus in a TLR2/MyD88 signal pathway-dependent manner. *Eur J Immunol*. **42**(10): 2655-2666

Allison, S. L., Stadler, K., Mandl, C. W., Kunz, C. & Heinz, F. X (1995) Synthesis and secretion of recombinant tick-borne encephalitis virus protein E in soluble and particulate form. *J. Virol*. **69**: 5816–5820

Bai F, Town T, Qian F, Wang P, Kamanaka M, Connolly TM, Gate D, Montgomery RR, Flavell RA, Fikrig E (2009) IL-10 signaling blockade controls murine West Nile virus infection. *PLoS Pathog*. **5**(10): 1-13

Bhattachan A, Amatya S, Sedai TR, Upreti SR, Partridge J (2009) Japanese encephalitis in hill and mountain districts, Nepal. *Emerg Infect Dis* 15: 1691–1692.

Bista MB, Shrestha JM. Epidemiological situation of Japanese encephalitis in Nepal. *JNMA J Nepal Med Assoc.* 2005 Apr-Jun;44(158):51-6. PubMed PMID: 16554872.

Biswas SM, Ayachit VM, Sapkal GN, Mahamuni SA, Gore MM (2009) Japanese encephalitis virus produces a CD4+ Th2 response and associated immunoprotection in an adoptive-transfer murine model. *J Gen Virol*. **90**(Pt 4): 818-826

Borah J, Dutta P, Khan SA, Mahanta J (2011) A comparison of clinical features of Japanese encephalitis virus infection in the adult and pediatric age group with Acute Encephalitis Syndrome. *J Clin Virol*. **52**(1): 45-49

Brinton, M. A (2002) The molecular biology of West Nile virus: a new invader of the western hemisphere. *Annu. Rev. Microbiol*. **56**: 371–402

Brooks DG, Trifilo MJ, Edelmann KH, Teyton L, McGavern DB, Oldstone MB (2006) Interleukin-10 determines viral clearance or persistence in vivo. *Nat Med*. **12**(11): 1301-1309

Cao QS, Li XM, Zhu QY, Wang DD, Chen HC, Qian P (2011) Isolation and molecular characterization of genotype 1 Japanese encephalitis virus, SX09S-01, from pigs in China. *Virol J.* **8**(472): 1-9

Cao S, Li Y, Ye J, Yang X, Chen L, Liu X, Chen H (2011) Japanese encephalitis Virus wild strain infection suppresses dendritic cells maturation and function, and causes the expansion of regulatory T cells. *Virol J.* **8**(39): 1-11

Chanama S, Sukprasert W, Sa-ngasang A, A-nuegoonpipat A, Sangkitporn S, Kurane I, Anantapreecha S (2005) Detection of Japanese encephalitis (JE) virus-specific IgM in cerebrospinal fluid and serum samples from JE patients. *Jpn J Infect Dis*. **58**(5): 294-296

Chao DY, Galula JU, Shen WF, Davis BS, Chang GJ (2015) Nonstructural protein 1-specific immunoglobulin m and g antibody capture enzyme-linked immunosorbent assays in diagnosis of flaviviral infections in humans. *J Clin Microbiol*. **53**(2): 557-566

Chen CJ, Ou YC, Chang CY, Pan HC, Liao SL, Chen SY, Raung SL, Lai CY (2012) Glutamate released by Japanese encephalitis virus-infected microglia involves TNF-α signaling and contributes to neuronal death. *Glia*. **60**(3): 487-501

Chen CJ, Ou YC, Li JR, Chang CY, Pan HC, Lai CY, Liao SL, Raung SL, Chang CJ (2014) Infection of pericytes in vitro by Japanese encephalitis virus disrupts the integrity of the endothelial barrier. *J Virol*. **88**(2): 1150-1161

Chen CJ, Ou YC, Lin SY, Raung SL, Liao SL, Lai CY, Chen SY, Chen JH (2010) Glial activation involvement in neuronal death by Japanese encephalitis virus infection. *J Gen Virol*. **91**(Pt 4): 1028-1037

Chiou CT, Hu CC, Chen PH, Liao CL, Lin YL, Wang JJ (2003) Association of Japanese encephalitis virus NS3 protein with microtubules and tumour susceptibility gene 101 (TSG101) protein. *J Gen Virol*. **84**(Pt 10): 2795-2805

Deng J, Pei J, Gou H, Ye Z, Liu C, Chen J (2014) Rapid and simple detection of Japanese encephalitis virus by reverse transcription loop-mediated isothermal amplification combined with a lateral flow dipstick. *J Virol Methods*. **213C:** 98-105

Deng X, Shi Z, Li S, Wang X, Qiu Y, Shao D, Wei J, Tong G, Ma Z (2011) Characterization of nonstructural protein 3 of a neurovirulent Japanese encephalitis virus strain isolated from a pig. *Virol J*. **8**(209): 1-10

Duong V, Sorn S, Holl D, Rani M, Deubel V, Buchy P (2011) Evidence of Japanese encephalitis virus infections in swine populations in 8 provinces of Cambodia:

implications for national Japanese encephalitis vaccination policy. *Acta Trop*. **120**(1-2): 146-150

Endy TP, Nisalak A, (2002) Japanese encephalitis virus: ecology and epidemiology. *Curr Top Microbiol Immunol*. **267***:* 11–48

Joshi AB, Banjara MR, Bhatta LR and Wierzba T (2004) Status and Trend of Japanese encephalitis Epidemics in Nepal: A Five-Year Retrospective Review. *Journal of Nepal Health Research Council*. **2**(1); 59-64

Ghosh D, Basu A (2009) Japanese encephalitis-a pathological and clinical perspective. *PLoS Negl Trop Dis*. **3**(9): 1-7

Gupta N, Hegde P, Lecerf M, Nain M, Kaur M, Kalia M, Vrati S, Bayry J, Lacroix-Desmazes S, Kaveri SV (2014) Japanese encephalitis virus expands regulatory T cells by increasing the expression of PD-L1 on dendritic cells. *Eur J Immunol*. **44**(5): 1363-1374

Hall RA, Scherret JH and Mackenzie JS: Kunjin virus, (2001) An Australian variant of West Nile? Ann N Y Acad. *Sci.* **951**: 153-160

Hanna JN, Ritchie SA, Phillips DA, Shield J, Bailey MC, Mackenzie JS, Poidinger M, McCall BJ and Mills PJ, (1995) An outbreak of Japanese encephalitis in the Torres Strait, Australia. *Med. J*. **165**: 256-260

Han XY, Ren QW, Xu ZY, Tsai TF (1988) Serum and cerebrospinal fluid immunoglobulins M, A, and G in Japanese encephalitis. *J Clin Microbiol*. **26**(5): 976-978

Hase T, Summers PL, Ray P (1990) Entry and replication of Japanese encephalitis virus in cultured neurogenic cells. *J Virol Methods*. **30**(2): 205-214

Jin R, Zhu W, Cao S, Chen R, Jin H, Liu Y, Wang S, Wang W, Xiao G (2013) Japanese encephalitis virus activates autophagy as a viral immune evasion strategy. *PLoS One.* **8**(1): 1-11

Kalia M, Khasa R, Sharma M, Nain M, Vrati S (2013) Japanese encephalitis virus infects neuronal cells through a clathrin-independent endocytic mechanism. *J Virol.* **87**(1): 148-162

Kakoti G, Prafulla Dutta, Bishnu Ram Das, Jani Borah, and Jagadish Mahanta (2013) Clinical Profile and Outcome of Japanese Encephalitis in Children Admitted with Acute Encephalitis Syndrome. *BioMed Research International.* **152656**: 1-5

Khan SU, Salje H, Hannan A, Islam MA, Bhuyan AA, Islam MA, Rahman MZ, Nahar N, Hossain MJ, Luby SP, Gurley ES (2014) Dynamics of Japanese Encephalitis Virus Transmission among Pigs in Northwest Bangladesh and the Potential Impact of Pig Vaccination. *PLoS Negl Trop Dis*. **8**(9): 1-9

Kimura-Kuroda J, Yasui K (1988) Protection of mice against Japanese encephalitis virus by passive administration with monoclonal antibodies. *J Immunol.* **141**(10): 3606-3610

Kumar JS, Parida M, Rao PV (2011) Monoclonal antibody-based antigen capture immunoassay for detection of circulating non-structural protein NS1: implications for early diagnosis of Japanese encephalitis virus infection. *J Med Virol.* **83**(6):1063-1070

Kumar P, Krishna VD, Sulochana P, Nirmala G, Haridattatreya M, Satchidanandam V (2004) Cell-mediated immune responses in healthy children with a history of subclinical infection with Japanese encephalitis virus: analysis of CD4+ and CD8+ T cell target specificities by intracellular delivery of viral proteins using the human immunodeficiency virus Tat protein transduction domain. *J Gen Virol*. **85**(Pt 2): 471-482

Kuno G (2003) Serodiagnosis of flaviviral infections and vaccinations in humans. *Adv Virus Res.* **61**: 3-65.

Kuo MD, Chin C, Hsu SL, Shiao JY, Wang TM, Lin JH (1996) Characterization of the NTPase activity of Japanese encephalitis virus NS3 protein. *J Gen Virol*. **77**(Pt 9): 2077-2084

Kurane, I., Brinton, M. A., Samson, A. L. & Ennis, F. A (1991) Dengue virus-specific, human CD4+ CD82 cytotoxic T-cell clones: multiple patterns of virus cross-reactivity recognized by NS3-specific T-cell clones. *J Virol.* **65**: 1823–1828

Larena M, Regner M, Lee E, Lobigs M (2011) Pivotal role of antibody and subsidiary contribution of CD8+ T cells to recovery from infection in a murine model of Japanese encephalitis. *J Virol*. **85**(11): 5446-5455

Larena M, Regner M, Lobigs M (2013) Cytolytic effector pathways and IFN-γ help protect against Japanese encephalitis. *Eur J Immunol*. **43**(7): 1789-1798

Lee Y, Ahn C, Han J, Choi H, Kim J, Yim J, Lee J, Provost P, Rådmark O, Kim S, Kim VN (2003) The nuclear RNase III Drosha initiates microRNA processing. *Nature*. **425**(6956): 415-419.

Lee Y, Kim M, Han J, Yeom KH, Lee S, Baek SH, Kim VN (2004) MicroRNA genes are transcribed by RNA polymerase II. *EMBO J*. **23**(20): 4051-4060.

Li F, Mei L, Li Y, Zhao K, Chen H, Wu P, Hu Y, Cao S (2011) Facile fabrication of magnetic gold electrode for magnetic beads-based electrochemical immunoassay: application to the diagnosis of Japanese encephalitis virus. *Biosens Bioelectron*. **26**(10): 4253-4256

Li L, Lok SM, Yu IM, Zhang Y, Kuhn RJ, Chen J, Rossmann MG (2008) The flavivirus precursor membrane-envelope protein complex: structure and maturation. *Science.* **319**(5871): 1830-1834

Li MH, Fu SH, Chen WX, Wang HY, Cao YX, Liang GD (2014) Molecular characterization of full-length genome of Japanese encephalitis virus genotype V isolated from Tibet, China. *Biomed Environ Sci*. **27**(4): 231-239

Li MH, Fu SH, Chen WX, Wang HY, Guo YH, Liu QY, Li YX, Luo HM, Da W, Duo Ji DZ, Ye XM, Liang GD (2011) Genotype v Japanese encephalitis virus is emerging. *PLoS Negl Trop Dis*. **5**(7): 1-7

Lindenbach B D, Thiel H J, Rice C M (2007) Flaviviridae: The Viruses and Their Replication, Vol V, Chapter 33, pub D. M. Knipe and P. M. Howley, Eds. Lippincott-Raven Publishers, Philadelphia: 1101-1152 pp

Lin RJ, Chang BL, Yu HP, Liao CL, Lin YL (2006) Blocking of interferon-induced Jak-Stat signaling by Japanese encephalitis virus NS5 through a protein tyrosine phosphatase-mediated mechanism. *J Virol*. **80**(12): 5908-5918

Lin YL, Chen LK, Liao CL, Yeh CT, Ma SH, Chen JL, Huang YL, Chen SS, Chiang HY (1998) DNA immunization with Japanese encephalitis virus nonstructural protein NS1 elicits protective immunity in mice. *J Virol*. **72**(1): 191-200.

Lindenbach, B. D. & Rice, C. M (2003) Molecular biology of flaviviruses. *Adv. Virus Res.* **59:** 23–61

Liu Y, Chen Q, Song Y, Lai L, Wang J, Yu H, Cao X, Wang Q (2011) MicroRNA-98 negatively regulates IL-10 production and endotoxin tolerance in macrophages after LPS stimulation. *FEBS Lett*. **585**(12): 1963-1968

Liu, W. J., Sedlak, P. L., Kondratieva, N. & Khromykh, A. A (2002) Complementation analysis of the flavivirus Kunjin NS3 and NS5 proteins defines the minimal regions essential for formation of a replication complex and shows a requirement of NS3 in cis for virus assembly. *J Virol*. **76:** 10766–10775

Livingston, P. G., Kurane, I., Dai, L. C., Okamoto, Y., Lai, C. J., Men, R., Karaki, S., Takiguchi, M. & Ennis, F. A (1995) Dengue virus-specific, HLA-B35-restricted, human CD8+ cytotoxic T lymphocyte (CTL) clones. Recognition of NS3 amino acids 500 to 508 by CTL clones of two different serotype specificities. *J Immunol*. **154**: 1287–1295

Lobigs M, Diamond MS (2012) Feasibility of cross-protective vaccination against flaviviruses of the Japanese encephalitis serocomplex. *Expert Review of Vaccines*. **11**(2): 177-187

Lobigs, M., Arthur, C. E., Mullbacher, A. & Blanden, R. V. (1994) The flavivirus nonstructural protein NS3 is a dominant source of cytotoxic T cell peptide determinants. *Virology* **202**: 195–201

Luca VC, AbiMansour J, Nelson CA, Fremont DH (2012) Crystal structure of the Japanese encephalitis virus envelope protein. *J Virol*. **86**(4): 2337-2346

Lund E, Güttinger S, Calado A, Dahlberg JE, Kutay U (2004) Nuclear export of microRNA precursors. *Science*. **303**(5654): 95-8.

Mackenzie JS, Gubler DJ, Petersen LR (2004) Emerging flaviviruses: the spread and resurgence of Japanese encephalitis, West Nile and dengue viruses. *Nat Med*. **10**(S): 98-109

Mathew, A., Kurane, I., Rothman, A. L., Zeng, L. L., Brinton, M. A. & Ennis, F. A (1996) Dominant recognition by human CD8+ cytotoxic T lymphocytes of dengue virus nonstructural proteins NS3 and NS1.2a. *J Clin Invest*. **98**: 1684–1691

Mathur A, Arora KL, Chaturvedi UC (1981) Congenital infection of mice with Japanese encephalitis virus. *Infect Immun*. **34**(1): 26-29

Mathur A, Kumar R, Sharma S, Kulshreshtha R, Kumar A, Chaturvedi UC (1990) Rapid diagnosis of Japanese encephalitis by immunofluorescent examination of cerebrospinal fluid. *Indian J Med Res*. **91**: 1-4

Mishra MK, Dutta K, Saheb SK, Basu A (2009) Understanding the molecular mechanism of blood-brain barrier damage in an experimental model of Japanese encephalitis: correlation with minocycline administration as a therapeutic agent. *Neurochem Int.* **55**(8): 717-723

Mogensen TH (2009) Pathogen recognition and inflammatory signaling in innate immune defenses. *Clin Microbiol Rev*. **22**(2): 240-273

Mohammed MA, Galbraith SE, Radford AD, Dove W, Takasaki T, Kurane I, Solomon T (2011) Molecular phylogenetic and evolutionary analyses of Muar strain of Japanese encephalitis virus reveals it is the missing fifth genotype. *Infect Genet Evol*. **11**(5): 855-862

Murthy, H. M. K., Clum, S. & Padmanabhan, R (1999) Dengue virus NS3 serine protease. Crystal structure and insights into interaction of the active site with substrates by molecular modeling and structural analysis of mutational effects. *J Biol Chem.* **274:** 5573–5580

Myint KS, Kipar A, Jarman RG, Gibbons RV, Perng GC, Flanagan B, Mongkolsirichaikul D, Van Gessel Y, Solomon T (2014) Neuropathogenesis of Japanese encephalitis in a primate model. *PLoS Negl Trop Dis*. **8**(8): 1-11

Nazmi A, Mukhopadhyay R, Dutta K, Basu A (2012) STING mediates neuronal innate immune response following Japanese encephalitis virus infection. *Sci Rep*. **2(**347): 1-10

Pant SD (2009) Epidemiology of Japanese Encephalitis in Nepal. *J Nepal Paediatr Soc* **29**: 35–37

Pareek S, Roy S, Kumari B, Jain P, Banerjee A, Vrati S (2014) MiR-155 induction in microglial cells suppresses Japanese encephalitis virus replication and negatively modulates innate immune responses*. J Neuroinflammation.* **11**(97): 1-13

Partridge J, Ghimire P, Sedai T, Bista MB, Banerjee M (2007) Endemic Japanese encephalitis in the Kathmandu valley, Nepal. Am J Trop Med Hyg 77: 1146–1149

Rodenhuis-Zybert IA, Moesker B, da Silva Voorham JM, van der Ende-Metselaar H,Diamond MS, Wilschut J, Smit JM (2011) A fusion-loop antibody enhances the infectious properties of immature flavivirus particles. *J Virol*. **85**(22): 11800-11808

Saraiva M, O'Garra A (2010) The regulation of IL-10 production by immune cells. *Nat Rev Immunol.* **10**(3): 170-181

Saxena SK (2008) Japanese encephalitis: Perspectives and new developments. *Future Neurol*. **3**: 515-521

Saxena S K, Tiwari S, Saxena R, Mathur A and Nair M P N (2013) Japanese Encephalitis Virus: The Complex Biology of an Emerging Pathogen, chapter 10, Pub Intech open science/open minds: 161-180 pp

Saxena SK, Mathur A, Srivastava RC (2001) Induction of nitric oxide synthase during Japanese encephalitis virus infection: evidence of protective role. *Arch Biochem Biophys.* **391**(1): 1-7

Schmittgen TD, Lee EJ, Jiang J, Sarkar A, Yang L, Elton TS, Chen C (2008) Real-time PCR quantification of precursor and mature microRNA. *Methods.* **44**(1): 31-8.

Schweitzer B, Chapman N (2009) Overview of the Flaviviridae with an Emphasis on the Japanese Encephalitis Group Viruses. *LabMedicine*. **40**: 493-499

Sharma A, Kumar M, Aich J, Hariharan M, Brahmachari SK, Agrawal A, Ghosh B (2009) Posttranscriptional regulation of interleukin-10 expression by hsa-miR-106a. *Proc Natl Acad Sci U S A.* **106**(14): 5761-5766

Sharma M, Bhattacharyya S, Nain M, Kaur M, Sood V, Gupta V, Khasa R, Abdin MZ, Vrati S, Kalia M (2014) Japanese encephalitis virus replication is negatively regulated by autophagy and occurs on LC3-I- and EDEM1-containing membranes. *Autophagy*. **10**(9): 1637-1651

Shirai K, Hayasaka D, Kitaura K, Takasaki T, Morita K, Suzuki R, Kurane I (2015) Qualitative differences in brain-infiltrating T cells are associated with a fatal outcome in mice infected with Japanese encephalitis virus. *Arch Virol.* **160**(3): 765-775

Solomon T (2004) Flavivirus encephalitis. *N Engl J Med*. **351**(4): 370-378

Solomon T, Dung NM, Kneen R, Gainsborough M, Vaughn DW, Khanh VT (2000) Japanese encephalitis. *J Neurol Neurosurg Psychiatry*. **68:** 405–415

Solomon T, Ni H, Beasley DW, Ekkelenkamp M, Cardosa MJ, Barrett AD (2003) Origin and evolution of Japanese encephalitis virus in Southeast Asia. *J Virol*. **77**(5): 3091-3098

Swami R, Ratho RK, Mishra B, Singh MP (2008) Usefulness of RT-PCR for the diagnosis of Japanese encephalitis in clinical samples. *Scand J Infect Dis.* **40**(10): 815-820

Swarup V, Ghosh J, Duseja R, Ghosh S, Basu A (2007) Japanese encephalitis virus infection decrease endogenous IL-10 production: correlation with microglial activation and neuronal death. *Neurosci Lett*. **420**(2): 144-149

Thakare JP, Rao TL and Padbidri VS, (2002) Prevalence of West Nile virus infection in India. *Southeast Asian J. Trop Med. Public Health*. **33**: 801-805

Thongtan T, Thepparit C, Smith DR (2012) The involvement of microglial cells in Japanese encephalitis infections. *Clin Dev Immunol.* **890586:** 1-7

Thounaojam MC, Kaushik DK, Kundu K, Basu A (2014) MicroRNA-29b modulates Japanese encephalitis virus-induced microglia activation by targeting tumor necrosis factor alpha-induced protein 3. *J Neurochem.* **129**(1): 143-154

Thounaojam MC, Kundu K, Kaushik DK, Swaroop S, Mahadevan A, Shankar SK, Basu A. (2014) MicroRNA 155 regulates Japanese encephalitis virus-induced inflammatory response by targeting Src homology 2-containing inositol phosphatase 1. *J Virol.* **88**(9): 4798-4810

Tiwari S, Chitti SVP, Mathur A and Saxena SK (2012) Japanese encephalitis virus: An emerging pathogen. *Am. J. Virol*. **1**: 1-8

Tiwari S, Singh RK, Tiwari R, Dhole TN (2012) Japanese encephalitis: a review of the Indian perspective. *Braz J Infect Dis*. **16**(6): 564-573

Utama A., Shimizu, H., Morikawa, S., Hasebe, F., Morita, K., Igarashi, A., Hatsu, M., Takamizawa, K. & Miyamura, T (2000) Identification and characterization of the RNA helicase activity of Japanese encephalitis virus NS3 protein. *FEBS Lett*. **465:** 74–78

Van den Hurk AF, Ritchie SA, Mackenzie JS (2009) Ecology and geographical expansion of Japanese encephalitis virus. *Annu Rev Entomol*. **54**: 17-35

Van den Hurk AF, Smith CS, Field HE, Smith IL, Northill JA, Taylor CT, Jansen CC, Smith GA, Mackenzie JS (2009) Transmission of Japanese Encephalitis virus from the black flying fox, Pteropus alecto, to Culex annulirostris mosquitoes, despite the absence of detectable viremia. *Am J Trop Med Hyg*. **81**(3): 457-462

Vrati S, Giri R, Razdan A, and Malik P (1999) Complete nucleotide sequence of an indian strain of japanese encephalitis virus: sequence comparison with other strains and phylogenetic analysis. *Am. J. Trop. Med*. **61**(4): 677–680

Wang L, Hu W, Soares Magalhaes RJ, Bi P, Ding F, Sun H, Li S, Yin W, Wei L, Liu Q, Haque U, Sun Y, Huang L, Tong S, Clements AC, Zhang W, Li C (2014) The role of environmental factors in the spatial distribution of Japanese encephalitis in mainland *China. Environ Int.* **73**: 1-9

Weaver SC, Barrett AD (2004) Transmission cycles, host range, evolution and emergence of arboviral disease. *Nat Rev Microbiol*. **2**(10): 789-801

Wilson EB, Brooks DG (2011) The role of IL-10 in regulating immunity to persistent viral infections. *Curr Top Microbiol Immunol*. **350**: 39-65

Xie N, Cui H, Banerjee S, Tan Z, Salomao R, Fu M, Abraham E, Thannickal VJ, Liu G (2014) miR-27a regulates inflammatory response of macrophages by targeting IL-10. *J Immunol.* **193**(1): 327-334

Xu LJ, Liu R, Ye S, Ling H, Zhu CM (2013) Genomic analysis of a newly isolated of Japanese encephalitis virus strain, CQ11-66, from a pediatric patient in China. *Virol J*. **10**(101): 1-6

Yamashita T, Unno H, Mori Y, Tani H, Moriishi K, Takamizawa A, Agoh M, Tsukihara T, Matsuura Y (2008) Crystal structure of the catalytic domain of Japanese encephalitis virus NS3 helicase/nucleoside triphosphatase at a resolution of 1.8 A. *Virology*. **373**(2): 426-436

Yang S, He M, Liu X, Li X, Fan B, Zhao S (2013) Japanese encephalitis virus infects porcine kidney epithelial PK15 cells via clathrin- and cholesterol-dependent endocytosis. *Virol J*. **10**(258): 1-8

Ye J, Zhu B, Fu ZF, Chen H, Cao S (2013) Immune evasion strategies of flaviviruses. *Vaccine*. **31**(3): 461-471

Yi R, Qin Y, Macara IG, Cullen BR (2003) Exportin-5 mediates the nuclear export of pre-microRNAs and short hairpin RNAs. *Genes Dev.* **17**(24): 3011-3016.

Zeng, L., Kurane, I., Okamoto, Y., Ennis, F. A. & Brinton, M. A (1996) Identification of amino acids involved in recognition by dengue virus NS3-specific, HLA-DR15-restricted cytotoxic CD4+ T-cell clones. *J Virol*. **70**: 3108–3117

Zhu YZ, Xu QQ, Wu DG, Ren H, Zhao P, Lao WG, Wang Y, Tao QY, Qian XJ, Wei YH, Cao MM, Qi ZT (2012) Japanese encephalitis virus enters rat neuroblastoma cells via a pH-dependent, dynamin and caveola-mediated endocytosis pathway. *J Virol*. **86**(24): 13407-13422

Zimmerman MD, Scott RM, Vaughn DW, Rajbhandari S, Nisalak A, Shrestha MP (1997) Short report: an outbreak of Japanese encephalitis in Kathmandu, Nepal. *Am J Trop Med Hyg*. **57**: 283–284.

APPENDICES

Appendix 1: PUBLICATIONS

❖ Saxena S.K., **Dahal S.** Ebola outbreak 2014: an overview of the experimental therapeutics. *Pharma Bio World.* 2014; 10: 26-31.

❖ Saxena S.K., **Dahal S.**, Srinivasulu G., Swamy MLA. Current trends in influenza therapeutics and prevention. *Fut. Virol.* 2014 (in press).

❖ **Dahal S.**, Saxena S.K. Emerging & re-emerging Japanese encephalitis: pathogenesis and host immune response. *Fut. Virol.* 2014 (in press).

Appendix 2: Presentations

❖ Poster presentation at National conference on Emerging and Re-emerging viral outbreaks in India-Clinical Challenges and Management entitled "**MOLECULAR MECHANISM OF IMMUNOPATHOGENESIS DURING JAPANESE ENCEPHALITIS VIRUS INFECTION**" and awarded as the best presentation award.

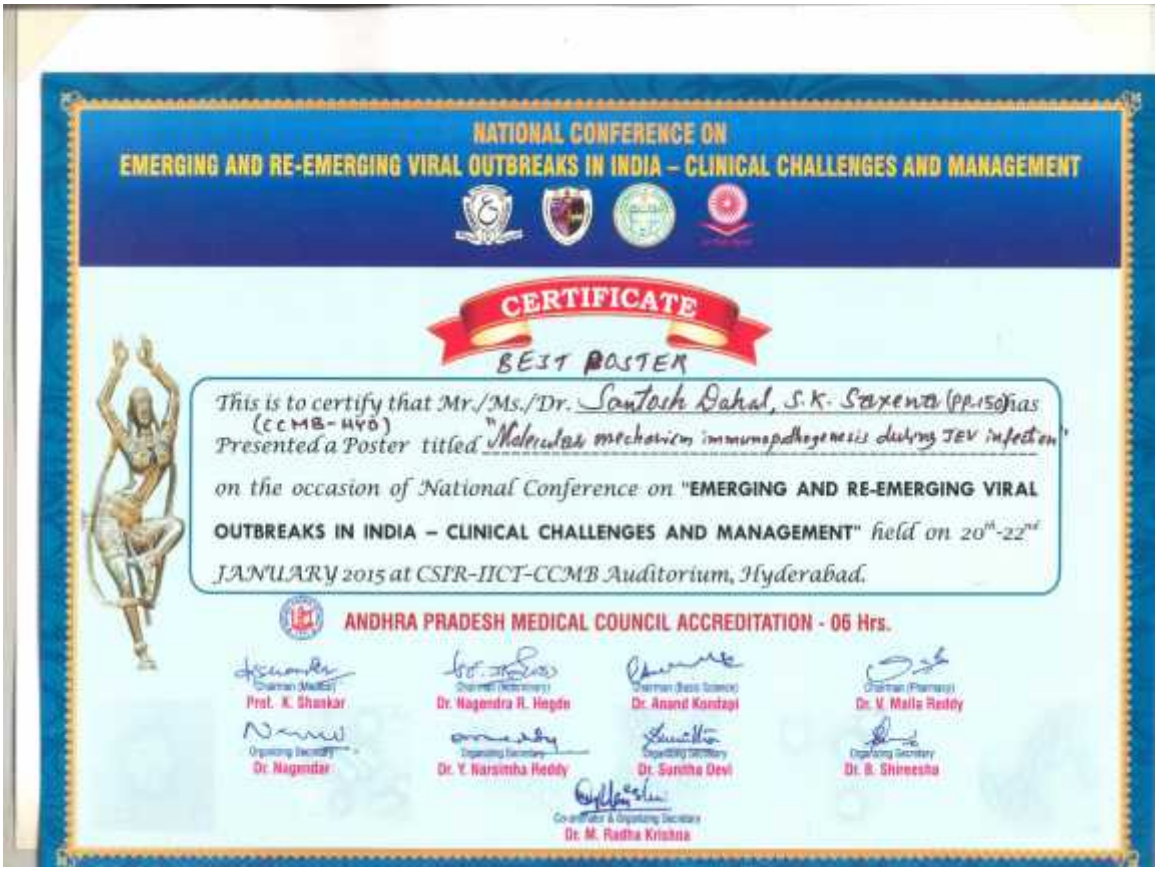

Receiving the certificate for best poster presentation

Appendix 3: Reagents Used

❖ **10X TAE Buffer**

Tris base	48.4 g
0.5M EDTA (pH 8.0)	20.0 ml
Glacial acetic acid	11.4 ml

Make final volume to one litre, final pH 8

❖ **Ethidium Bromide**

Ethidium Bromide	10.0 mg
DDW	1.0 ml

❖ **Protein loading dye (5x)**

50mM Tris-HCl (pH 6.8)
100mM Dithiothreitol
2% SDS
0.1% Bromophenol blue
10% Glycerol

❖ **Running Buffer (5x)**

Tris base	15.1g
Glycine	94g
10% SDS	50mL
Water	800mL

Make up the final volume to 1000ml

❖ **30% acrylamide**

Acrylamide	29gm
Bis-acrylamide	1gm

Dissolve in 100ml MQ water in dark. Filter with Whatman filter paper, cover with foil and store at 4^{o}C

❖ **Ammonium per sulphate (10%)**

Ammonium per sulphate	1gm
Distilled water	10ml

❖ **Sodium dodecyl sulphate (10%)**

Sodium dodecyl sulphate	1gm
Distilled water	10ml

❖ **Transfer buffer**

Tris base	5.8gm
Glycine	2.9gm
SDS	0.37gm

Make the volume to 800ml with distilled water, then add 200ml methanol

❖ **Blocking solution**

Powdered nonfat milk	10gm
Tween 20	500µl

Make to 1L with 1X PBS. Store at 4^{o}C for no more than 1 week

❖ **PBST (1X)**

Dissolve the following in 800ml of distilled water

NaCl	8gm
KCl	0.2gm
Na_2HPO_4	1.44gm
KH_2PO_4	0.24gm
Tween-20	2ml

Adjust pH to 7.2 and make final volume to 1L with distilled water

❖ **4% Formaldehyde solution**

Formaldehyde	4ml
1X PBS	96ml

❖ **15% resolving gel**

MilliQ	2.3 mL
30% acrylamide gel	5.0 mL
1.5M Tris (pH 8.8)	2.5 mL
10% SDS	100 µL
10% ammonium persulfate	100 µL
TEMED	4 µL

❖ **STACKING GEL (5mL)**

MilliQ	3.4mL
30% acrylamide gel	830µL
1.5M Tris (pH 8.8)	630 µL
10% SDS	50 µL
10% ammonium persulfate	5 µL
TEMED	5 µL

❖ **80% Ethanol (100ml)**

Absolute alcohol	80ml
Distilled Water	20ml

❖ **3M Sodium Acetate**

Sodium acetate	24.61gm
Distilled water	100ml

Appendix 4: Instruments

Autoclave	:	Asian Engineering Pvt. Ltd., India.
Freezer (-80 ^{0}C)	:	Thermo Forma, USA.
DNA sequencer	:	3730xl Automated DNA Sequencer Applied Biosystems, USA
Inverted microscope		Leitz LABOVERT
Electronic balance	:	Afcoset FX-1200
Hemocytometer	:	Thoma weber
Electrophoresis apparatus	:	Amersham Biorad
Incubator shaker (37oC)	:	Innova 40 (New Brunswick Scientific)
Biosafety Cabinet	:	Biosafety Cabinet Class II
Microcentrifuge (5417R)	:	Eppendorf, Germany
Plate centrifuge		Eppendorf, Germany
Thermocycler	:	Eppendorf epgradient
Fluorescent microscope	:	Zeiss, AXIO, Imager.Z1
Imaging system	:	Versa Doc
UV-Vis spectrophotometer	:	Shimadzu UV-1601, Japan
Water-bath	:	Julabo SW23
Gel documentation	:	Syngene